Mechanisms of Water Storage in the Unsaturated Zone of the Chalk Aquifer

The University of Reading

R&D Technical Report W50

Further copies of this report are available from:

Foundation for Water Research, Allen House, The Listons,
Liston Rd, Marlow, Bucks SL7 1FD. Tel: 01628-891589, Fax: 01628-472711

Mechanisms of water storage in the unsaturated zone of the Chalk aquifer

R G Low
C McCann
M Price

Research Contractor
The University of Reading

Environment Agency
Rio House
Waterside Drive
Aztec West
Almondsbury
Bristol
BS12 4UD

The University of Reading
Whiteknights
Reading
RG6 6AB

R&D Technical Report W50

Publishing Organisation
Environment Agency
Rio House
Waterside Drive
Aztec West
Almondsbury
Bristol
BS12 4UD

Tel. 01454 624400 Fax 01454 624409

TH-04/97-AXZZ

This report is the result of work funded jointly by the Environment Agency and The University of Reading.

Dissemination Status
Internal: Released to Regions
External: Released to Public Domain

Statement of Use: This document is for information only and will form the basis of further research work on the drainage and recharge behaviour of the Chalk. The report has been circulated to other Environment Agency regions for comment.

Research contractor:
This document was produced under R & D Project 612 by:

Postgraduate Research Institute for Sedimentology
The University of Reading
Whiteknights
PO Box 227
Reading
Berkshire
RG6 6AB

Tel. 0118 931 6713 Fax 0118 931 0279

Environment Agency's Project Manager
The Environment Agency's Project Manager for R & D Project 612 was
Mrs Sue Hunter - Environment Agency, Thames Region

FOREWORD

This Technical Report describes the findings of a study of the relationship between fissure storage and matric porosity storage in the unsaturated zone of the Chalk, Britain's most important aquifer.

The project was initiated by The University of Reading, and funded jointly by the Environment Agency (formerly the National Rivers Authority) and the University.

The work was carried out at the University by Robert Low, Clive McCann and Michael Price. The Environment Agency Project Leader was Sue Hunter (Thames Region).

The authors are grateful for the assistance, practical help and advice of Solomon Assefa, John Jack, Jeremy Sothcott and David Thornley of the University, and of Professor Rory Mortimore (University of Brighton). Mercury intrusion measurements were undertaken by Dr John Bloomfield and staff of the British Geological Survey at Wallingford. The help, encouragement and advice of staff of the Environment Agency, particularly Sue Hunter and Nicola Bailey, during the inception and execution of the project, is also gratefully acknowledged.

CONTENTS

LIST OF FIGURES

EXECUTIVE SUMMARY

In 1993 Lewis *et al.* reported the results of a study, by the British Geological Survey (BGS), on the amount of water in storage in the Chalk aquifer in England under various conditions. One part of that study compared the volumes of water leaving two Chalk catchments as baseflow during long recessions with the estimated changes in groundwater storage in the catchments during the same periods. In all cases there appeared to be more water leaving the catchments than could be accounted for by the measured fall in the water table, suggesting that there was some additional source of water in the catchments. Lewis *et al.* concluded that the most likely source of water was slow drainage from the unsaturated zone, a process that they termed delayed recharge.

It was estimated that this storage would need to be about 0.25 to 0.30 per cent of bulk volume, but that in order to explain the delay in drainage it would most probably have to derive from the matrix of the chalk rather than from the fissure porosity. This seemed at odds with conventional thinking on Chalk hydrogeology, which was that the matric porosity of chalk remained essentially filled with water, even in the unsaturated zone; changes in storage were believed to result from the emptying and filling of the fissure porosity.

The issue is worth understanding. If the extra drainable storage is taken as 0.25 per cent, and the average thickness of the unsaturated zone is assumed to be 20 m, the additional storage in the unsaturated zone would amount to 1000 million m^3 of water (five times the gross storage of Kielder Reservoir).

Previously some workers have suggested that chalk may contain large pores ('macropores') and be intersected by networks of fine fissures ('microfissures') that might be expected to drain under gravity and therefore could contribute this additional storage. The present study was undertaken to determine whether or not the matrix of chalk contains drainable elements that could account for the extra water apparently revealed by the BGS study.

The project used a variety of methods to answer this question:

- Air-water capillary drainage (AWCP)
- Mercury-intrusion porosimetry (MICP)
- Acoustic velocity and attenuation
- Resin impregnation to produce pore casts

These tests were carried out on samples of chalk from three sites in southern England.

The AWCP studies indicated that apparently unfissured blocks of chalk have specific yields (drainage measured over the range of suctions likely to occur in the unsaturated zone) of 0.15 to 1.2 per cent of bulk volume, with the larger values associated with smaller samples that include some or all surfaces that are naturally or artificially fractured (i.e. rough and irregular). This suggests that the drainage is occurring at least partly from irregularities on the block walls rather from within the blocks. This conclusion is supported by the MICP data, which show greater apparent intrusion into samples broken into fragments than into those which are left whole.

The acoustic studies were designed to determine the presence or absence of microfissures within the chalks. Ultrasonic signals were passed through the samples as the effective stress was increased; if microfissures were present it would be expected that they would close at the higher stresses, leading to an observed change in the acoustic properties. No such significant change was observed, and it is concluded that the samples do not contain microfissures.

Finally, samples were impregnated with resin and the chalk partly dissolved away to reveal the resin pore casts, which were examined using a scanning electron microscope (SEM). Macropores and microfissures should then be revealed as concentrations of resin. Macropores were present, but their connections with surrounding pores were so small that they would not drain under the normal suctions present in the unsaturated zone. A few very localised microfissures were found, but there was no evidence of microfissure networks that could contribute significantly to drainage.

The key findings are that, on the basis of the samples studied, there is significant drainable storage in the unsaturated zone of the Chalk, and this drainage is of the magnitude required to explain the additional water predicted by the BGS study. This drainage does not occur from within the matric pores, but from irregularities on the block or fissure walls. Simple modelling confirms that small irregularities that are present even on apparently smooth surfaces would hold sufficient water to explain the observed drainage. Microfissures are not present to any significant degree, and macropores do not contribute significantly to drainage or permeability.

The findings are seen to be of great relevance to studies of Chalk hydrogeology and water resources. The extra storage explains why the Chalk aquifer has proved to be more resilient to drought than expected. The nature of the storage, as irregularities which fill as pore-water suctions fall during recharge, helps explain the manner in which fissure flow is generated in the unsaturated zone, and the rate of response of the water table to recharge events, including the initiation of flooding in Chalk catchments.

The nature of the recharge pathway - whether by matric pore space or through fissures - is of importance to solute transport, and particularly to the entry of pollutants into the aquifer. Transport through fissures is more rapid and more dispersive than flow through matric pores. A pollutant pulse that enters the top of the unsaturated zone may take years or decades to reach the water table if transported by matric flow. If transport is via fissures it may reach the water table in days or weeks.

However, it has to be stressed that the study has been based on relatively few samples, and further experimental and modelling work is recommended to verify the results and predictions.

KEY WORDS

Chalk aquifer, delayed drainage, macropore, microfissure, specific yield, storage, unsaturated zone, water resources.

1. INTRODUCTION

1.1 Origins of the project

In 1993 Lewis *et al.* reported the results of a study to determine the amount of water in storage in the Chalk aquifer in England. The basic approach used was to determine volumes of chalk between various defined surfaces, such as potentiometric surfaces on various dates, or a potentiometric surface and some other surface such as a fixed elevation, and multiply these volumes by the specific yield. The specific yields were weighted to take account of factors such as rock province, lithology, topography, and declining yield with depth.

In addition, studies were made of two river catchments (the Itchen and the Kennet) and their subcatchments. These catchment studies calculated the volume of water in storage in the saturated zone of the Chalk on two dates, and compared the difference with the volume of water flowing from the catchment between those dates. In every case it was found that substantially more water left the catchment as streamflow than could be accounted for by the change in position of the water table, unless an unrealistically large value was assumed for the specific yield. A similar discrepancy, based on a simpler analysis, had already been noted for the Itchen catchment by Ineson and Downing (1964). In many cases the difference was an order of magnitude or greater. Neither catchment contained significant superficial deposits, so no source of water other than the Chalk could be invoked. The most likely explanation for the discrepancy was thought to be slow release of water by drainage of chalk in the unsaturated zone. Calculations suggested that drainage of water equivalent to around 0.25 to 0.30 per cent of the volume of rock in the unsaturated zone would be sufficient to account for the anomaly (Lewis *et al.*, 1993). Because it was assumed that the fissure porosity would drain relatively quickly, the most likely source of water seemed to be the matric porosity. However, this conclusion seemed at odds with much of the conventional thinking on the Chalk, which was that the specific yield is contributed entirely by the fissures and that the matric pore space does not drain to any significant degree. The present study was undertaken to determine whether or not the matric pore space contains drainable elements that could account for the apparent 'extra' water, which was termed **delayed recharge** by Lewis *et al.*

The issue is worth understanding. The outcrop area of the Chalk in England is approximately 20 000 km^2 If the average thickness of the unsaturated zone is assumed to be 20 m, then a drainage of 0.25 per cent from the unsaturated zone would yield 1000 million m^3 of water (five times the volume of Kielder Reservoir).

1.2 Capillary-pressure theory

Water is a wetting fluid to most minerals. This causes water in contact with a solid to spread over the solid so as to achieve the maximum area of contact between water and solid. Water in a capillary tube or cylindrical pore throat will be drawn into the tube or capillary and will resist removal or drainage. Increasing the suction on the water, or increasing the pressure of the air on the other side of the air-water interface, will reduce the radius of curvature of the interface (the meniscus). If the pressure or suction is increased sufficiently, the radius of curvature will reduce to that of the tube or throat. Any further reduction in the radius of curvature will result in the water leaving the pore. The air pressure that must be applied to the concave side of the meniscus to cause this drainage is called the air-entry pressure.

Any small water-filled tube, pore or fissure will retain water against gravity. To expel the water and replace it with air, a positive pressure equal to the air-entry pressure must be applied to the air, or a suction of equal magnitude must be applied to the water. For a circular capillary, or a cylindrical pore throat draining a pore, filled with pure water at 10°C, the magnitude of this suction, h_c, in millimetres, is given by

$$h_c = 30/d \qquad (1.1)$$

where d is the diameter of the capillary or pore throat in millimetres. For a parallel-plate fissure the equivalent suction h_b is given by

$$h_b = 15/b \qquad (1.2)$$

where b is the plate separation or fissure aperture in millimetres.

Most rocks and soils contain pores and pore throats of varying sizes, which drain at varying pressures or suctions. A useful tool for describing the behaviour of a rock or soil is a curve that relates drainage to applied pressure or suction. Such curves are known by a variety of names such as soil-water characteristics, pore-water characteristics, and air-water capillary pressure (AWCP) curves; the last name will be used in this document. An AWCP curve is produced by placing a saturated sample of rock or soil on a porous plate or membrane that forms the floor of a sealed container; the air pressure in the container is increased in steps and the water loss from the sample is recorded for each pressure step (Section 3) Because the air-entry pressure is dependent on the diameter of the pore throat, the AWCP curve can be converted into a curve of pore-size distribution by making assumptions about the pore throat shape and the properties of water.

Mercury is a non-wetting fluid to most materials. This means that mercury in contact with a solid will assume the minimum surface area of contact. Mercury will not enter a tube or pore throat unless a pressure is applied to the mercury or suction to the air in the pore. Increasing the differential pressure between the mercury and air will cause the radius of curvature of the mercury to decrease; when the radius of curvature of the mercury falls below that of the pore throat, mercury will enter the pore throat and the larger pore behind it. This property makes it possible to construct a curve of mercury intrusion against pressure - a mercury-intrusion capillary pressure (MICP) curve. The MICP curve, like the AWCP curve, can be converted into a pore-size distribution curve by making certain assumptions; hence an MICP curve can be converted to an equivalent AWCP or water-drainage curve.

1.3 Recharge and drainage of the unsaturated zone of the Chalk

During winter, water is added to the top of the unsaturated zone by recharge and moves downward towards the water table. Water is also removed from the profile by evaporation and plant growth during spring and summer. If these influences could be removed for a long period, water would drain downward through the profile until equilibrium was reached. At this

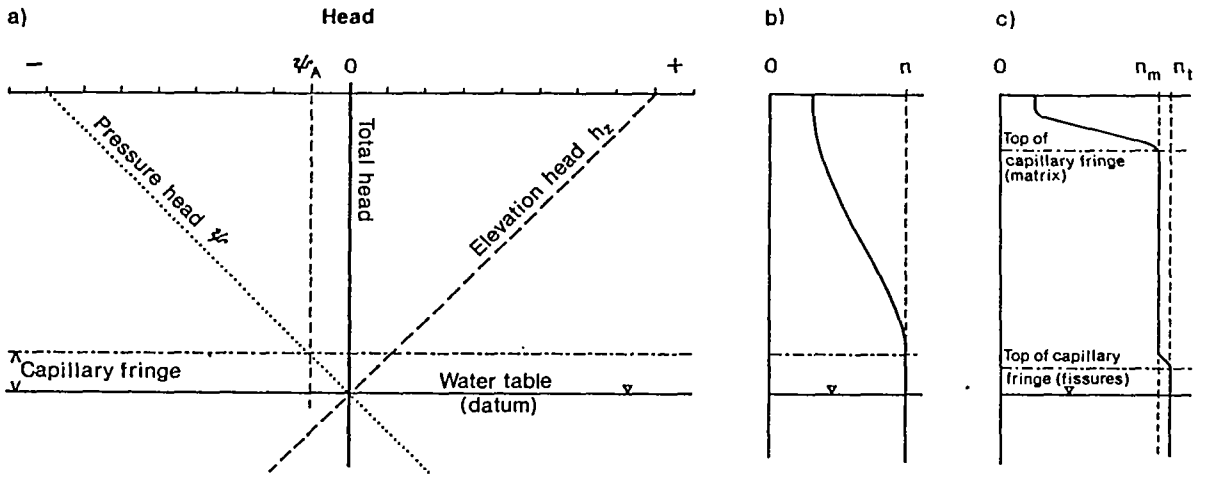

Figure 1.1 Theoretical relationships between head, depth and water content in the unsaturated zone of an aquifer after drainage to equilibrium: (a) head relationships; (b) water content in a uniform granular aquifer; (c) water content in a dual-porosity aquifer such as the Chalk (after Price *et al.*, 1993).

n = porosity of granular aquifer

n_t = total porosity of dual-porosity aquifer

n_m = matric porosity of dual-porosity aquifer

ψ_A = air-entry pressure

equilibrium the total head at every depth in the profile would be equal to the head at every other depth (Figure 1.1). For this to be achieved, the pressure head at any point z metres above the water table would be -z, so that the sum of elevation head and pressure head, measured relative to the water table, would be zero. A negative pore-pressure head is referred to as a pore-water suction, so there would be a pore-water suction (a negative pressure head) of z metres at that point. Although this condition is never completely achieved in Britain, it is approached in summer.

Because the water table in the Chalk is frequently many tens of metres below ground level, much of the unsaturated zone is many tens of metres above the water table. It follows that the pore-water suctions in much of the unsaturated zone as equilibrium is approached will be very high. Under these suctions the fissure space is effectively drained and does not transmit water.

The pore throats in the Chalk are very small, typically less than 1 μm (Price *et al.*, 1976), and the suction needed to drain chalk pores is therefore likely to be in excess of 30 m. It was therefore widely believed that, even at equilibrium, the pore space in the matrix would not drain under the suctions likely to be present in the unsaturated zone, except within the top two or three metres where plant roots could be exerting much higher suctions. Some workers (e.g. Reeves, 1979) have suggested that chalk may contain 'macropores' and 'microfissures' that might drain under gravity and contribute to specific yield, but no physical evidence of their presence has been forthcoming.

1.4 Rationale of this project

The aim of the current project was to determine whether or not the matric porosity of typical chalks contains elements that are capable of draining under field conditions, and to assess the magnitude (in ratio or percentage terms) of any such drainable space. In particular, it was necessary to determine whether or not chalk contains macropores or microfissures that might provide this additional source of water. The strategy adopted to try to answer these questions involved collecting samples of chalk and then studying them using a combination of laboratory methods. The techniques chosen were:

- Air-water capillary drainage
- Mercury-intrusion porosimetry
- Acoustic velocity and attenuation
- Resin impregnation to produce pore casts

Both air-water capillary drainage and mercury intrusion porosimetry are techniques to study the drainage characteristics of porous materials. An introduction to capillary theory was given in Section 1.2. Surprisingly little previous AWCP work has been done on chalks. Previous MICP studies (Price *et al.*, 1976) showed that about 2-3 per cent of the pore space in many chalks could be expected to drain at suctions below 20 m of water. This is equivalent to about 1 per cent of the bulk volume, so that matric pores could contribute about 1 per cent to the specific yield. However, the samples used in the 1976 study were very small (typically about 2 g) and it was considered possible that much of the mercury intrusion at low pressures was occurring into irregularities on the surface of the sample. It is therefore equally possible that

drainage of water from chalks in AWCP tests might occur from such irregularities. Equally, it is possible that, under field conditions, drainage from chalks may be from irregularities on fissure surfaces rather than from the pore space in the matrix. To try to resolve this, a testing strategy was developed that involved using various types and shapes of samples, in both AWCP and MICP tests (Sections 3 and 4).

The acoustic method is based on the fact that microfissures slow down and attenuate ultrasonic acoustic signals passed through a sample of rock. As the effective stress on the sample increases, the microfissures close up, the speed of the wave increases and less of the acoustic energy is 'lost'. In the tests used in this study, cores of rock are held in a high-pressure testing rig in the laboratory and subjected to increasing confining stress as ultrasonic signals are passed through them. If microfissures are present, the acoustic wave speeds up and attenuation decreases as the stress is increased and the microfissures close. If there is no significant change in velocity and attenuation with increasing stress at low stress levels, microfissures are unlikely to be present.

Resin impregnation fills the pore space (including any microfissures present) with a resin. The chalk can then be removed by etching with acid, leaving a 3-dimensional cast of the pore space. This cast can be prepared and examined using a scanning electron microscope (SEM). Resin impregnation of chalks has been carried out by other workers, but always on small samples (typically ~ 10 mm or less) These samples have not revealed any evidence of microfissures, but it could be argued that this is because the samples had broken along microfissures and so did not include them. One aim of the present study was to construct a new and much larger rig, permitting impregnation of samples so large that, if microfissures really exist in chalks, these samples must contain them.

2. SAMPLING

The initial plan was to take a total of up to 20 samples from several sites from a range of stratigraphical horizons and geographical locations in England, to represent the range of chalk lithologies. After discussion within the Environment Agency and with Professor Rory Mortimore (Department of Civil Engineering, University of Brighton) it was decided that sufficient lithological variation existed over short stratigraphical intervals, and it was agreed that samples would be taken from three localities - Play Hatch Quarry (SU 740765), near Reading; Shoreham Cement Works Quarry (TQ 203087); and Cherry Hinton Quarry (TL 484556), near Cambridge. Quarry sites were chosen to enable reasonably fresh material to be collected.

As part of the effort to ensure that microfissures, if present, would be sampled, large blocks were collected from all three sites. From Shoreham, seven blocks were collected on 13 March 1996. The blocks were taken from the Upper Lewes Chalk, either from adjacent to the quarry face or by small-scale excavating. The blocks had an average largest dimension of 0.4 m. Three of the blocks were chosen to include natural fracture or weathering surfaces, as it was suspected that these could have a major influence on drainage.

Seven blocks of similar dimensions, and also with fracture and weathering surfaces, were taken from Cherry Hinton Quarry on 15 March 1996. The stratigraphy of Cherry Hinton is not well documented but it is believed that all the samples were from the Lower Chalk. Several visits were made to Play Hatch Quarry during the winter of 1995-96. In addition to large blocks, smaller fragments bounded by natural fractures were taken from a thinly bedded sequence.

All of the samples were assigned sample numbers and were photographed.

3. AIR-WATER CAPILLARY PRESSURE MEASUREMENTS

3.1 Introduction

As explained in Section 1.3, in the absence of recharge or evaporative loss, drainage of the unsaturated zone will theoretically continue until the profile is in equilibrium with the water table (Figure 1.1). In most rock types drainage will progressively slow down as the larger pores empty and the unsaturated hydraulic conductivity is correspondingly reduced. Usually the air-entry pressure is relatively low, and only a small thickness of the profile, immediately above the water table, remains fully saturated; this is the capillary fringe or tension saturated zone. In the Chalk, the air-entry pressure is high, and the 'capillary fringe' frequently extends for the full thickness of the unsaturated zone. Because there is little drainage of the matric pores, the hydraulic conductivity of the matrix remains fairly constant over a wide range of pore-water suctions.

To assess the specific yield of a particular horizon, it would theoretically be possible to collect a sample from that horizon, take it to the laboratory, saturate it, place it on a porous plate and apply a suction corresponding to the position of the sample horizon above the water table. The amount of water drained, expressed as a fraction or percentage of the bulk volume of the sample, would be the specific yield. In practice this approach is not adopted. Instead a complete AWCP curve is built up for each sample, and the specific yield is estimated by assuming the suction that the rock will drain to in the field.

In the case of the present study, we needed to determine whether any of the matric pore space in the Chalk will drain at suctions below about 30-50 m and thus contribute to specific yield. In addition, answers were needed to two questions:

- does drainage come from the bulk of the rock or predominantly from the block surface?
- do different types of surface, in particular 'natural' fissure surfaces, affect the degree of drainage?

3.2 Experimental methods

3.2.1 Sample preparation and saturation

To achieve the aims outlined in Section 3.1, samples had to be carefully selected. To determine whether drainage was occurring mainly from the block surface or from the bulk of the rock, samples were needed with different ratios of surface area to volume. In essence, this ratio will be greater for small samples than for large ones, so the sample suite had to include blocks of varying sizes. To determine the effects of different types of surface, those types had to be represented in the samples. Ideally each sample would have only one type of surface, but we accepted that this would not always be possible.

In practice, selection of samples for testing was limited by the size and geometry of the blocks that had been collected from the three sites, and it proved difficult to create an ideal sample set without producing too many samples. In the end, a representative sub-set of 16 samples was selected from a set of 50 samples that included all the main properties thought necessary. All

three sites were equally represented in the full sample set, but as the samples in the sub-set were selected on the basis of size and shape, Play Hatch was over represented in this final suite.

When the samples had been selected, they were cut from the larger blocks using a bandsaw. A flat surface was ground on one side, and they were photographed and described. They were then dried in an oven at 100°C until their weights stabilised, a process which took three days. The stable weight of each sample was taken as the dry weight.

After drying the samples were placed in a stainless steel pressure vessel which was evacuated using an Edwards E2M8 two-stage vacuum pump An absolute pressure of 2.7 Pa (compared with standard atmospheric pressure of 101 325 Pa) was achieved after three days, when the vessel was isolated from the vacuum pump and slowly filled with de-aired water. The samples were left for two days under 0.5 m head of water to ensure the fullest possible saturation. The saturated samples were then weighed, in air and submerged in water, to permit calculation of porosity and grain density using Archimedes' principle:

$$V_p = (W_a - W_d)/\rho_L \quad (3.1)$$

$$V_b = (W_a - W_s)/\rho_L \quad (3.2)$$

$$V_g = (W_d - W_s)/\rho_L \quad (3.3)$$

$$n = V_p/V_b = (W_a - W_d)/(W_a - W_s) \quad (3.4)$$

$$\rho_g = W_d/V_g \quad (3.5)$$

where:

V_p = pore volume

V_b = bulk volume

V_g = grain volume

n = interconnected porosity

W_d = dry weight of sample in air

W_a = saturated weight of sample in air

W_s = saturated weight of sample submerged in liquid

ρ_L = density of liquid used for saturation and submersion

ρ_g = grain density of sample

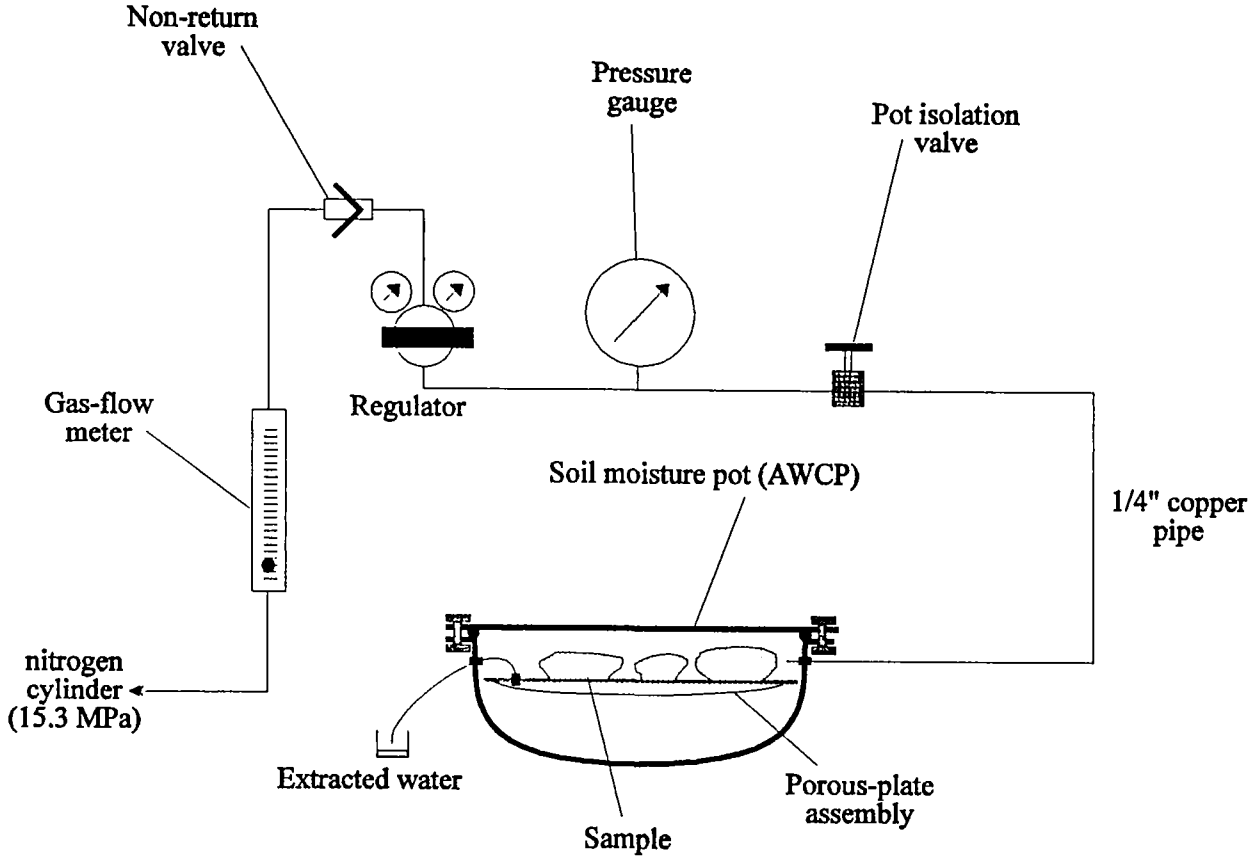

Figure 3.1 Diagrammatic representation of the air-water capillary pressure (AWCP) apparatus

3.2.2 Procedure for AWCP determination

The AWCP apparatus used in this study is shown schematically in Figure 3.1. To carry out an AWCP determination and produce a curve, the porous plate was first saturated. This was done by flooding the plate with distilled water containing a small amount of formalin to act as a biocide. The AWCP vessel was then sealed and the gas pressure inside the container increased to a pressure less than the air-entry pressure of the plate. This caused most of the water to drain from the vessel but left the plate saturated.

The saturated samples were then weighed and placed on the porous plate with the cut surface of the sample as the base. To ensure good capillary contact between sample and plate, a thin film of kaolin was placed on the plate beneath each sample, with a suitably sized Whatman No. 1 filter paper between the kaolin and the base of the sample to prevent kaolin entering the pores of the sample. A small dish of water was placed inside the vessel to maintain a humid atmosphere and prevent water being lost from the samples by evaporation. The vessel was then sealed and the pressure inside increased using nitrogen from a commercial gas cylinder. Every 2-3 days the vessel was depressurised and the samples removed, quickly weighed and returned to the vessel which was repressurised. When the weights of all the samples had stabilised, the pressure was raised to the next step. At each pressure step, the pressure was increased by between 50 and 100 per cent, with smaller percentage increases at the start of the experiment and at what were expected, by reference to previous pore-size distribution studies (e.g. Price *et al.*, 1976), to be critical pressure increments.

Ideally, when the samples were placed in the AWCP vessel, their pores would have been completely filled with water but no water would be adhering to their surfaces. A slight increase in pressure above atmospheric would then lead to the drainage of pores with large pore throats and of large irregularities on the surfaces of the samples; this drainage would be detected by decreases in the weights of the samples. In practice this condition could not be achieved, because it is impossible to guarantee that there is no water clinging by surface tension to the outsides of the samples. The procedure adopted to overcome this was to make the first increase in pressure above atmospheric as small as possible. It was hoped that this pressure increment would cause drainage of the 'skin' of water adhering to the sample surface, but not cause drainage of pores, fissures or irregularities. The minimum pressure increment above atmospheric that could be reliably maintained and measured with the regulators and transducers available was about 4.9 kPa, so this was chosen as the first step. When the weights of the samples had stabilised at this pressure, the weights were recorded as the initial weights for the experiment, i.e. any drainage that had occurred at this pressure was ignored.

In reality, this initial pressure although the lowest step that could be achieved with the sensitive equipment available, was higher than would ideally be needed to determine drainage from small fissures and large pores. Equations (1.1) and (1.2) show that at a pressure of 4.9 kPa, drainage could be expected of pores with diameters greater than 60 μm and of fissures with apertures greater than 30 μm. For practical purposes, in determining how much drains from chalks in the field, it was close to ideal. Field studies of pore-water suctions in the unsaturated zone of the chalk indicate that the suction rarely falls below about 0.5-1 m of water (Wellings, 1984); at lower suctions, fissure flow could be expected.

Porous plates with a range of air-entry pressures were available. Above its air-entry pressure a plate becomes permeable to air or nitrogen and can no longer be used. Plates with lower air-

entry pressures are more permeable and allow more rapid drainage to equilibrium at any pressure. To achieve maximum drainage rates and to allow drainage to continue to higher pressures, a low air-entry plate (10^5 Pa) was used initially, and replaced with a high air-entry plate (5×10^5 Pa) at the appropriate time. The main purpose of the AWCP study was to determine whether drainage occurs from matric pore space in the unsaturated zone of the Chalk, i.e. at suctions of around 10-50 m of water. Therefore although it was intended to continue drainage to the highest equivalent suction possible in the time available, most attention was paid to drainage at relatively low pressures (less than 30 m head of water, or about 300 kPa).

3.3 Results

The values derived during the saturation experiments are presented in Table 3.1. Chalk - especially Middle and Upper Chalk - is generally almost pure calcite, and can be expected to have a grain density around 2710 kg/m^3 (2.71 g/cm^3). Most of the grain density values in Table 3.1 are very close to this figure, except those for samples PH5/1-PH5/3. These samples are small, so errors in weighing would have a greater relative significance. The most likely explanation for the discrepancy is that the submerged weight was too low, perhaps because of incomplete saturation or slight sample loss. With these exceptions the similarity of the grain densities to that for calcite is reassuring. The porosity values given in Table 3.1 are also similar to those reported from other studies.

Bloomfield *et al* (1995) presented a summary of the chalk matrix porosity values held in the aquifer properties database at BGS, Wallingford. Mean porosity values derived for both Shoreham (36.3 %) and Play Hatch (38.8 %) compare well with the mean value 38.8 % quoted for Southern/Thames and Chiltern Upper Chalk (Bloomfield *et al* 1995). A mean of 34.25 % for the Cherry Hinton samples also compares well with the quoted mean for East Anglian Middle and Lower Chalk of 34.3 %.

Examples of the AWCP curves are presented in Figures 3.2 to 3.5. Each of these figures also includes a photograph of the sample, with a bar scale in centimetres, and details of the sample surface. The findings are summarised in Figure 3.6, which compares the AWCP curves from the four samples, two large and two small, with cut surfaces and natural fissure surfaces.

The results shown in Figures 3.2 to 3.6 imply that in the absence of irregular surfaces, such as those formed by natural fissures, drainage at suctions of 10-15 m is of the order of 0.5-1 per cent of pore space, or about 0.15-0.4 per cent of bulk volume, with the smaller value applicable to large blocks and the larger value applicable to small blocks. Where irregular surfaces are present (Figures 3.4 and 3.5) the drainage for the same suctions is in the range 1.5 to 3 per cent of pore space, or about 0.5 to 1.2 per cent of bulk volume, with the larger value again associated with the smaller sample size. The variation with size of tested blocks implies clearly that there is a surface effect in the drainage behaviour. This conclusion is strengthened by the fact that drainage is significantly greater from samples that include one or more rough surfaces - either natural fissure surfaces or artificially broken surfaces.

Table 3.1 Pore/grain related parameters for the AWCP samples

Sample	Dry weight (g)	Saturated weight in air (g)	Pore volume (cm^3)	Saturated weight immersed (g)	Bulk volume (cm^3)	Grain density (g/cm^3)	Porosity (%)
SH4/7	32.92	39.58	6.67	20.75	18.86	2.70	35
SH5/4	213.96	267.26	53.39	134.76	132.71	2.70	40
SH5/5	97.06	115.77	18.74	60.68	55.18	2.66	34
PH1/4	112.95	139.86	26.95	71.32	68.65	2.71	39
PH1/5	70.48	87.21	16.76	44.05	43.23	2.66	39
PH2/3	55.48	70.04	14.58	34.76	35.34	2.67	41
PH2/4	47.50	58.49	11.01	30.00	28.54	2.71	39
PH4/1	50.18	62.50	12.34	31.70	30.85	2.71	40
PH5/1	13.34	16.33	2.99	8.05	8.29	2.52	36
PH5/2	11.79	14.32	2.53	6.98	7.35	2.45	34
PH5/3	12.60	15.60	3.00	7.54	8.07	2.49	37
PH6/4	215.31	270.02	54.80	135.54	134.69	2.69	41
PH7/6	45.18	56.49	11.33	28.41	28.12	2.69	40
PH7/8	17.27	21.77	4.51	10.86	10.93	2.69	41
CH4/4	52.52	63.54	11.04	32.88	30.71	2.67	36
CH6/4	87.48	103.76	16.31	54.81	49.03	2.67	33
CH6/6	57.06	67.72	10.68	35.41	32.36	2.63	33
CH6/7	58.52	70.46	11.96	36.44	34.07	2.65	35

Figure 3.2 AWCP results for sample PH1/4

PH1/4

Dry weight in air (g) 112.95

Pressure (bar)	Weight (g)	Pore space drained (%)	Pressure (kPa)
0.05	139.57	0.00	5
0.16	139.51	0.23	16
0.3	139.48	0.34	30
0.637	139.46	0.41	63.7
1.135	139.44	0.49	113.5
1.56	139.4	0.64	156
2.27	138.57	3.76	227

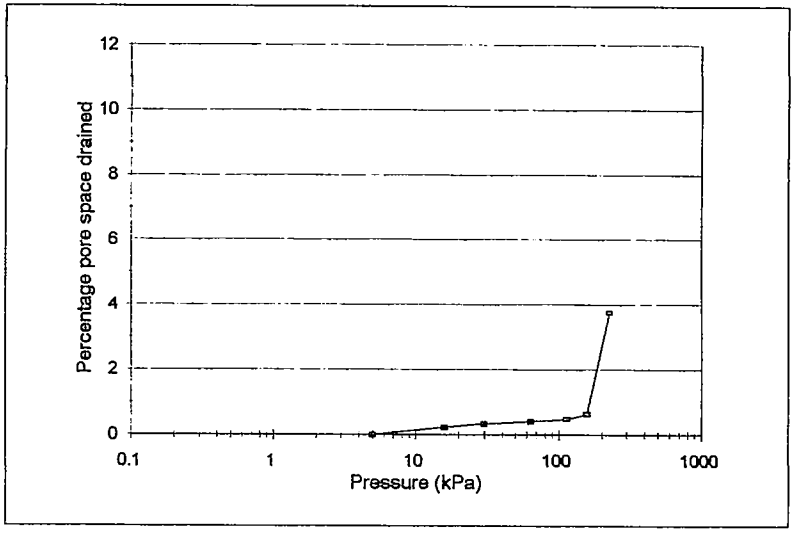

Sample description: 100 % cut surface (core radius)

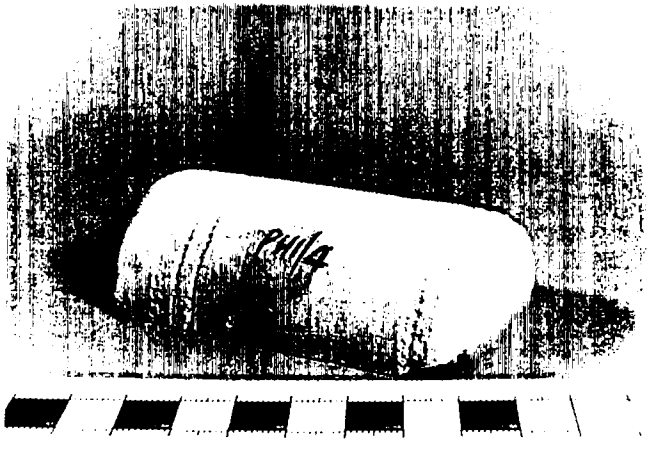

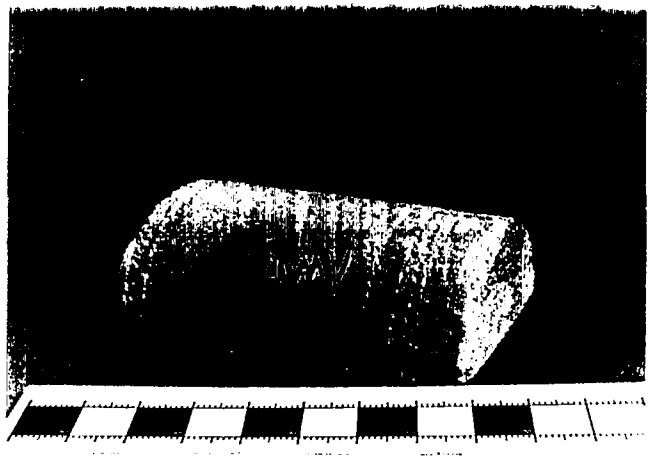

Figure 3.3 AWCP results for sample PH7/8

PH7/8

Dry weight in air (g) 17.27

Pressure (bar)	Weight (g)	Pore space drained (%)	Pressure (kPa)
0.05	21.7	0.00	5
0.16	21.7	0.00	16
0.3	21.67	0.68	30
0.637	21.67	0.68	63.7
1.135	21.66	0.90	113.5
1.56	21.64	1.35	156
2.27	21.33	8.35	227
3.4	20.01	38.15	340

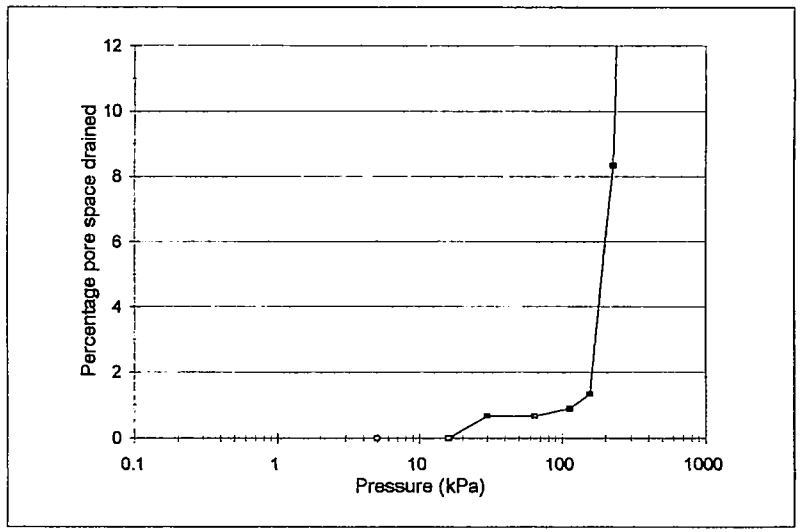

Sample description: 70 % cut surface (radius of 25 mm core), 20 % plain cut flat surface

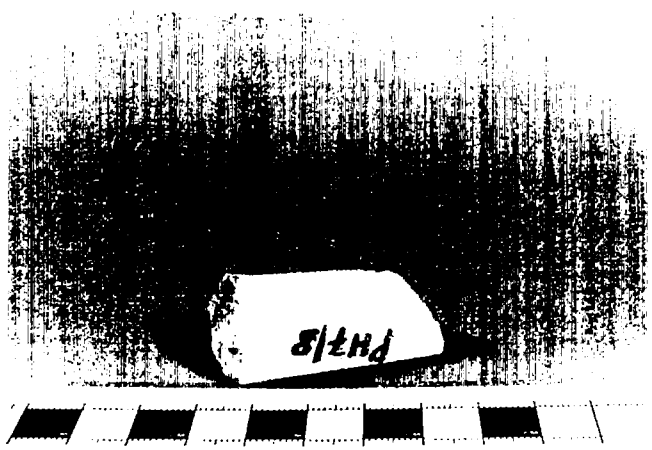

Figure 3.4 AWCP results for sample SH5/5

SH5/5

Dry weight in air (g) 97.06

Pressure (bar)	Weight (g)	Pore space drained (%)	Pressure (kPa)
0.05	115.38	0.00	5
0.145	115.31	0.38	14.5
0.296	115.21	0.93	29.6
0.63	115.13	1.36	63
1.04	115.05	1.80	104
1.56	114.84	2.95	156

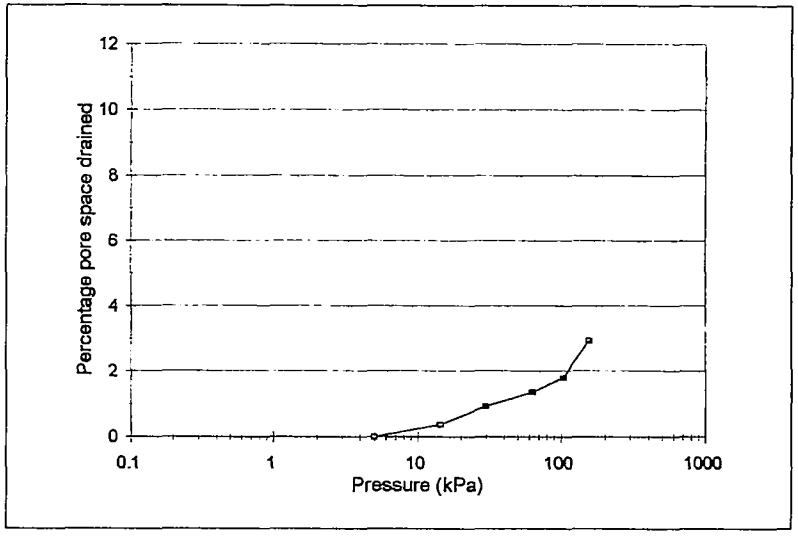

Sample description: 75 % natural block surface (rough, some dark staining), 25 % newly fractured surface

Figure 3.5 AWCP results for sample PH5/1

PH5/1

Dry weight in air (g) 13.34

Pressure (bar)	Weight (g)	Pore space drained (%)	Pressure (kPa)
0.05	16.26	0.00	5
0.16	16.22	1.37	16
0.3	16.21	1.71	30
0.637	16.21	1.71	63.7
1.135	16.18	2.74	113.5
1.56	16.18	2.74	156
2.27	16.03	7.88	227
3.4	15.36	30.82	340

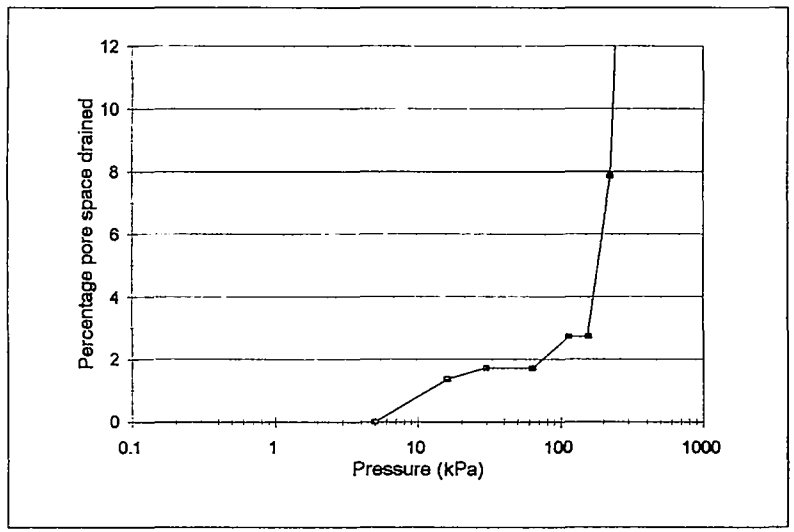

Sample description: 100 % natural block surface (smooth with light yellow staining)

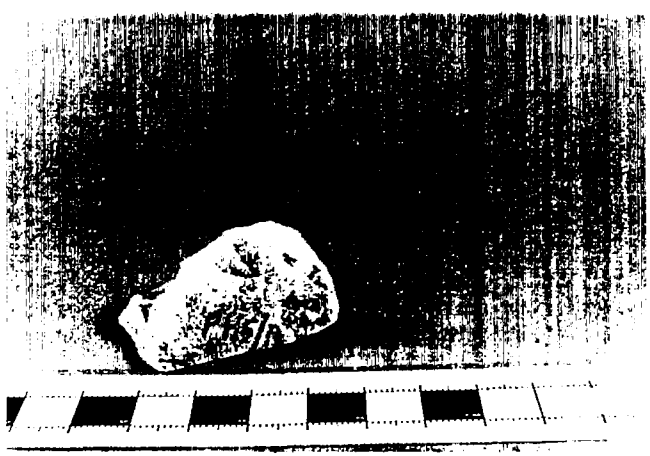

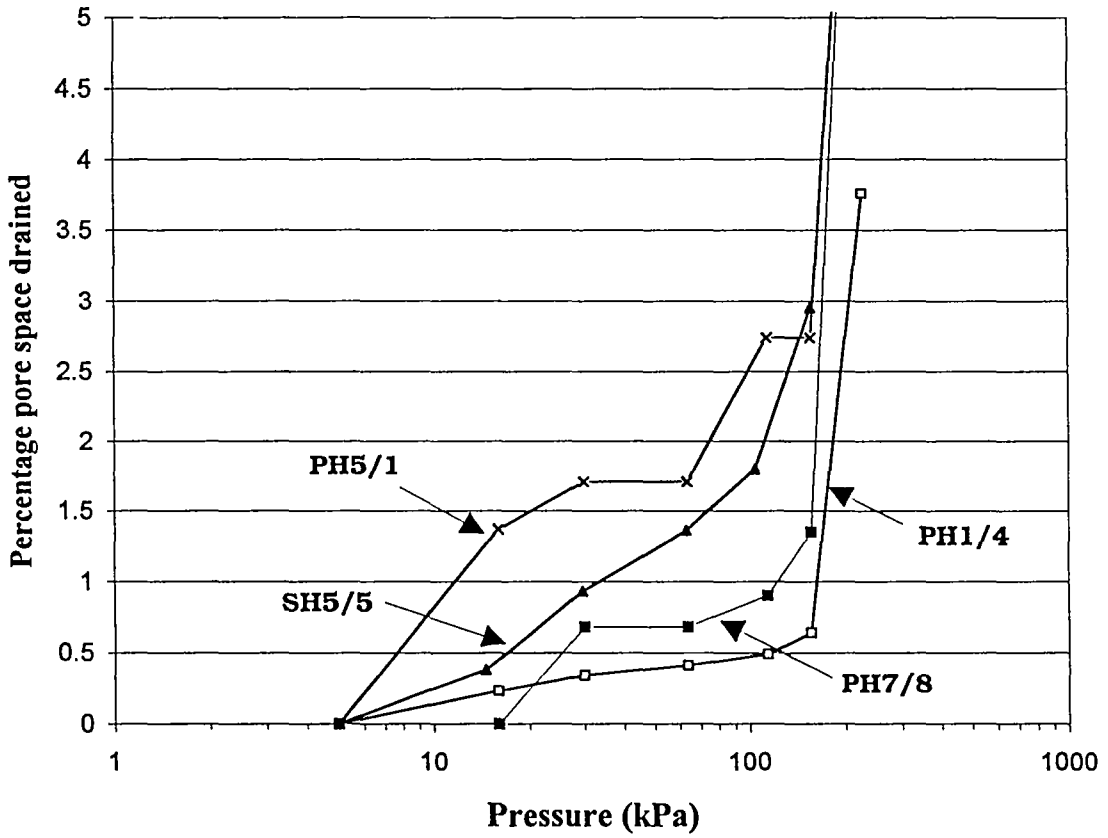

Figure 3.6 Summary of AWCP results for samples PH1/4, PH7/8, SH5/5 and PH5/1

4. MERCURY INTRUSION MEASUREMENTS

4.1 Introduction

The mercury-intrusion technique was developed by Ritter and Drake (1945) as a means of determining the pore-size distribution of a porous solid. It is based on the principle that mercury is a non-wetting fluid to most solids (the angle of contact between mercury and the solid is greater than 90°) so that mercury must be pressurised if it is to be forced into small openings (Section 1.2). The pressure required is dependent on the size of the opening. In converting from measured pressure to pore throat diameter, it is generally assumed that the pores in the material are spherical and the interconnecting pore throats are cylindrical.

In a mercury-intrusion porosimeter, a small sample of the material to be tested is placed in a penetrometer (Figure 4.1). This is essentially a glass capillary with an enlarged bulbous end. The large end of the penetrometer, which holds the sample, is sealed with a metal disc (Figure 4.1a), and the penetrometer and sample are placed in a filling device where they are evacuated. The tip of the open (capillary) end of the penetrometer is then introduced into a pool of mercury, and the air pressure in the filling device is increased slightly to cause mercury to flow into the penetrometer and around the sample (Figure 4.1b). At this stage any very large pores or depressions on the surface of the sample will also be filled; the size of the openings that are filled with mercury will depend on the air pressure and hence the pressure on the mercury. The tip of the filling device is then removed from the mercury pool, leaving the penetrometer bulb and stem completely filled with mercury. This is the condition from which pressure increments and mercury intrusion are measured; the volume of any pores already filled at this stage will not be determined, so it is important that this first pressure should be as low as possible consistent with achieving the filling of the penetrometer.

The air pressure in the filling device is then increased slowly in increments, increasing the pressure on the mercury and forcing mercury from the capillary stem into the larger pores of the sample. At each step the volume of mercury that has moved from the capillary stem into the sample is determined; in early instruments this was done visually, but it is now often done automatically by measuring the change in capacitance between the mercury column and a metal sheath surrounding the penetrometer.

When the pressure in the filling device has increased to atmospheric pressure, or slightly above, the penetrometer assembly is removed from the filling device and transferred to a high-pressure chamber. There the penetrometer is surrounded by liquid, usually alcohol or oil, which can be pressurised by a hydraulic pump or ram. The pressurising fluid is able to enter the open end of the penetrometer and continue the process of forcing mercury from the penetrometer stem into the sample as the pressure is increased (Figure 4.1c). The decrease in length of the mercury column is a measure of the volume of mercury being forced from the penetrometer stem into the sample. This decrease in length is monitored remotely; Ritter and Drake used an electrical resistance method, but modern instruments normally use the capacitance principle outlined above.

4.2 Experimental methods

In the present study, the mercury intrusion measurements were undertaken by the British Geological Survey (BGS) laboratories at Wallingford, using a Micromeritics

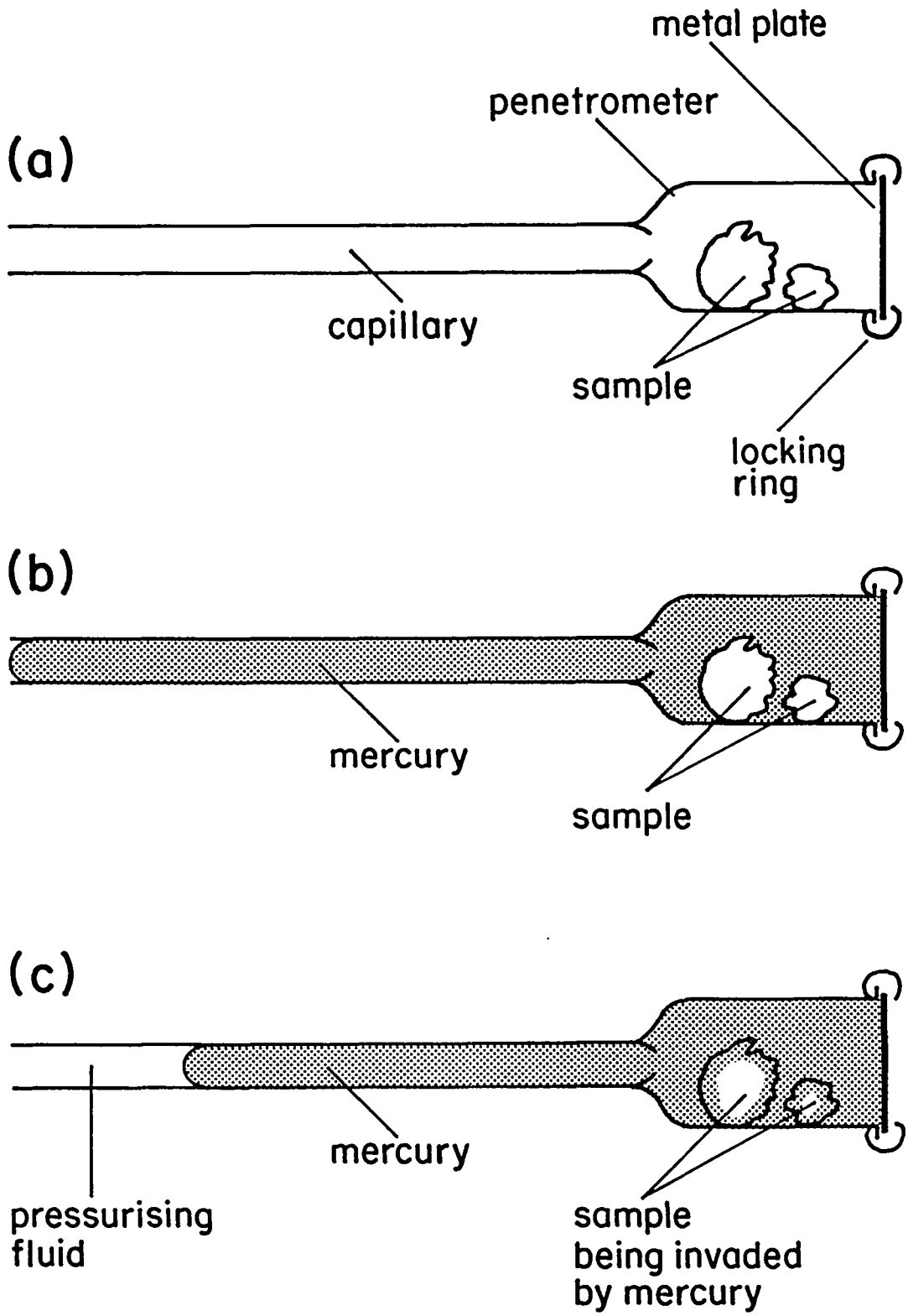

Figure 4.1 Diagrammatic representation of the sequence of mercury intrusion into a sample in a penetrometer.

AutoPore III 9410 porosimeter. This is a newly acquired instrument in which operation, data collection and processing are controlled by a microcomputer.. The low-pressure (filling device) portion of the instrument operates to a pressure of 345 kPa, and the high-pressure chamber operates to a maximum pressure of 414 MPa. This maximum pressure theoretically allows the instrument to intrude pore throats as small as 0.003 μm.

Subsamples in the form of cores approximately 9 mm in diameter were taken from ten of the samples used in the AWCP study. Each sub sample was broken into two. One half was tested intact in the mercury porosimeter, and the other half was broken and tested as fragments. The aim of this was to study further the effects of surface area and surface irregularities on the pore-size distribution, and hence on drainage behaviour, for comparison with the AWCP study.

Problems were experienced by BGS in the use of this porosimeter. The curves produced from the first samples studied were of the usual 'S'-shape, with the steep central limb indicating that most of the porosity is accessible through pore throats of a narrow size range. After some operating problems, repairs and modifications were made to the machine by the manufacturers' technician. Curves produced from subsequent samples showed a double 'S' shape, with a second steep limb at about 105 MPa, corresponding to intrusion into pores smaller than about 0.012 μm. The amount of intrusion was believed to be impossible, and this effect has been dismissed as an error in the software. Because of this problem, the curves presented are terminated at an intrusion pressure of 69 MPa.

4.3 Results

MICP curves from four samples are show in Figures 4.1 to 4.4. Those for whole samples show less intrusion at low pressure than those on fragmented material from the same subsamples. This is seen as confirmatory evidence that intrusion occurs into surface irregularities.

This filling of irregularities on the surfaces of samples is recognised in the oil industry, where it is known as conformance (Vavra *et al.*, 1992). In oil reservoir studies results are corrected for conformance before they are applied to field problems; however, most oil reservoirs are at such depth that open fissures are rare, and irregularities on fissure surfaces will be insignificant for reservoir behaviour. In the Chalk aquifer, and particularly in its unsaturated zone, we believe that irregularities on fissure walls may represent significant storage.

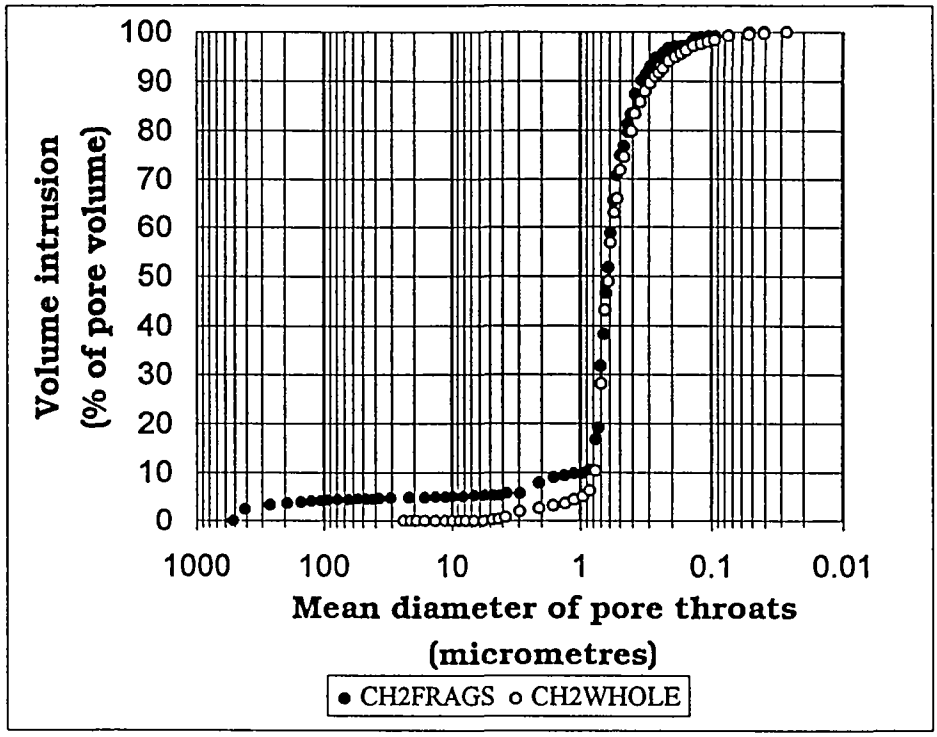

Figure 4.2 Mercury-intrusion capillary pressure curves for whole and fragmented samples of chalk from Cherry Hinton (sample CH2).

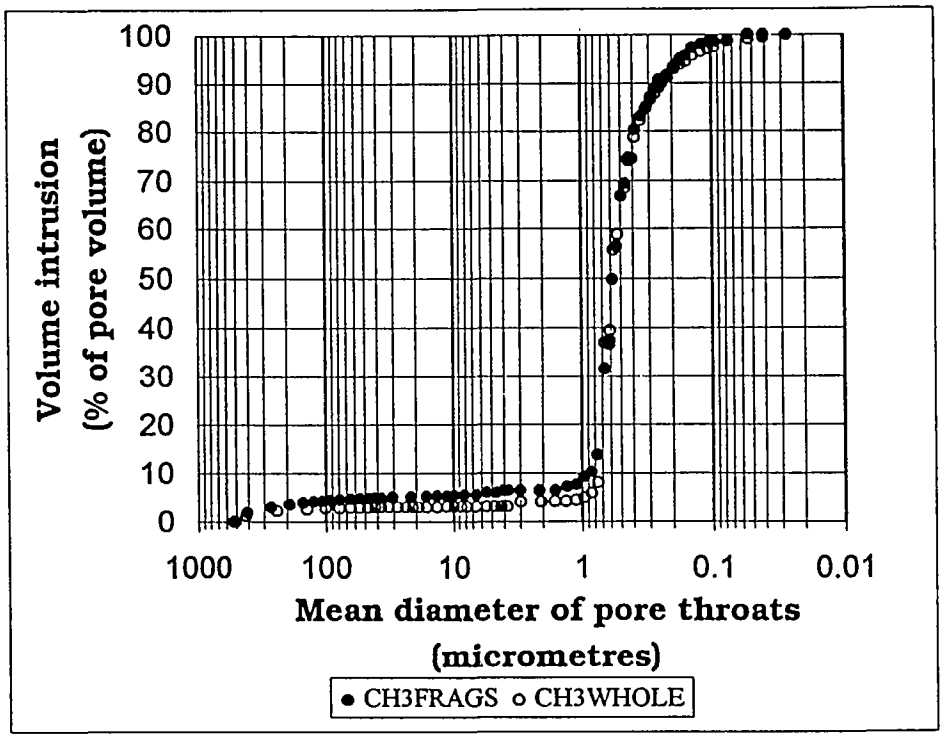

Figure 4.3 Mercury-intrusion capillary pressure curves for whole and fragmented samples of chalk from Cherry Hinton (sample CH3).

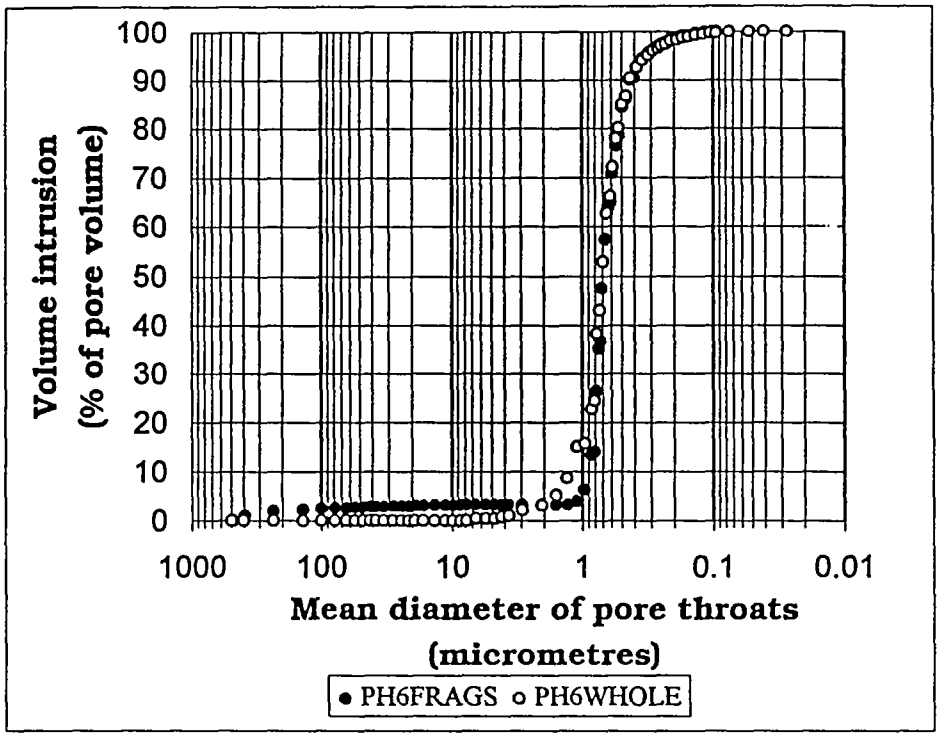

Figure 4.4 Mercury-intrusion capillary pressure curves for whole and fragmented samples of chalk from Play Hatch (sample PH6).

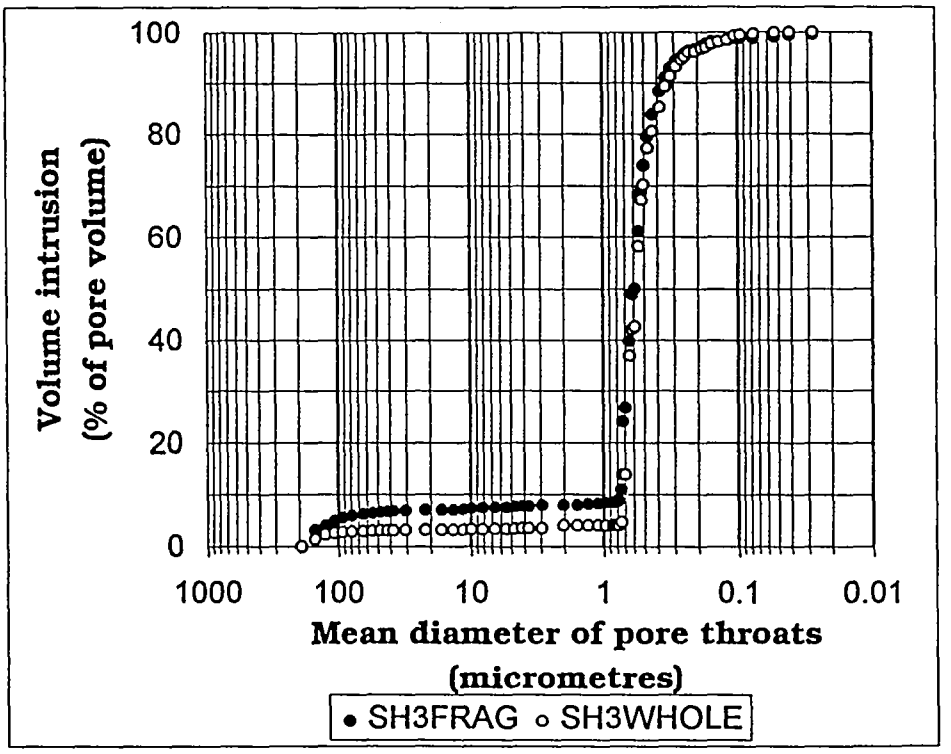

Figure 4.5 Mercury-intrusion capillary pressure curves for whole and fragmented samples of chalk from Shoreham Quarry (sample SH3).

5. ACOUSTIC MEASUREMENTS

5.1 Introduction

The acoustic studies are based on the work of Winkler and Plona (1982) and McCann and Sothcott (1992), who demonstrated that it is possible to measure the compressional and shear-wave velocities of rock samples at ultrasonic frequencies (0.85 MHz) and at confining pressures up to 60 MPa with an accuracy of +/- 0.3%. They also showed that the inelastic loss (attenuation) of energy through the rock could be measured simultaneously with an accuracy of +/- 0.1 dB/cm. The inelastic attenuation of a seismic wave propagating through a material is defined by the attenuation coefficient α, the reduction in amplitude per unit distance. As α is experimentally observed to be approximately proportional to frequency, it is convenient to express the transmission properties of the material in terms of the seismic quality factor, Q, which is approximately independent of frequency. Q is related to α by:

$$Q = (\pi f)/(\alpha(f)V(f)) \qquad (5.1)$$

where: Q is the quality factor

f is the measurement frequency

$\alpha(f)$ is the measured attenuation coefficient at frequency f

V(f) is the measured seismic velocity at frequency f

Peacock *et al.* (1994a, 1994b) showed that the variations of velocity and attenuation of each rock sample with confining pressure were related to the concentration of cracks or microfractures within the rock fabric. Figure 5.1 shows the increase of compressional-wave velocity and shear-wave velocity, and Figure 5.2 the increase of compressional-wave quality factor (see note below) and shear-wave quality factor with pressure for a vacuum dry sample of a fine grained sandstone.

Peacock *et al.* (1994a, 1994b) derived relationships between the differential high and low pressure velocity/attenuation values with the crack density. Measurements of the compressional-wave velocity and shear-wave velocity, and of the quality factor, of rock samples as a function of pressure enable the degree of microfracturing within the fabric to be determined.

5.2 Sample preparation

Cores of 50 mm diameter were drilled from blocks of chalk from Shoreham Quarry, Play Hatch Quarry and Cherry Hinton. Samples of each rock of about 20 mm in length were cut from these cores and end faces, flat and parallel to better than +/- 0.005 mm, were cut on a milling machine. The samples were evacuated to a residual pressure of 0.1 MPa and stored in an oven at a constant temperature of 40°C. Experience has shown that samples of relatively weak rocks such as chalk tend to disintegrate during the saturation and acoustic measurement process, whereas the oven dry samples are more robust. As it had been established by Peacock *et al.* (1994a, 1994b) that the density of microfractures was related to the pressure dependence

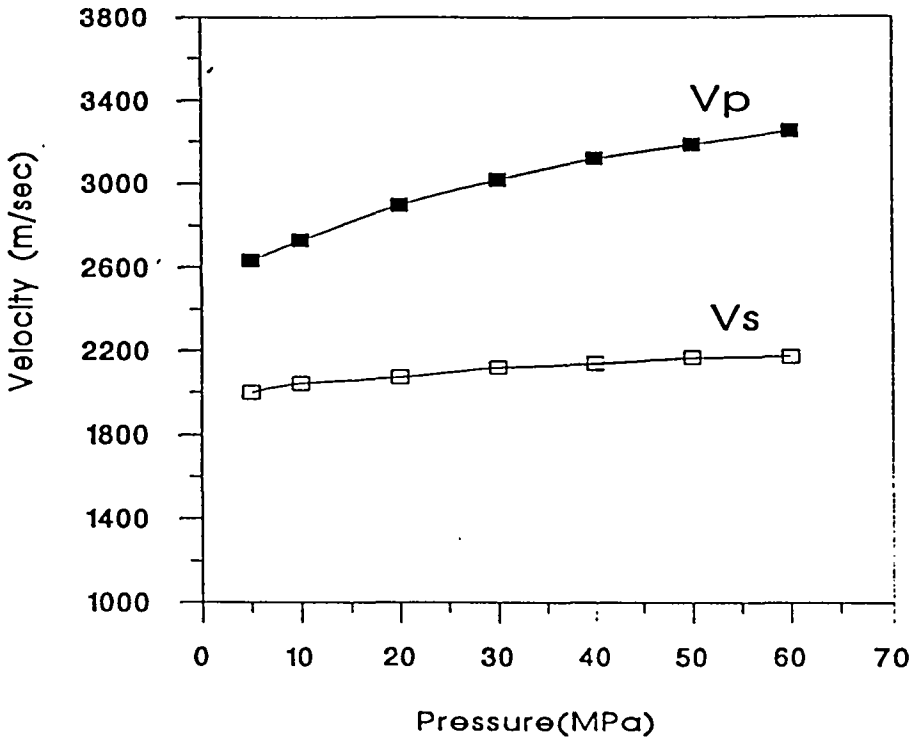

Figure 5.1 Compressional (Vp) and shear (Vs) wave velocities versus pressure for vacuum-dry sandstone

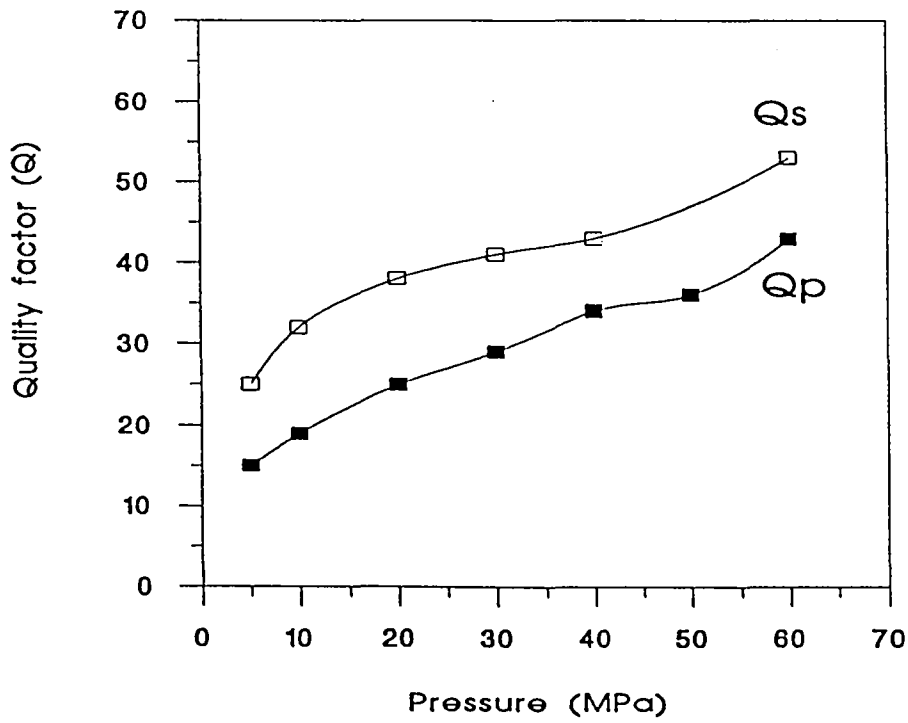

Figure 5.2 Compressional (Qp) and shear (Qs) wave quality factors versus pressure for vacuum-dry sandstone

of the velocity and quality factor of both dry and saturated samples, it was decided to undertake the ultrasonic measurements on dry samples of the chalks.

5.3 Ultrasonic measurements

Compressional- and shear-wave velocities and attenuations were measured at confining pressures of 5 MPa, 10 MPa, 15 MPa, 20 MPa, 30 MPa, 40 MPa, 50 MPa and 60 MPa. The seismic measurements were carried out using the reflection technique described by Winkler and Plona (1982), Klimentos and McCann (1990) and McCann and Sothcott (1992). The equipment is illustrated schematically in Figure 5.3. The sample is sandwiched between two perspex buffer rods. A dual compressional-wave/shear-wave transducer is mounted on the top buffer rod and protected with a stainless-steel housing. The buffer rod/sample/housing system is confined by an oil-proof rubber jacket constrained by O-rings inside a Wykeham Farrance hydraulic pressure cell. A hydraulic ram penetrates through the pressure cell from the top.

Figure 5.4 shows the chalk sample (diameter 50 mm) being mounted on the lower buffer rod within the pressure cell. Figure 5.5 shows the completed measurement system awaiting the mounting of the body of the pressure cell. The dual compressional/shear-wave transducer is mounted on the top buffer rod inside the stainless-steel pressure housing. The electrical leads running through are also visible. Figure 5.6 shows the base plate about to be raised up to the pressure cell body. Visible in this photograph is the vernier gauge which is used to measure the movement of the hydraulic ram, which is in contact with the top of the stainless steel transducer housing. As the confining pressure is increased the length of the sample decreases. By placing the ram in contact with the top of the transducer housing the exact position of the housing can be measured with the vernier gauge, and the decrease in the length of the sample can be determined. Figure 5.7 shows the completed pressure cell, together with the hydraulic pumps and gauges, and in the foreground the digital oscilloscope used for making the ultrasonic measurements.

The ultrasonic measurements of velocity and quality factor are made as follows. A compressional- or shear-wave signal is transmitted through the buffer rod and is partially reflected at the interface between the rock and buffer rod. At each pressure the amplitude and travel time of the third peak of a single frequency pulsed sine wave (toneburst) are measured at a frequency of about 0.85 MHz. Comparison of the amplitudes and travel times of the signals reflected from the top and the base of the sample enables the quality factor and velocity of the sample to be deduced. Use of the toneburst enables the velocity to be measured with great accuracy from the phase delay between specified cycles of the two reflected signals (McCann and Sothcott, 1990). Figure 5.8 shows the compressional-wave and Figure 5.9 the shear-wave signals for sample SH1/1 at a confining pressure of 60 MPa. In each case the first toneburst signal is the reflection from the top of the chalk sample and the second signal is from the base of the sample. The data require correction for the diffraction effects of the transducers and for the impedance contrasts at the buffer rod/rock interface. The data given here have been corrected for transducer diffraction effects using the tables published by Benson and Kiyohara (1974). Impedance effects have been calculated from the measured velocities and densities of the rock samples and of the perspex buffer rods. The raw seismic data have been corrected for these effects using a spreadsheet designed by A. I. Best. Confidence limits estimated at 95% have been determined for the results using the calibration results of McCann and Sothcott (1992).

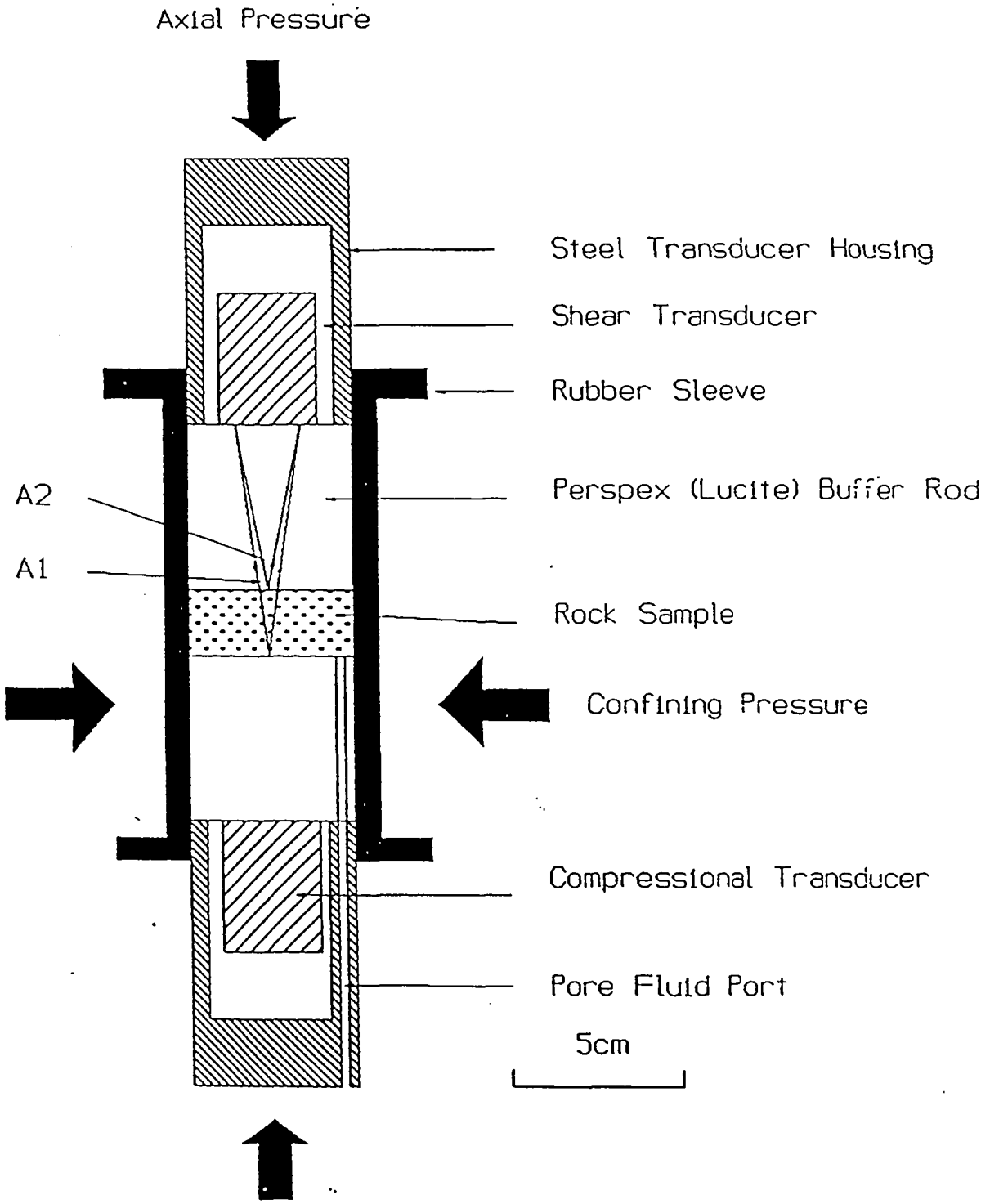

Figure 5.3 Schematic arrangement of the pulse reflection system

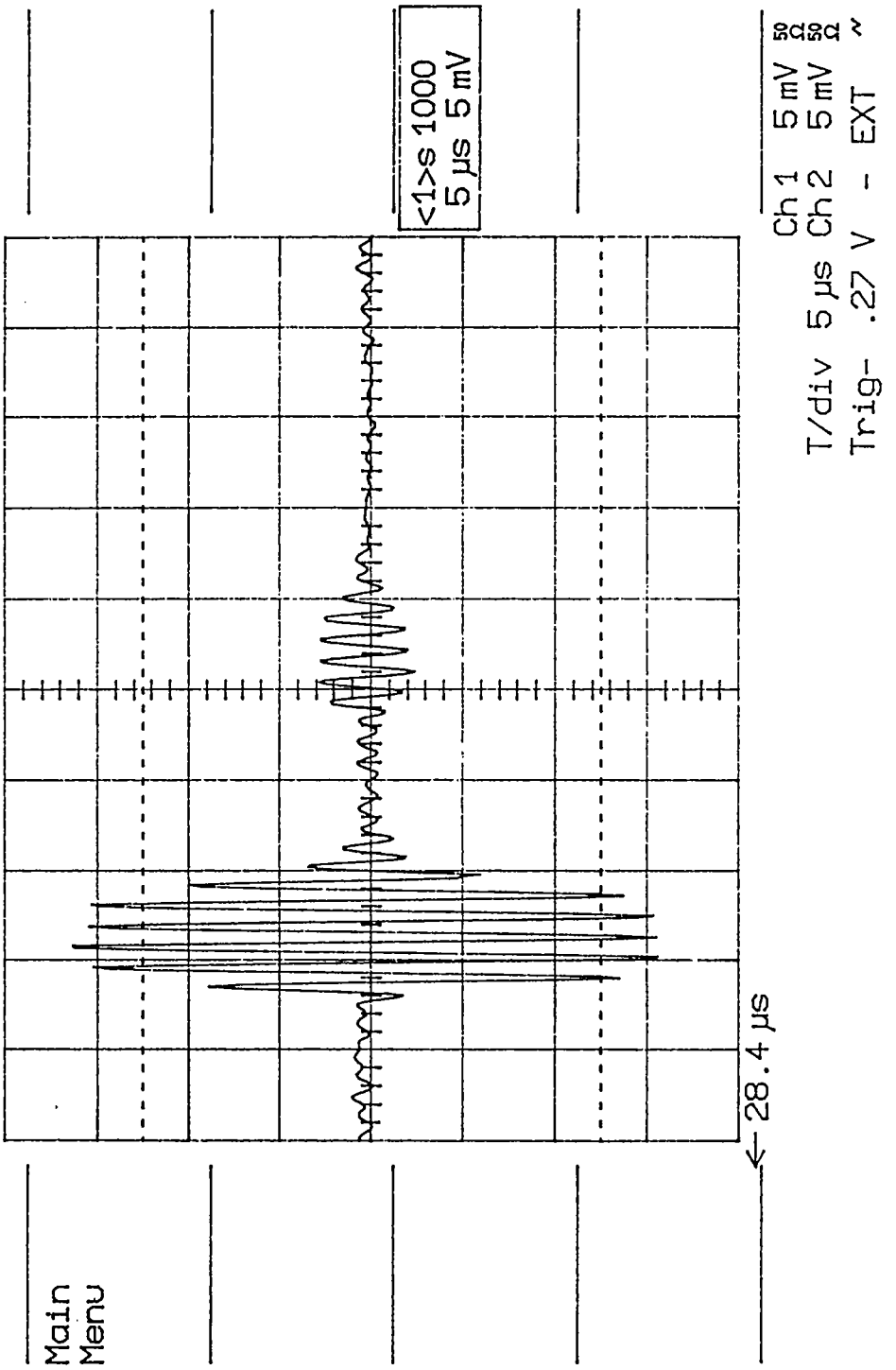

Figure 5.8 Compressional-wave reflections from the top (left) and bottom (right) of the chalk sample

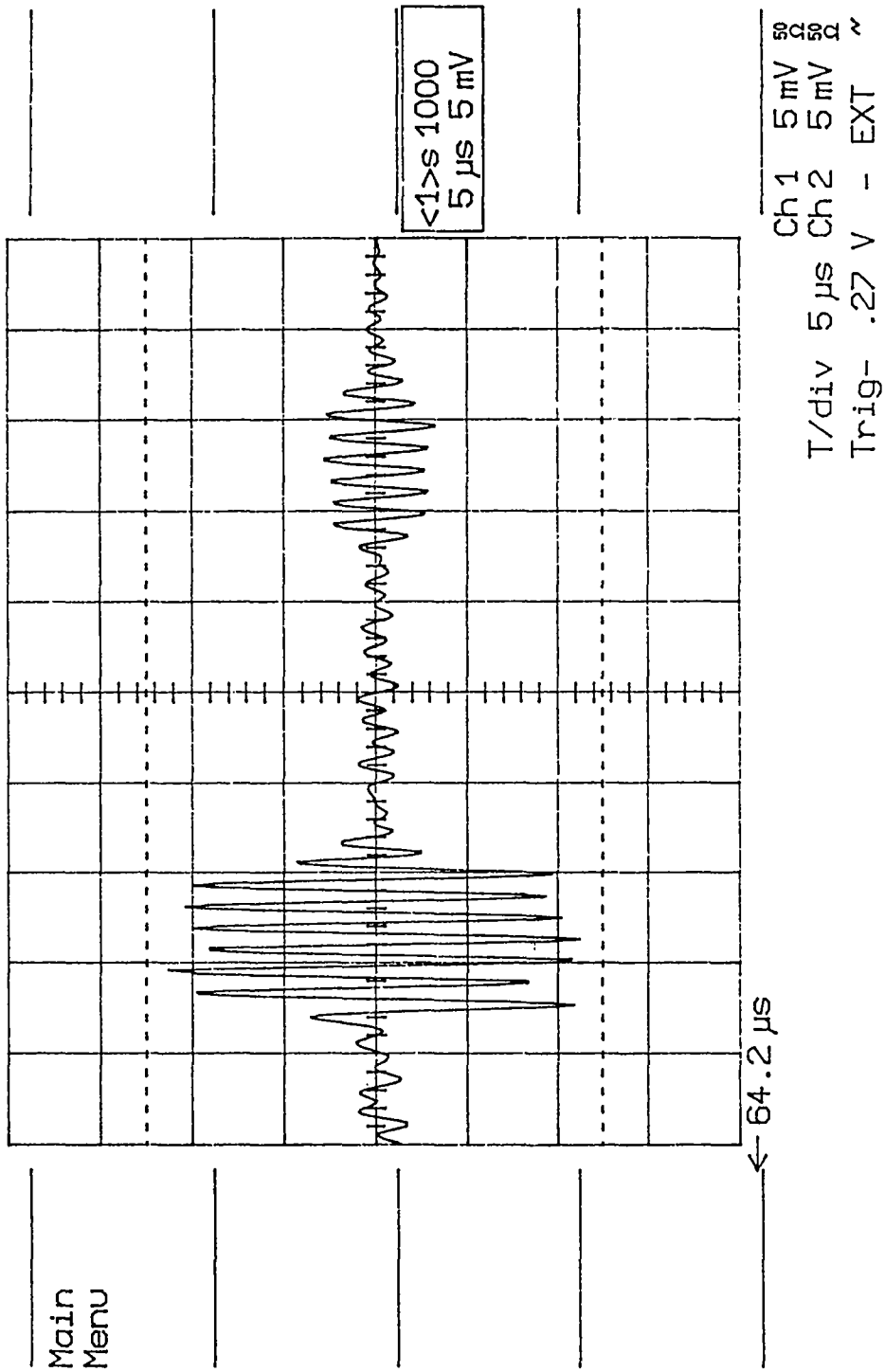

Figure 5.9 Shear-wave reflections from the top (left) and bottom (right) of the chalk sample

The seismic quality factors were computed from the attenuation coefficients of each sample using Equation 5.1.

5.4 Calibration measurements on the Wykeham Farrance pressure cell

In order to test the stability of the velocity measurements a sample of "Dural" was placed in the cell. Figures 5.10 and 5.11 show the compressional-wave and shear-wave velocities respectively of the Dural plotted against confining pressure. It should be noted that there is a small increase of both velocities with increasing confining pressure from 5 MPa to 10 MPa and that the velocities remain constant with further increase in confining pressure. The increase in the velocities at low pressure is an artefact of the system; the buffer rods are not in perfect welded contact with the sample at the lowest pressure. This will almost certainly not apply to the chalk samples. The Dural sample is very smooth and hard and it is much more difficult to attain the welded contact than with the soft chalk.

5.5 Sample shortening measurements

As explained above the Wykeham Farrance cell contains an adjustable hydraulic ram which enables the shortening of the sample to be measured. The perspex buffer rods also decrease significantly in length with increasing confining pressure, and this has to be separately measured to obtain the net decrease in the lengths of the samples. The overall shortening of the samples with increase in confining pressure are shown in Figures 5.12, 5.13, 5.14, 5.15, 5.16, 5.17, 5.18, 5.19 and 5.20. The point to be made about these data is that the chalk samples show decreases in length from room pressure to a confining pressure of 60 MPa of between 0.3 mm and 0.8 mm. Comparison of this magnitude of shortening over the same pressure range with that of an average sandstone, about 0.03 mm, demonstrates the significant irreversible effects on the chalk matrix of this large confining pressure.

5.6 Discussion of the ultrasonic results

All of the ultrasonic results are presented as combined graphs of the compressional and shear velocities of each sample versus confining pressure and the compressional- and shear-wave quality factors of each sample versus confining pressure. The following commentary describes the significance of the sets of data for each sample.

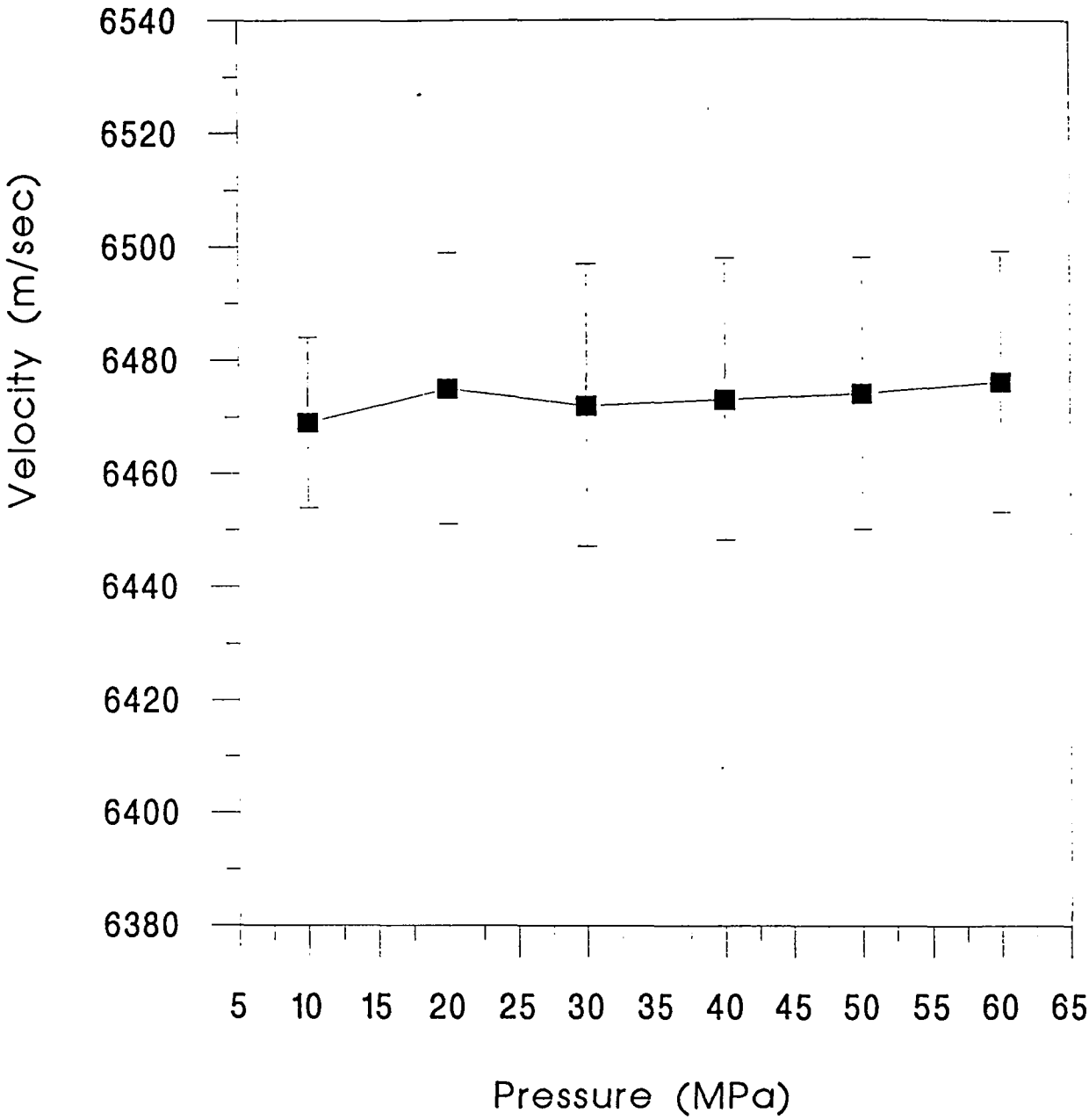

Figure 5.10 Compressional wave velocity of Dural versus confining pressure

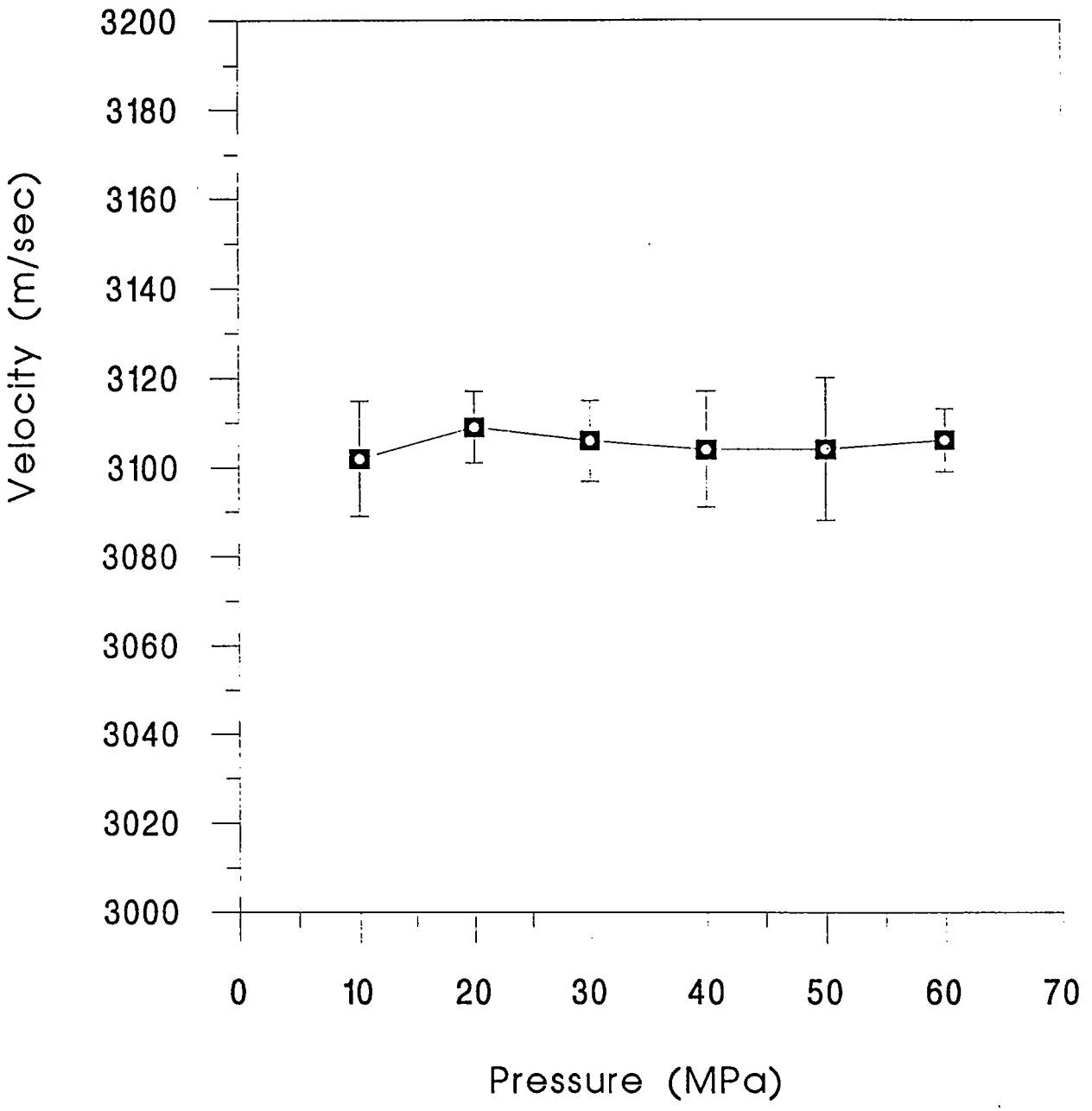

Figure 5.11 Shear wave velocity of Dural versus confining pressure

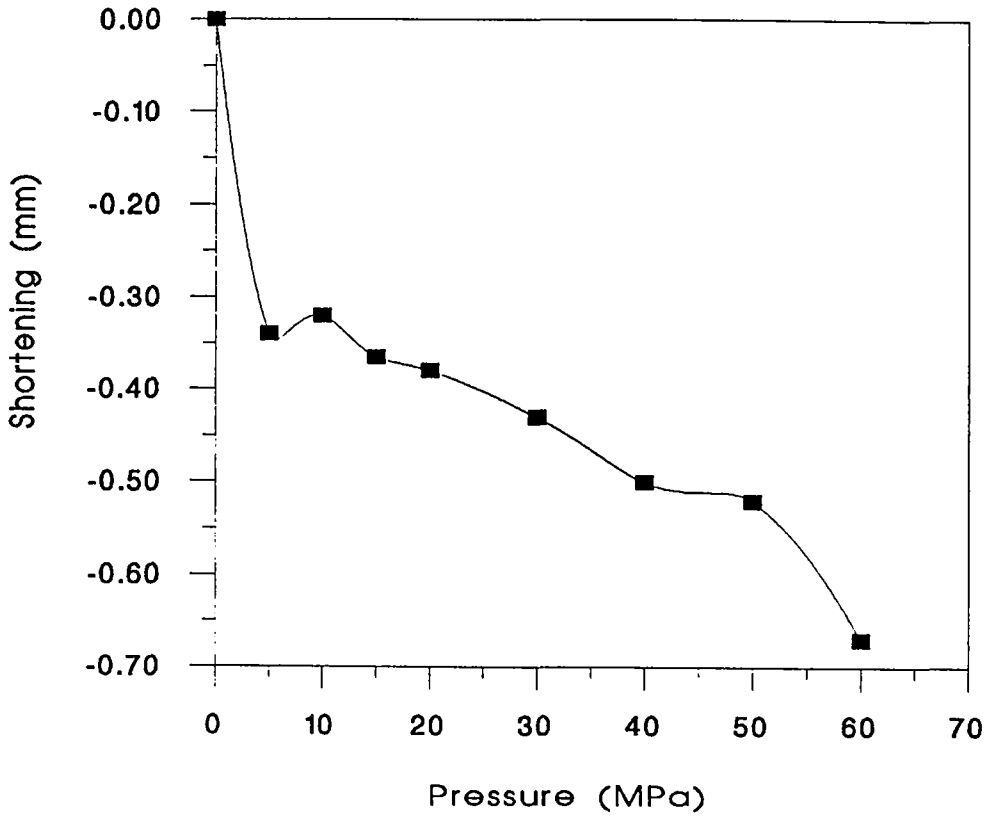

Figure 5.12 Sample shortening versus confining pressure for SH1/1

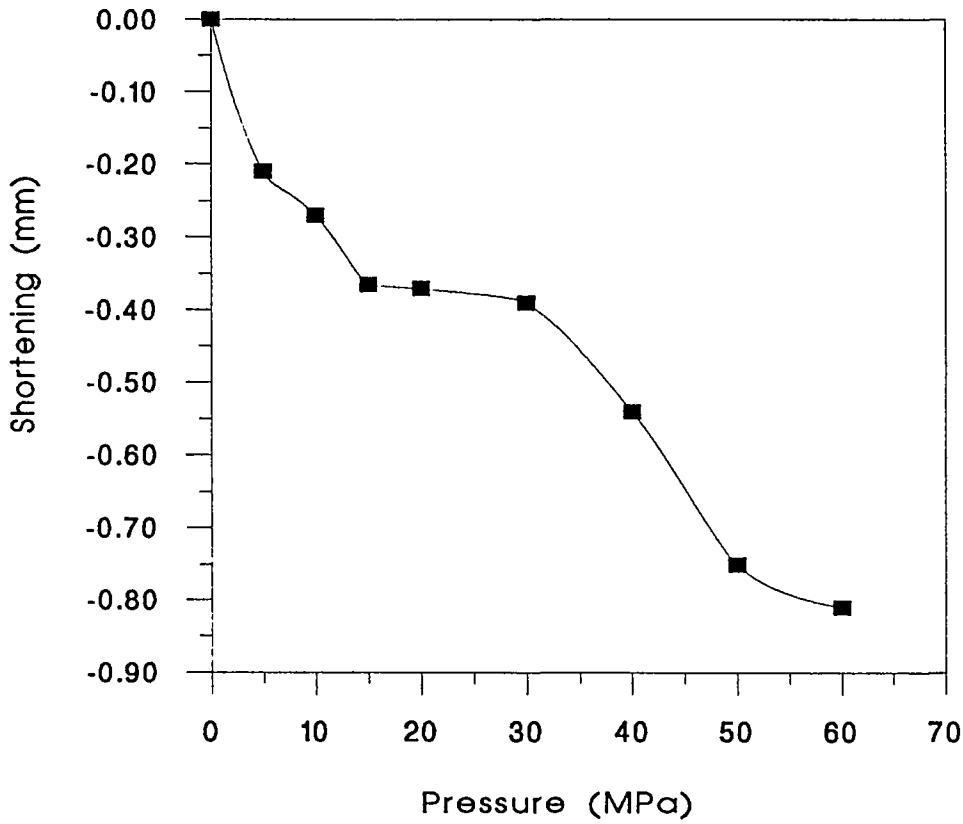

Figure 5.13 Sample shortening versus confining pressure for SH4/1

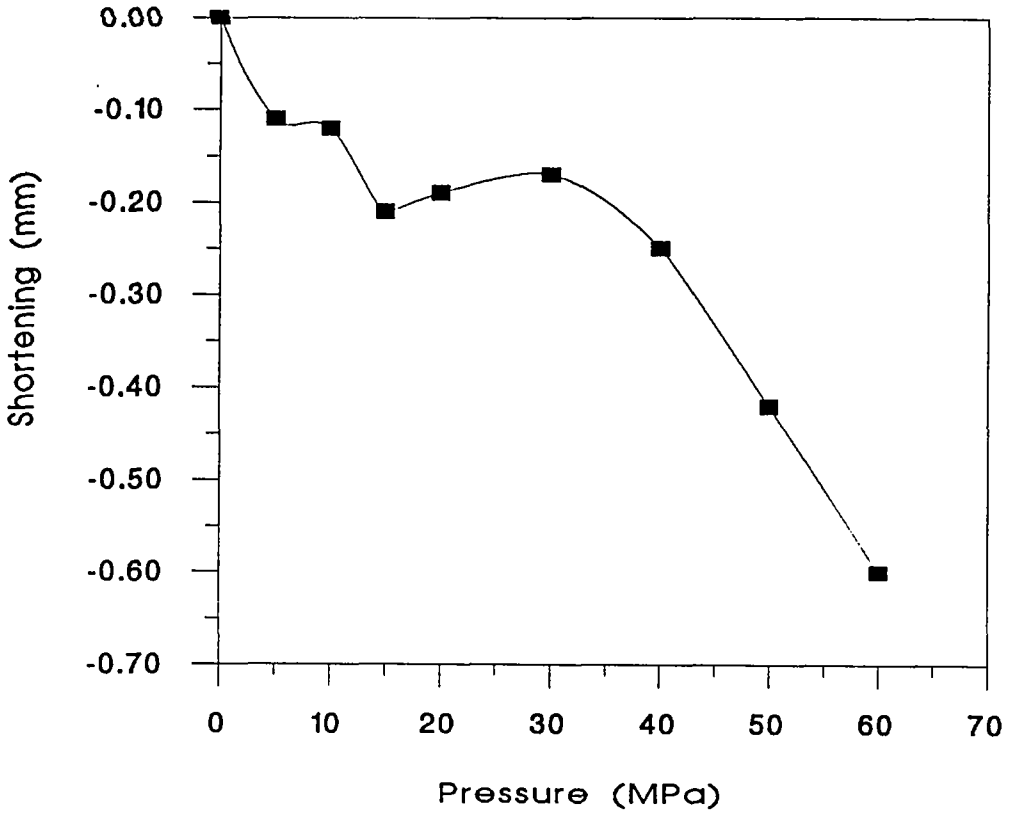

Figure 5.14 Sample shortening versus confining pressure for SH5/1

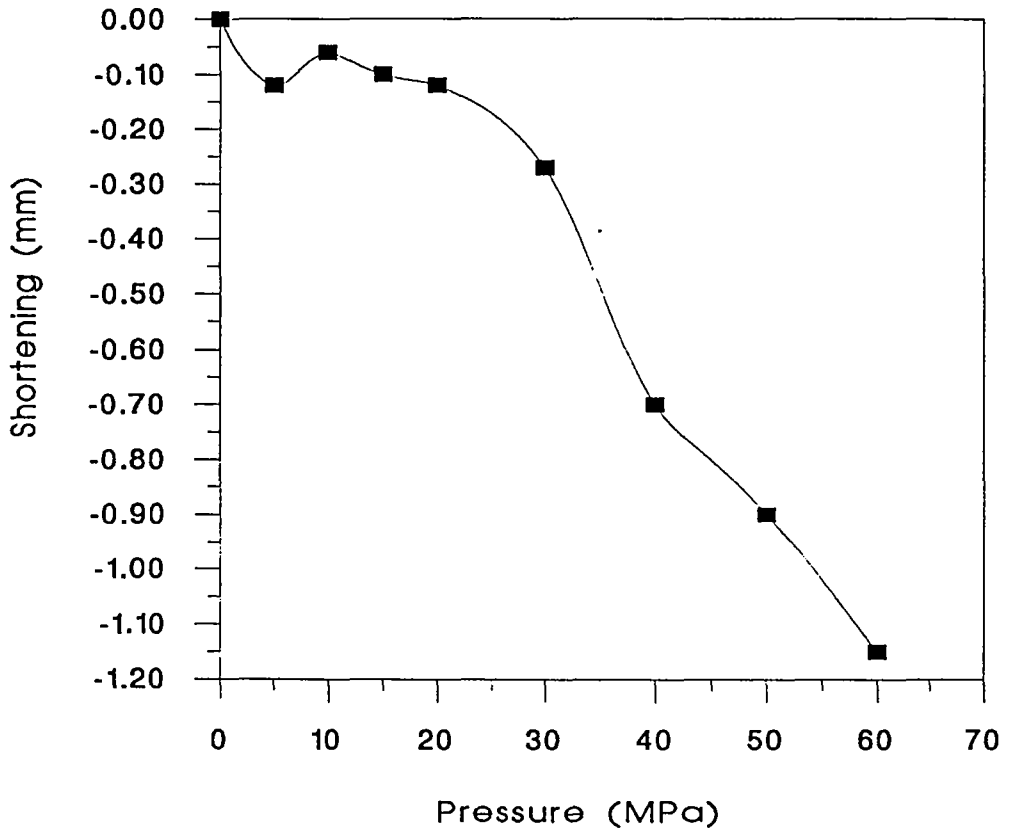

Figure 5.15 Sample shortening versus confining pressure for PH6/1

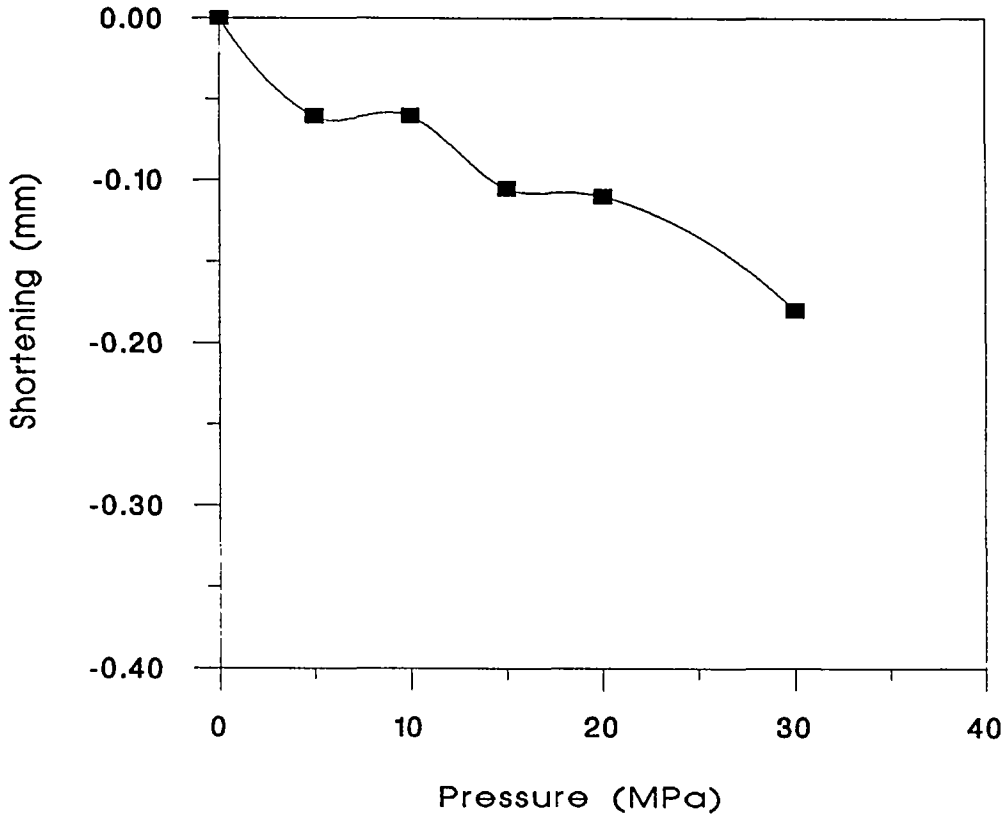

Figure 5.16 Sample shortening versus confining pressure for PH7/1

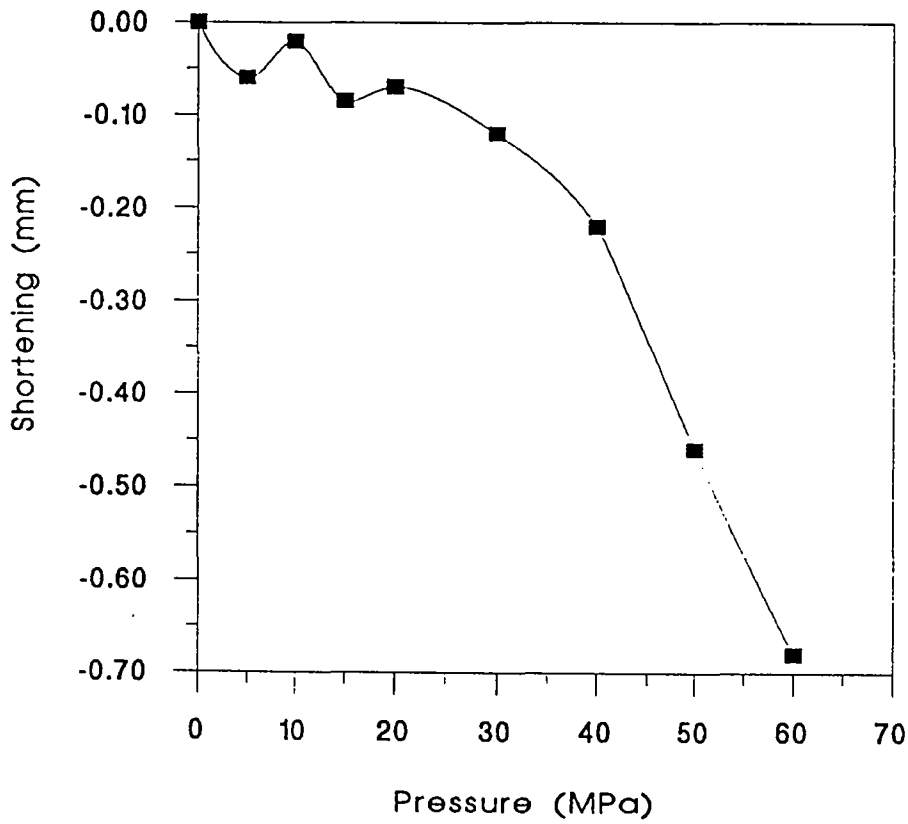

Figure 5.17 Sample shortening versus confining pressure for CH2/1

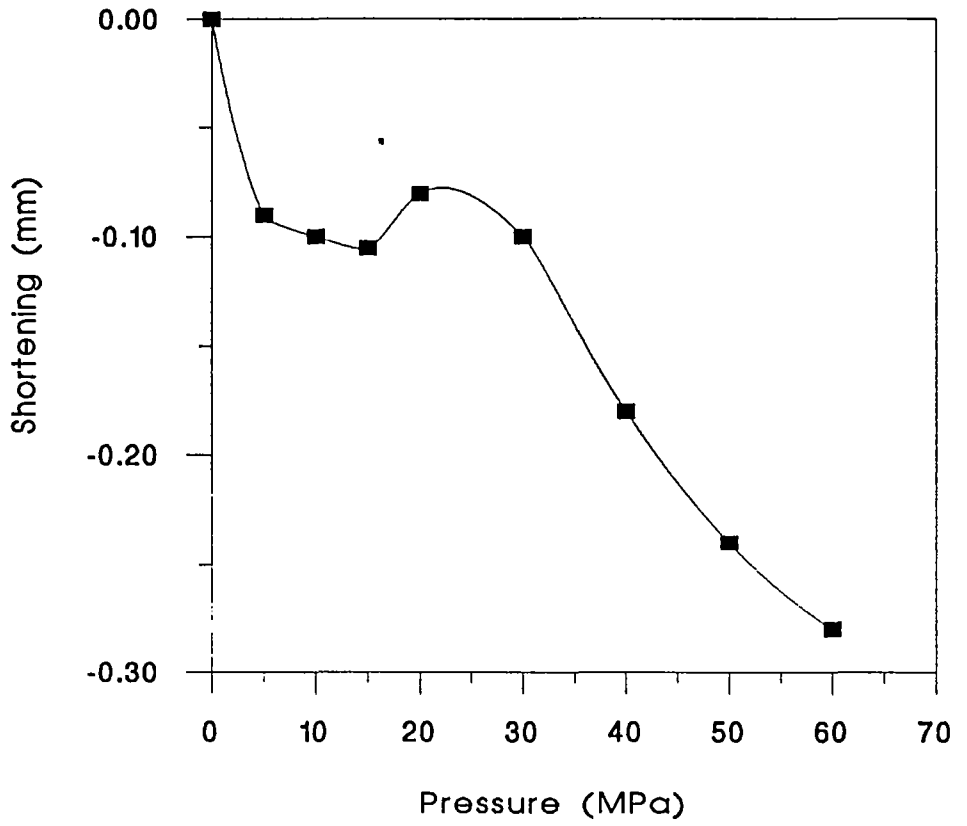

Figure 5.18 Sample shortening versus confining pressure for CH5/1

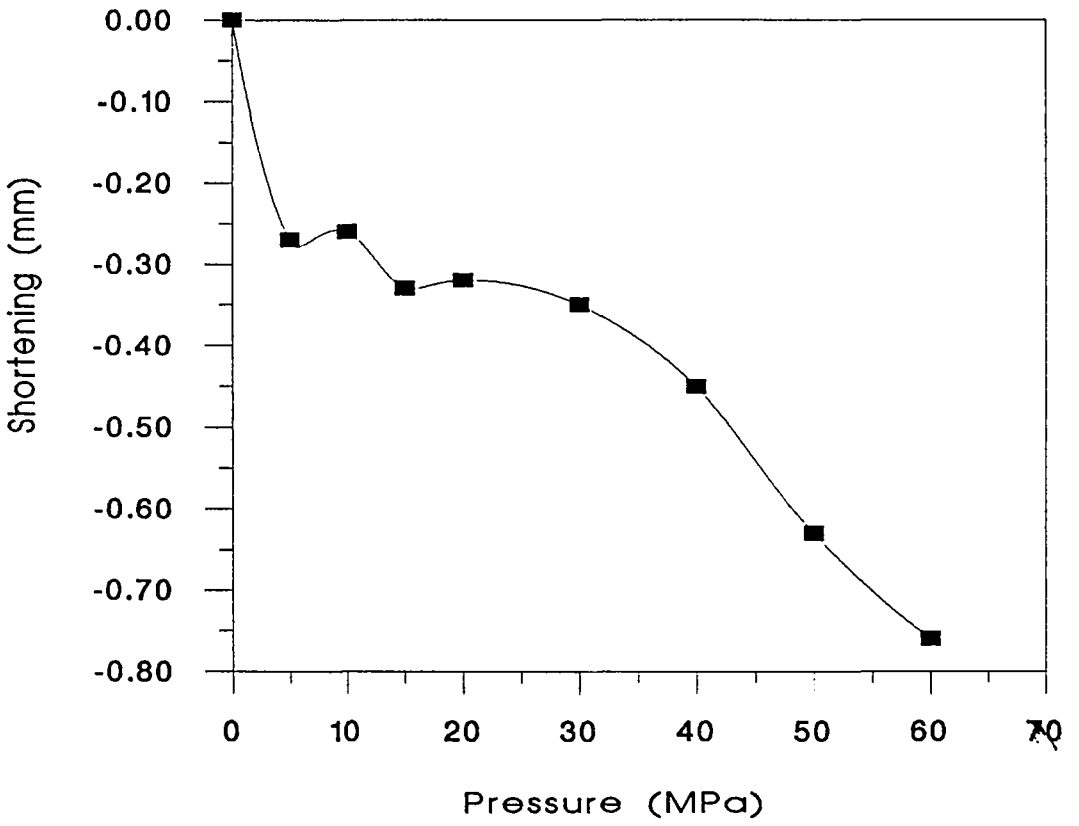

Figure 5.19 Sample shortening versus confining pressure for CH6/1

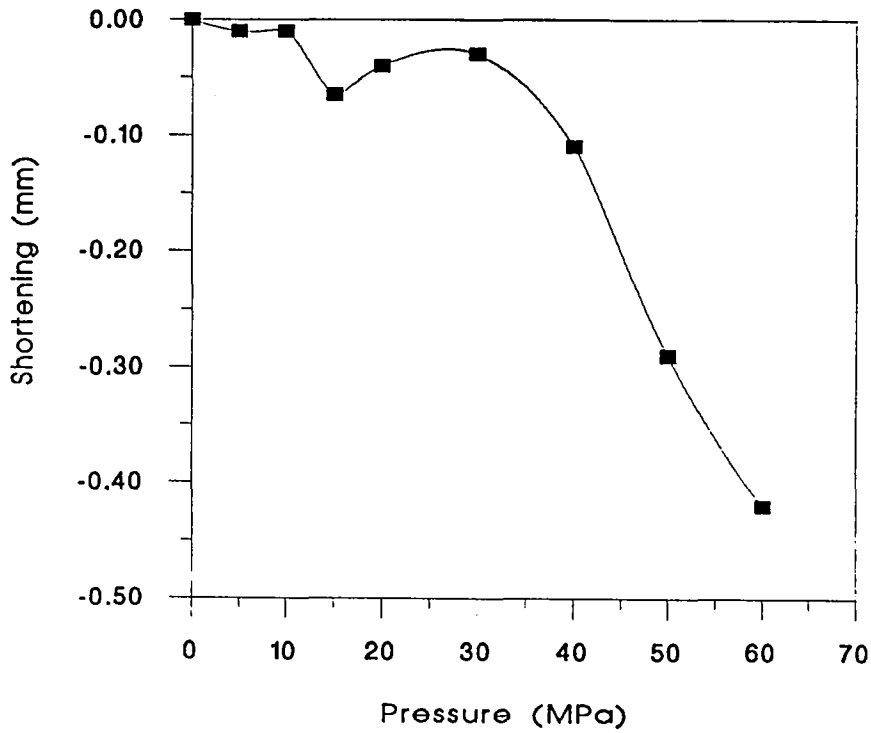

Figure 5.20 Sample shortening versus confining pressure for CH7/1

5.6.1 Shoreham Quarry samples

Figures 5.21a and 5.21b shows the velocity and quality factor data plotted as a function of confining pressure for Shoreham Quarry sample SH1/1. Figure 5.21a shows that both the compressional-wave velocity, Vp, and the shear-wave velocity, Vs, remain virtually constant with increasing confining pressure up to 20 MPa and then decrease to about 93% of their low pressure values at 60 MPa. Figure 5.21b shows that both the compressional-wave and shear-wave quality factor values decrease with increasing confining pressure.

Figures 5.22a and 5.22b show the velocity and quality factor data as a function of pressure for Shoreham Quarry sample SH4/1. The velocity data show similar low pressure behaviour to that of SH1/1. The shear-wave velocity shows a sudden increase in value at 30 MPa which is not matched by a similar increase in the compressional-wave velocity. After an initial increase in the compressional-wave quality factor with pressure between 5 MPa to 10 MPa, both the compressional- and shear-wave quality factors show similar behaviour to that of SH1/1.

Figures 5.23a and 5.23b show the velocity and quality factor data as a function of pressure for Shoreham Quarry sample SH5/1. The shear-wave quality factor of this sample decreased rapidly with increasing pressure such that no signal could be observed at confining pressures above 30 MPa. The shear-wave velocity decreased slightly with increasing pressure up to this point. The compressional-wave velocity decreased from its low pressure value up to a confining pressure of 40 MPa and then showed some instability. The compressional-wave quality factor showed dramatic instability throughout the pressure range and declined to a low value above 50 MPa.

Comparison of Figures 5.21a, 5.22a and 5.23a with Figure 5.1, and Figure 5.21b, 5.22b and 5.23b with Figure 5.2 shows that the acoustic properties of the Shoreham Quarry samples are not consistent with those of a microfractured rock. Figures 5.1 and 5.2 show that both the velocities and the quality factors of a microfractured rock increase with increasing confining pressure. The compressional- and shear-wave velocities show an initial rapid increase up to a confining pressure of about 40 MPa, followed by a continuing linear increase at higher pressures. The quality factors show an initial rapid increase to about 40 MPa to a plateau of constant value at higher pressures. Apart from some instabilities, the pattern of the acoustic behaviour of the Shoreham samples is of a decrease in both the velocities and the quality factors with increasing confining pressure. This behaviour suggests that the increasing confining pressure is generating new microfractures or pore collapse within an existing unfractured matrix. It is concluded that the Shoreham Quarry chalks contain no significant concentration of microfractures.

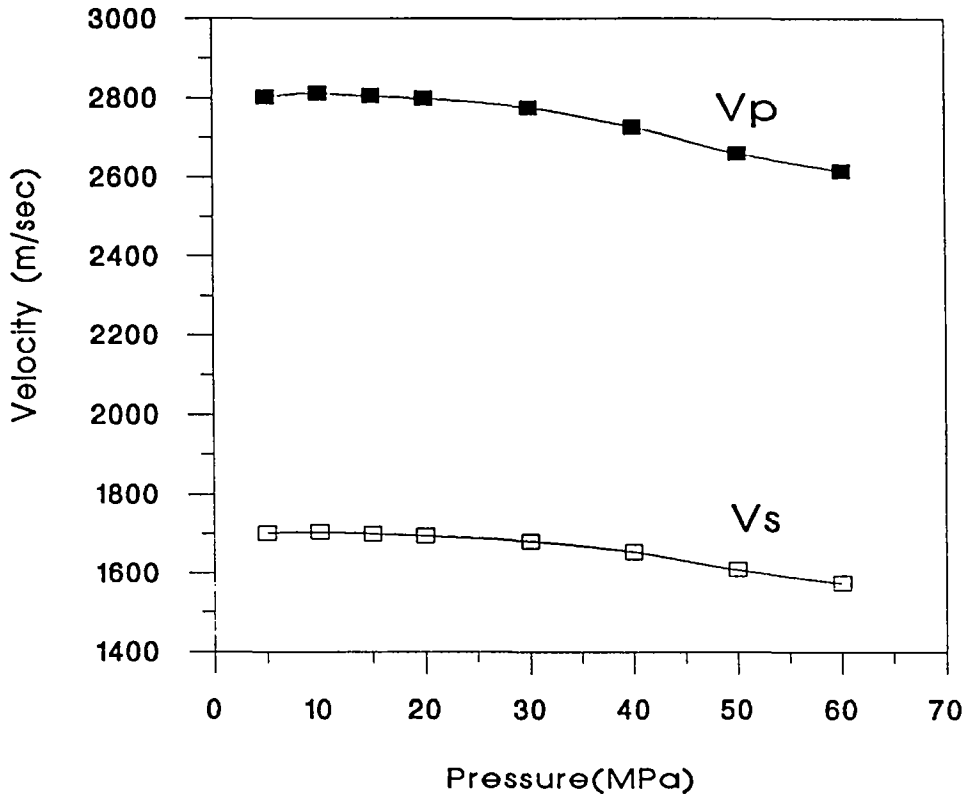

Figure 5.21a Compressional (Vp) and shear (Vs) velocities versus pressure for sample SH1/1

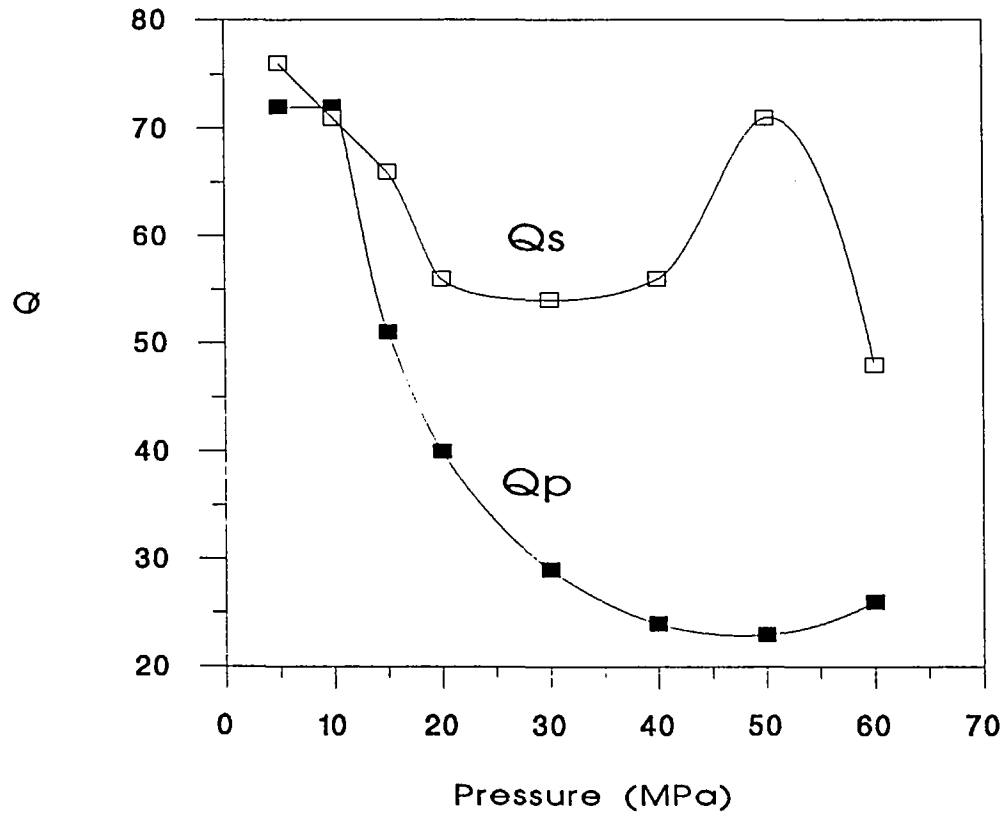

Figure 5.21b Compressional (Qp) and shear (Qs) quality factors versus pressure for sample SH1/1

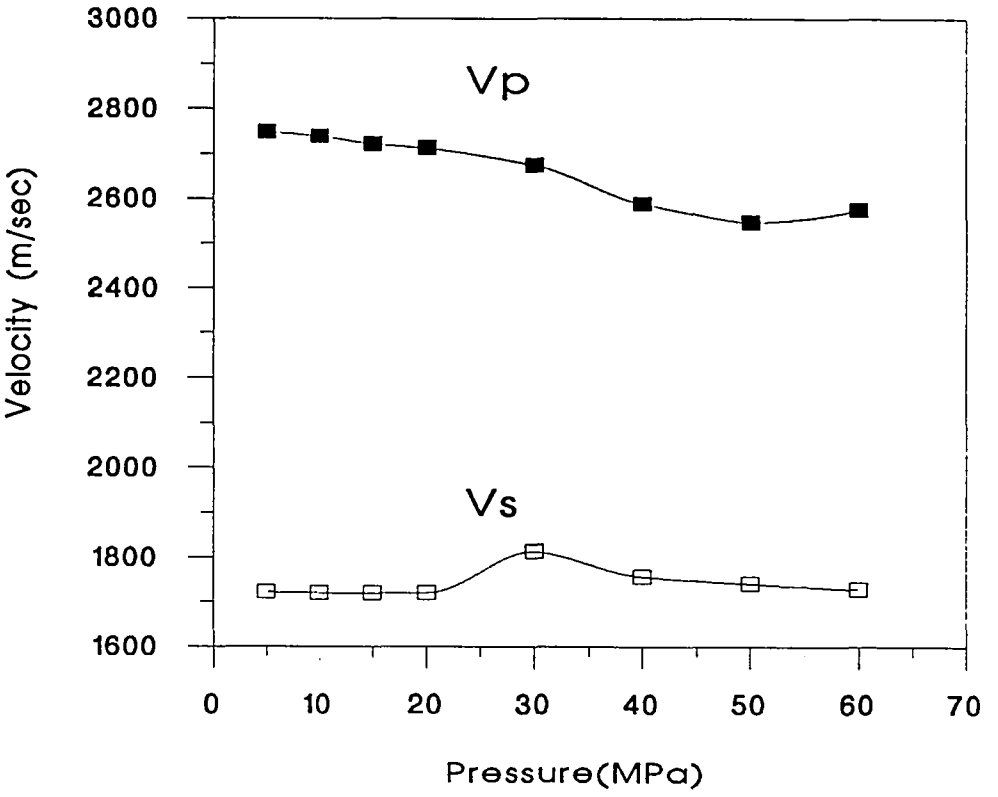

Figure 5.22a Compressional (Vp) and shear (Vs) velocities versus pressure for sample SH4/1

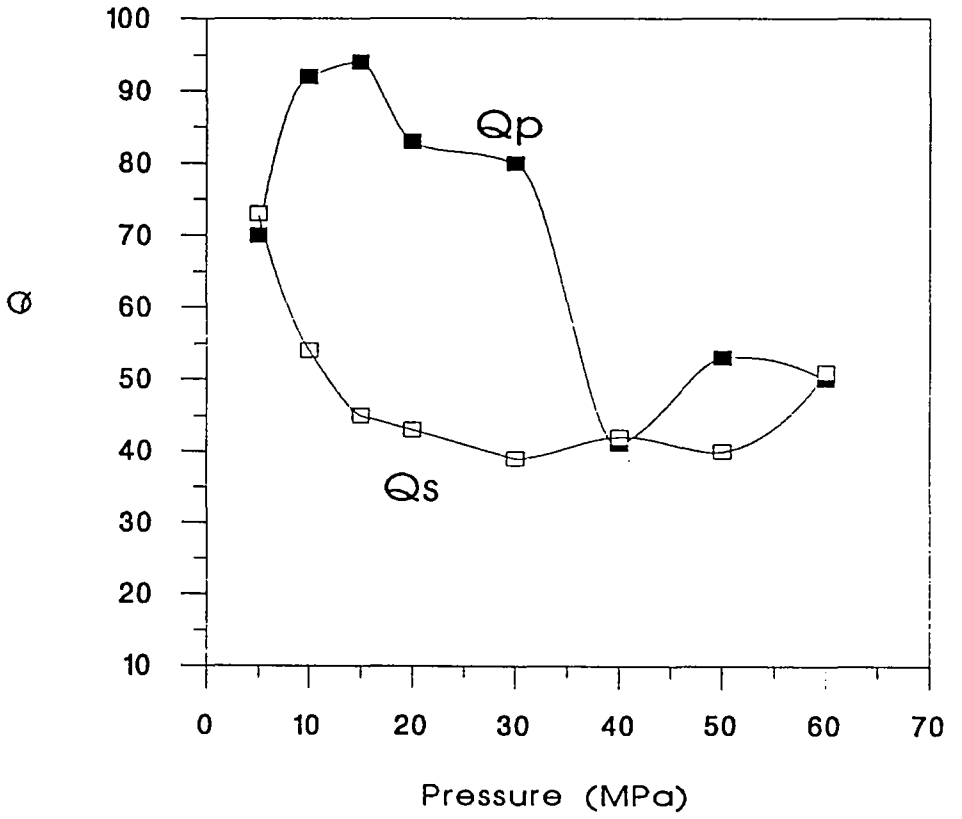

Figure 5.22b Compressional (Qp) and shear (Qs) quality factors versus pressure for sample SH4/1

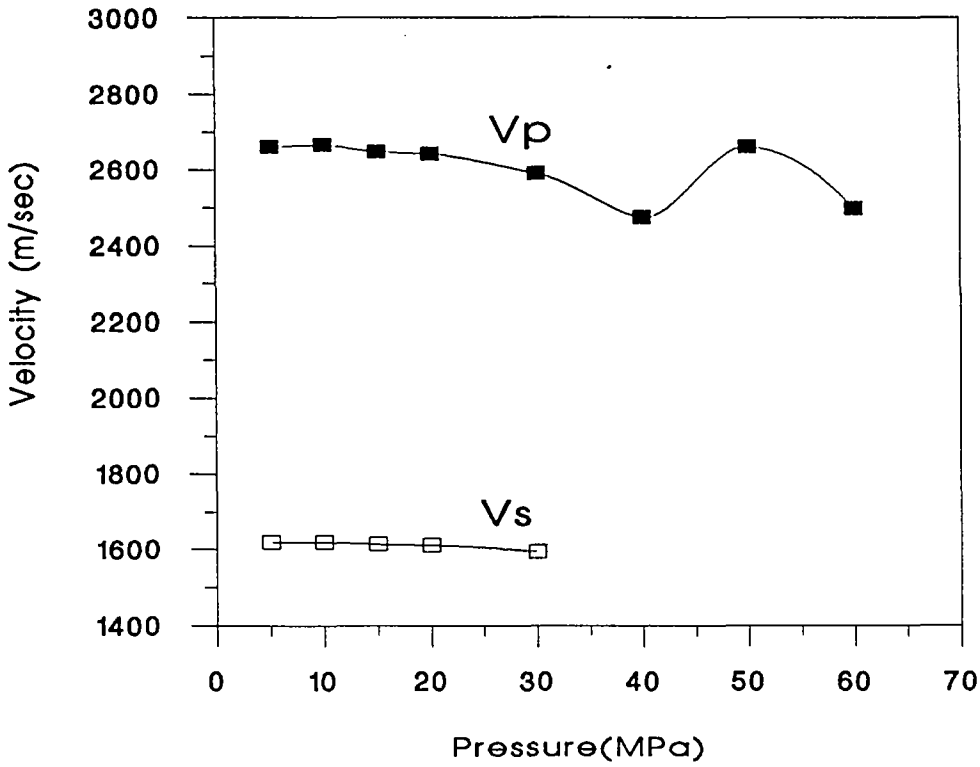

Figure 5.23a Compressional (Vp) and shear (Vs) velocities versus pressure for sample SH5/1

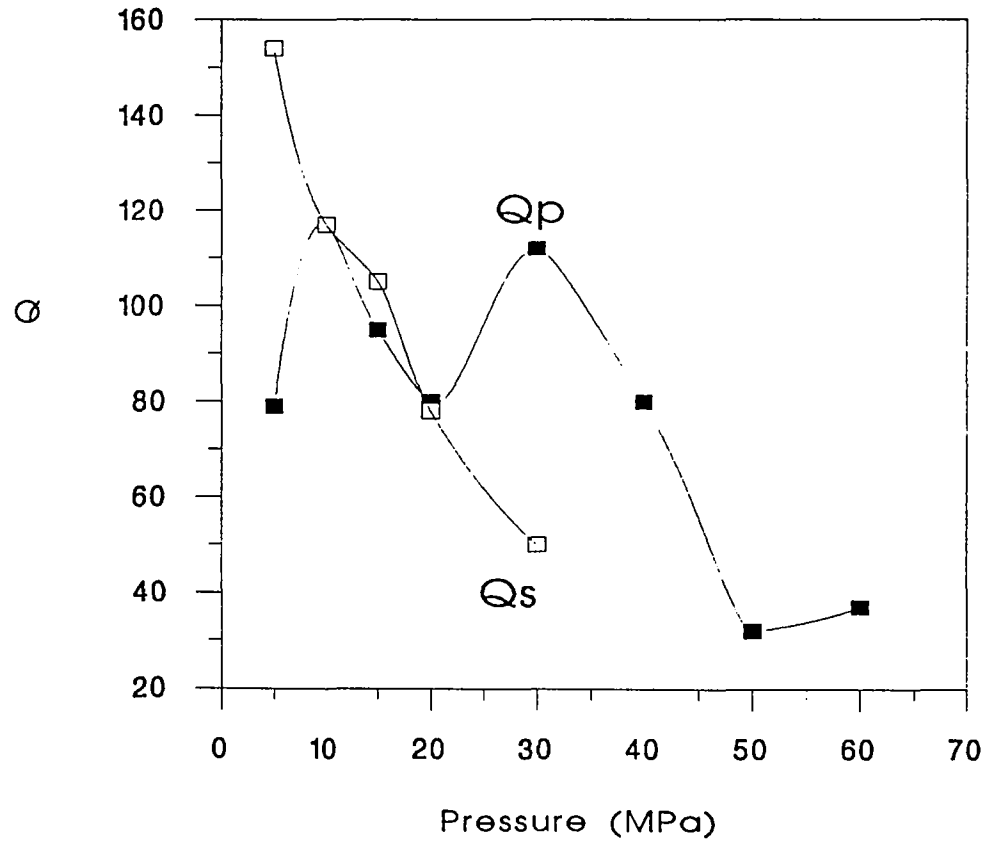

Figure 5.23b Compressional (Qp) and shear (Qs) quality factors versus pressure for sample SH5/1

5.6.2 Play Hatch Quarry samples

Figures 5.24a and 5.24b shows the velocity and quality factor data plotted as a function of confining pressure for Play Hatch sample PH6/1. The decrease in shear-wave quality factor with increasing pressure caused the signal to disappear above 20 MPa confining pressure. Figure 5.24a shows that both the compressional-wave velocity, Vp, and the shear-wave velocity, Vs, are virtually constant with increasing confining pressure. Figure 5.24b shows that both the compressional- and shear-wave quality factor values increase initially from 5 MPa to 10 MPa confining pressure and then decrease with further increase in confining pressure.

Figures 5.25a and 5.25b show the velocity and quality factor data as a function of pressure for Play Hatch Quarry sample PH7/1. No signals were detectable at a confining pressure greater than 20 MPa. Figure 5.25a shows that the compressional-wave velocity increases between a confining pressure of 5 MPa and 10 MPa; no similar increase is observed in the shear-wave velocity. Figure 5.25b shows the compressional-wave quality factor increasing with increasing confining pressure; the shear-wave quality factor is almost constant. The disappearance of the compressional- and shear-wave signals at confining pressures greater than 20 MPa indicates very low quality factors at high confining pressures.

Comparison of Figures 5.24a and 5.25a with Figure 5.1, and Figure 5.24b and 5.25b with Figure 5.2 shows that the acoustic properties of the Play Hatch Quarry samples are not consistent with those of a microfractured rock. As previously discussed in connection with the Shoreham Quarry samples, Figures 5.1 and 5.2 show that both the velocities and the quality factors of a microfractured rock increase with increasing confining pressure. The general pattern of the acoustic behaviour of the Play Hatch samples does not conform to this steady increase in both the velocities and the quality factors with increasing confining pressure. Although there is some instability the general behaviour of the Play Hatch samples is similar to that of the Shoreham samples, suggesting that the increasing confining pressure is generating new microfractures or pore collapse within an existing unfractured matrix. It is concluded that there is no significant evidence for an existing concentration of micro fractures within the Play Hatch chalk samples.

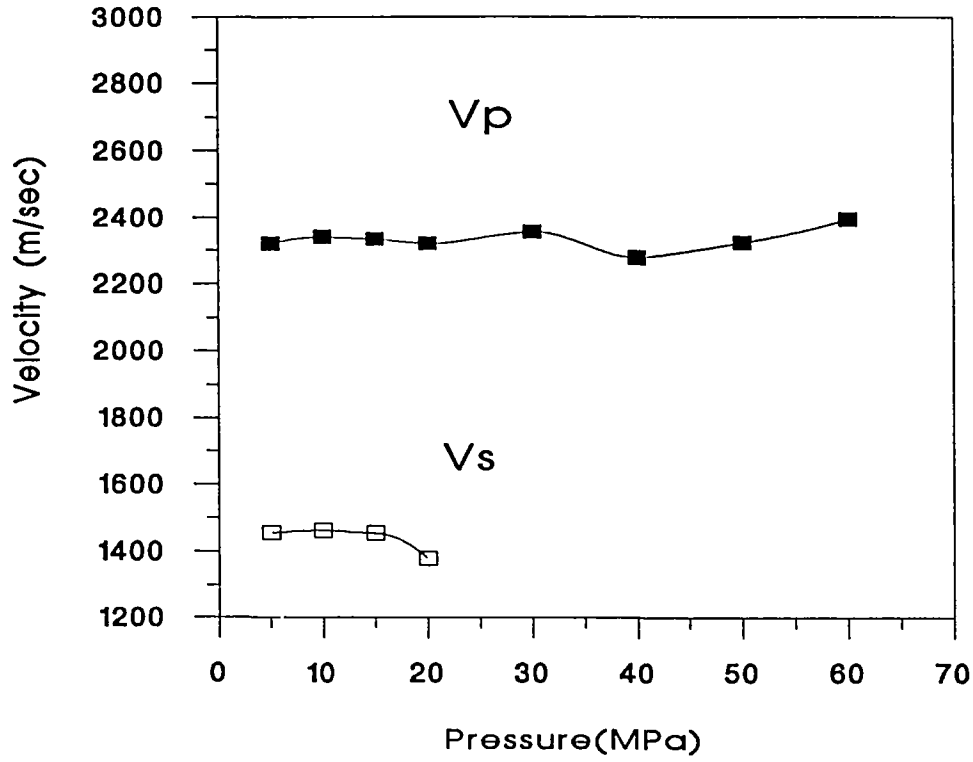

Figure 5.24a Compressional (Vp) and shear (Vs) velocities versus pressure for sample PH6/1

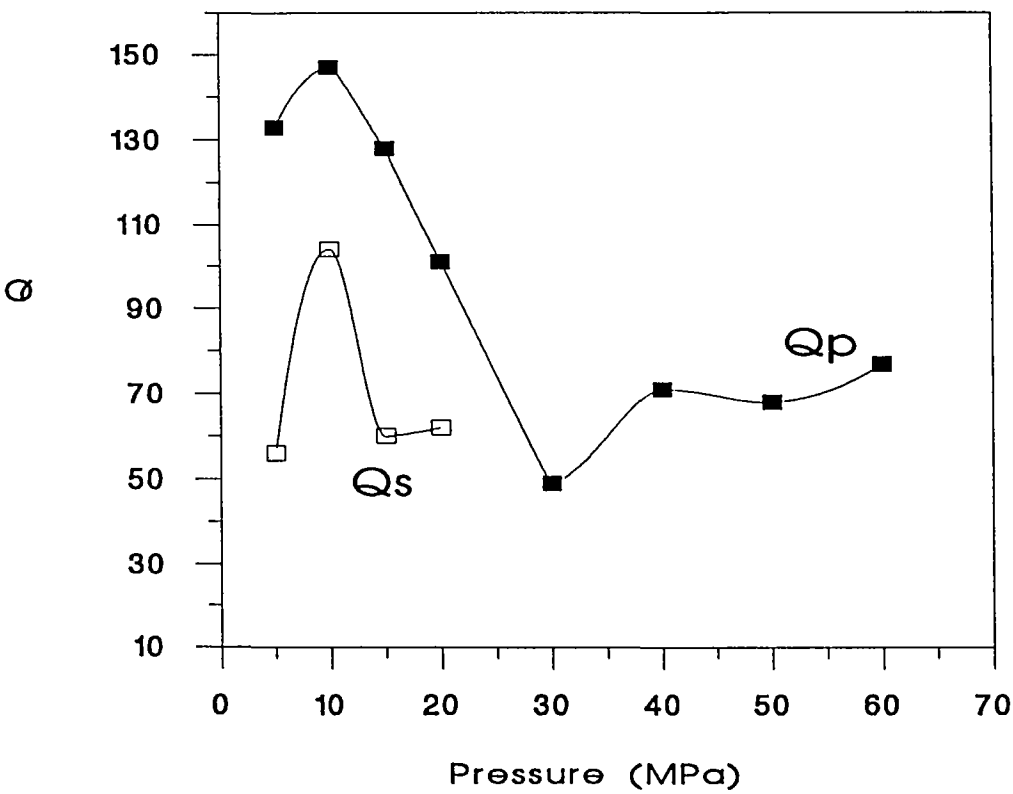

Figure 5.24b Compressional (Qp) and shear (Qs) quality factors versus pressure for sample PH6/1

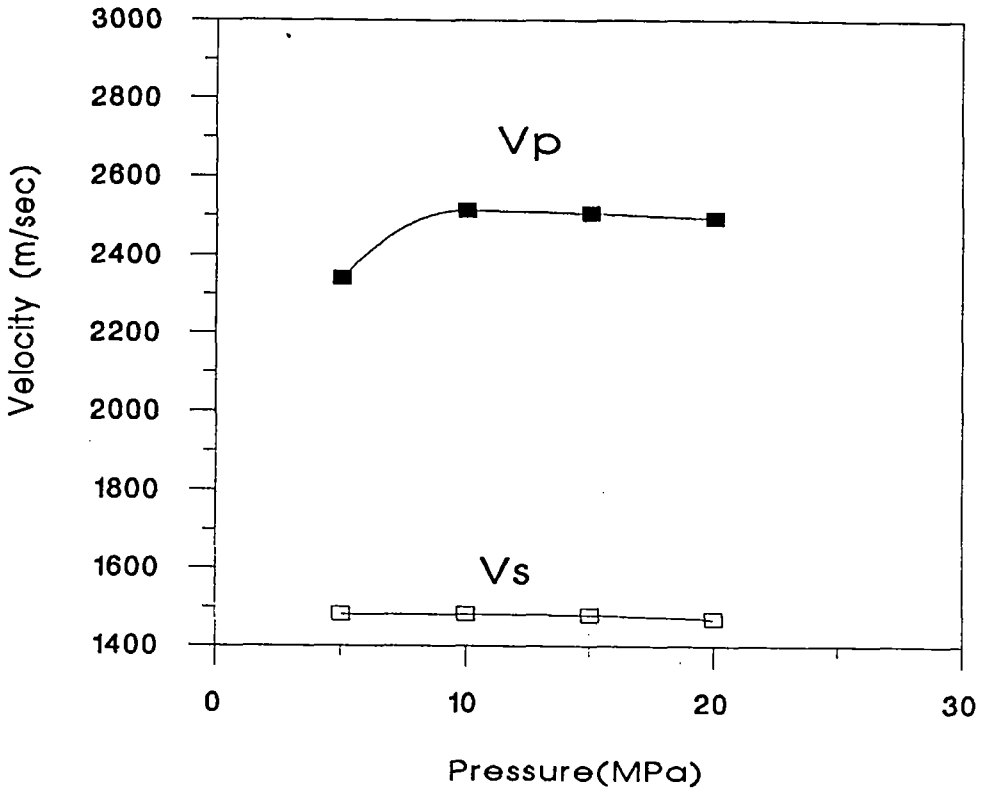

Figure 5.25a Compressional (Vp) and shear (Vs) velocities versus pressure for sample PH7/1

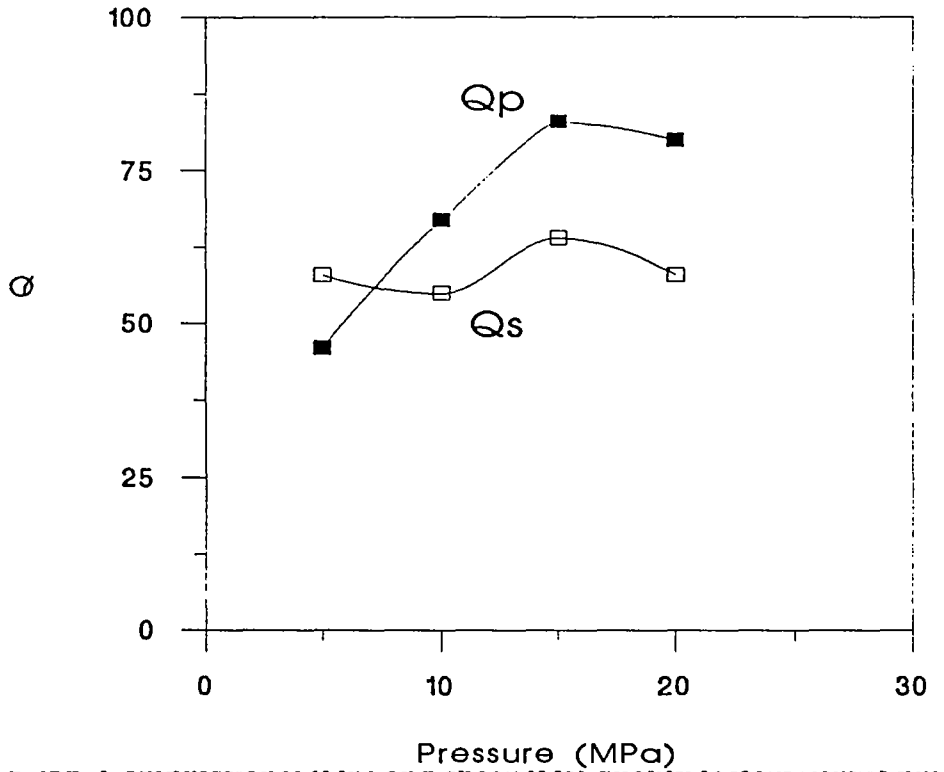

Figure 5.25b Compressional (Qp) and shear (Qs) quality factors versus pressure for sample PH7/1

5.6.3 Cherry Hinton samples

Figures 5.26a and 5.26b show the velocity and quality factor data plotted as a function of confining pressure for Cherry Hinton sample CH2/1. Figure 5.26a shows that both the compressional-wave velocity, Vp, and the shear-wave velocity, Vs, remain virtually constant up to 20 MPa and then decrease with further increase of confining pressure. Figure 5.26b shows that, after an initial increase as the confining pressure is increased from 5 MPa to 10 MPa, both the compressional- and shear-wave quality factor values decrease with increasing confining pressure.

Figures 5.27a and 5.27b show the velocity and quality factor data as a function of pressure for Cherry Hinton sample CH5/1. No shear-wave signal was detectable at confining pressures above 5 MPa. Both the compressional-wave velocity and quality factor show a consistent increase in value as the confining pressure is increased from 5 MPa to 20 MPa. At greater confining pressures the velocity starts to decrease, whilst the quality factor remains roughly constant.

Figures 5.28a and 5.28b show the velocity and quality factor data as a function of pressure for Cherry Hinton sample CH6/1. No shear-wave signal was detectable at confining pressures above 20 MPa. Both the compressional-wave velocity and shear-wave velocity show consistent increases in value as the confining pressure is increased from 5 MPa to 20 MPa. At greater confining pressures the compressional velocity decreases slightly, then increases rapidly. The compressional-wave and shear-wave quality factors show an initial increase as the confining pressure is increased from 5 MPa.

Figures 5.29a and 5.29b show the velocity and quality factor data as a function of pressure for Cherry Hinton sample CH7/1. Both the compressional-wave and the shear-wave velocities increase as the confining pressure is increased from 5 MPa to 30 MPa, remaining roughly constant with further increase in confining pressure. The compressional-wave quality factor shows an initial rapid increase between 5 MPa and 15 MPa confining pressure, followed by a rapid decrease with further increase in confining pressure. The shear-wave quality factor is virtually independent of confining pressure.

Comparison of Figures 5.26a with Figure 5.1, and Figure 5.26b with Figure 5.2 shows that the acoustic properties of Cherry Hinton sample CH2/1 are not consistent with those of a microfractured rock. As with the Shoreham and Play Hatch samples the pattern of the acoustic behaviour of CH2/1 is of a decrease in both the velocities and the quality factors with increasing confining pressure. This behaviour suggests that the increasing confining pressure is generating new microfractures or pore collapse within an existing unfractured matrix. It is concluded that Cherry Hinton sample CH2/1 contains no significant concentration of microfractures.

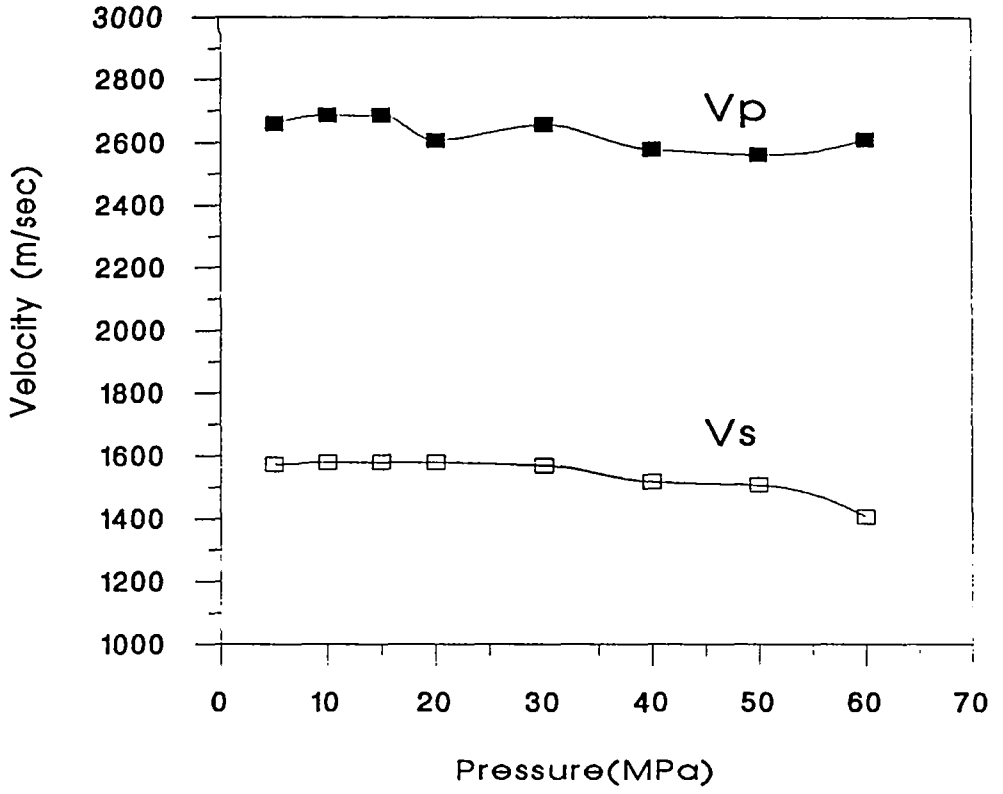

Figure 5.26a Compressional (Vp) and shear (Vs) velocities versus pressure for sample CH2/1

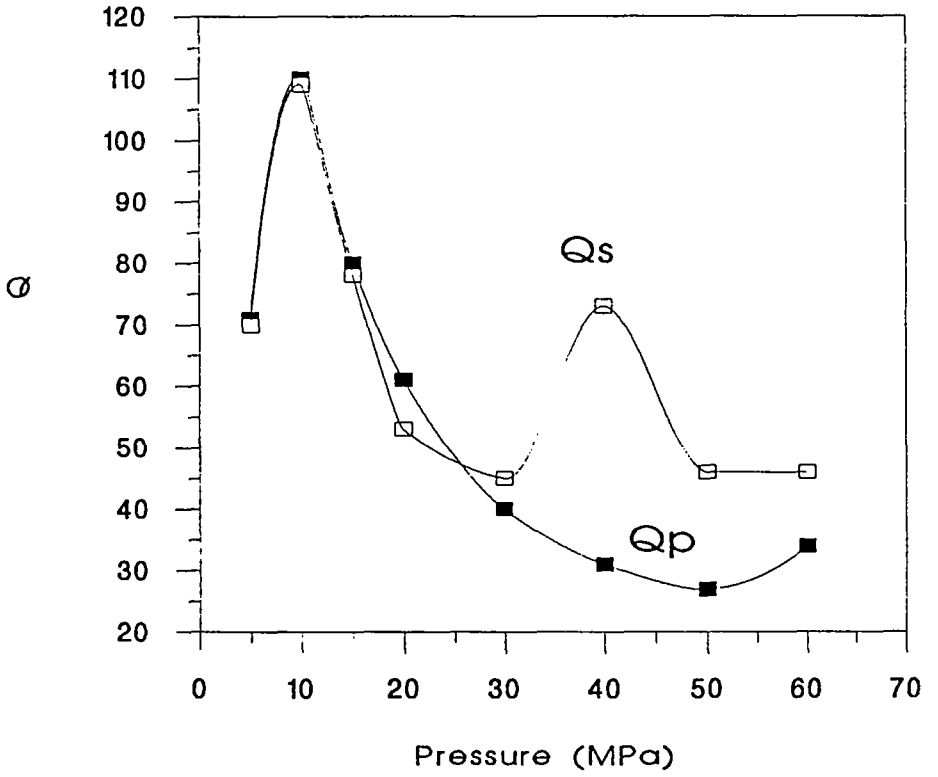

Figure 5.26b Compressional (Qp) and shear (Qs) quality factors versus pressure for sample CH2/1

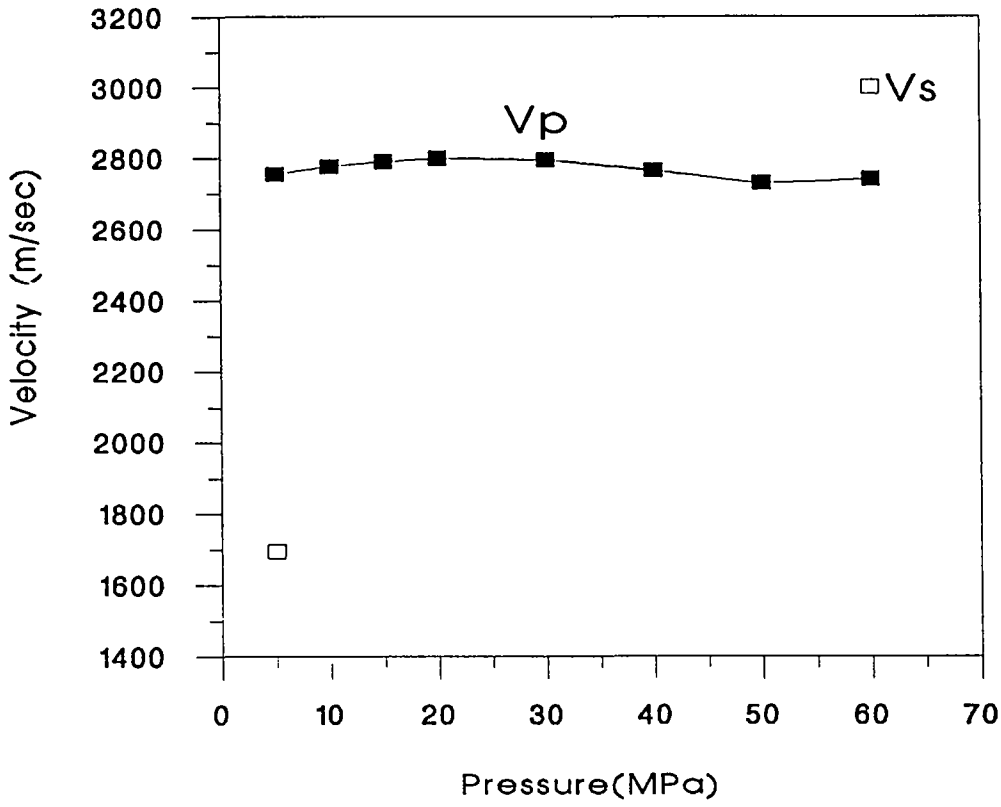

Figure 5.27a Compressional (Vp) and shear (Vs) velocities versus pressure for sample CH5/1

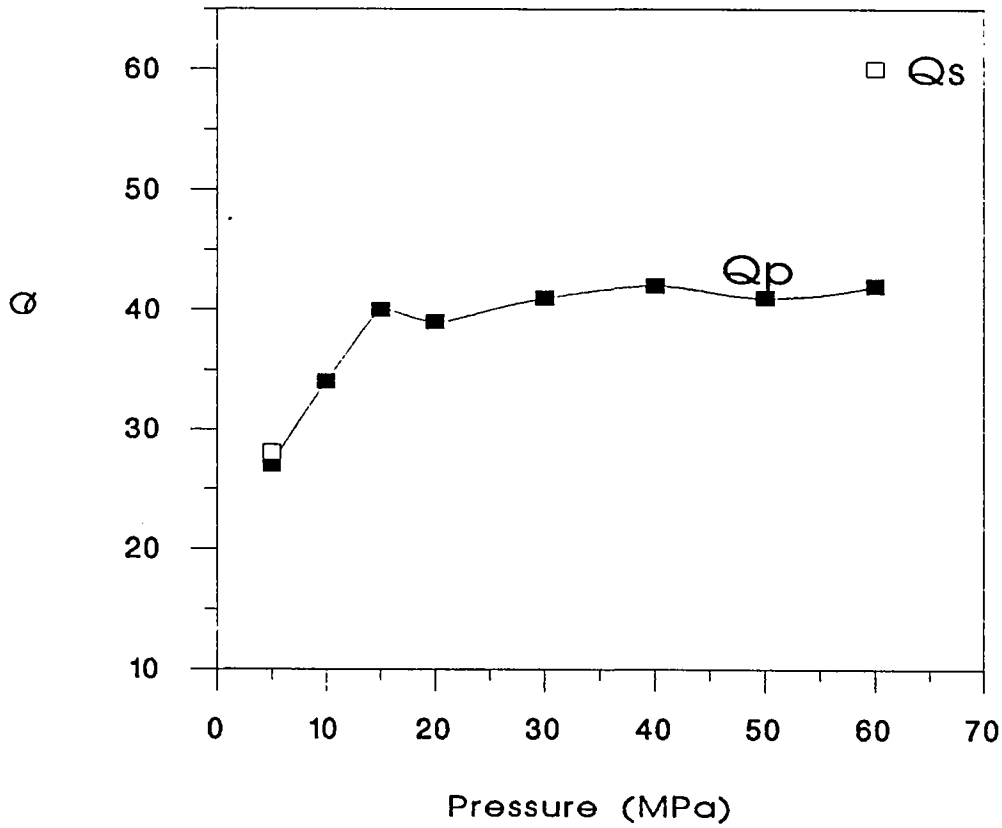

Figure 5.27b Compressional (Qp) and shear (Qs) quality factors versus pressure for sample CH5/1

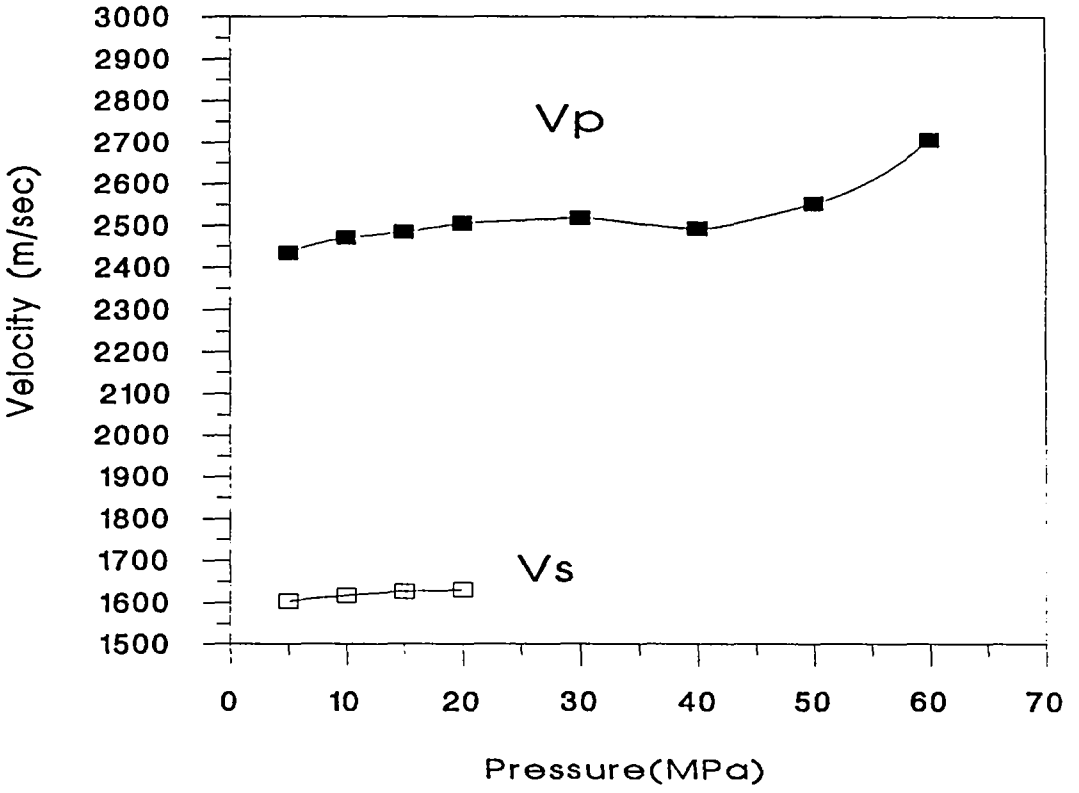

Figure 5.28a Compressional (Vp) and shear (Vs) velocities versus pressure for sample CH6/1

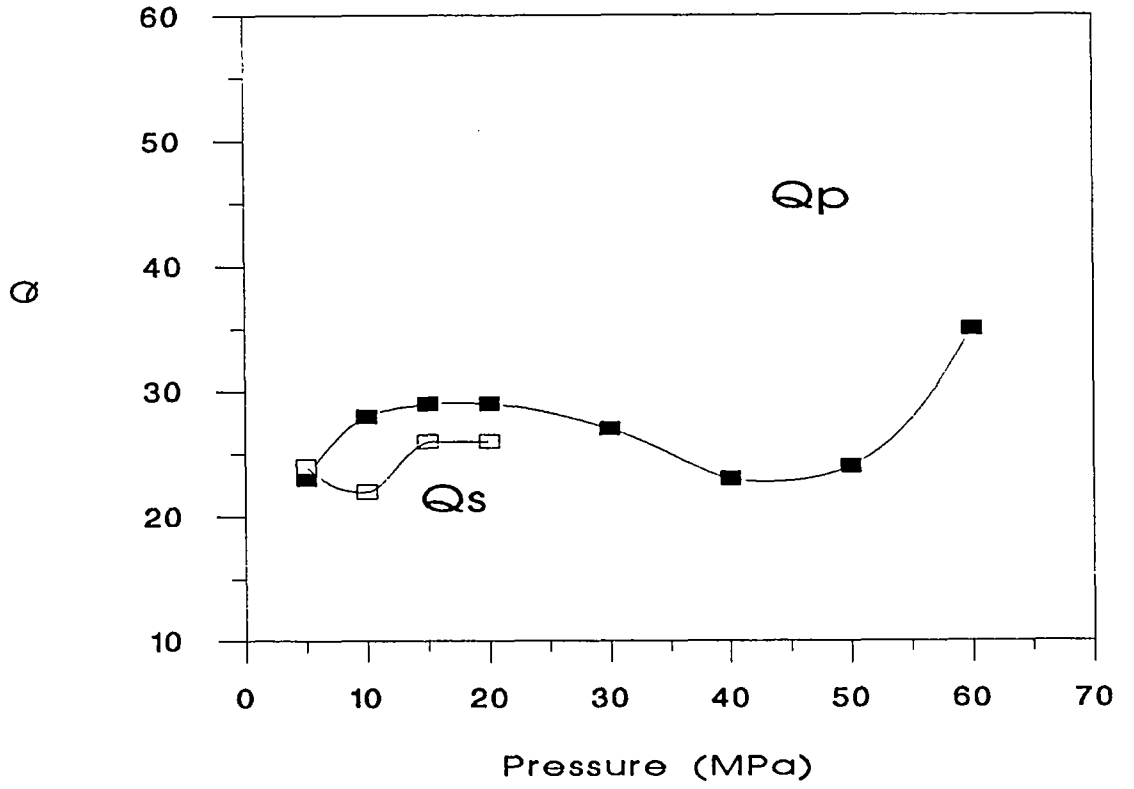

Figure 5.28b Compressional (Qp) and shear (Qs) quality factors versus pressure for sample CH6/1

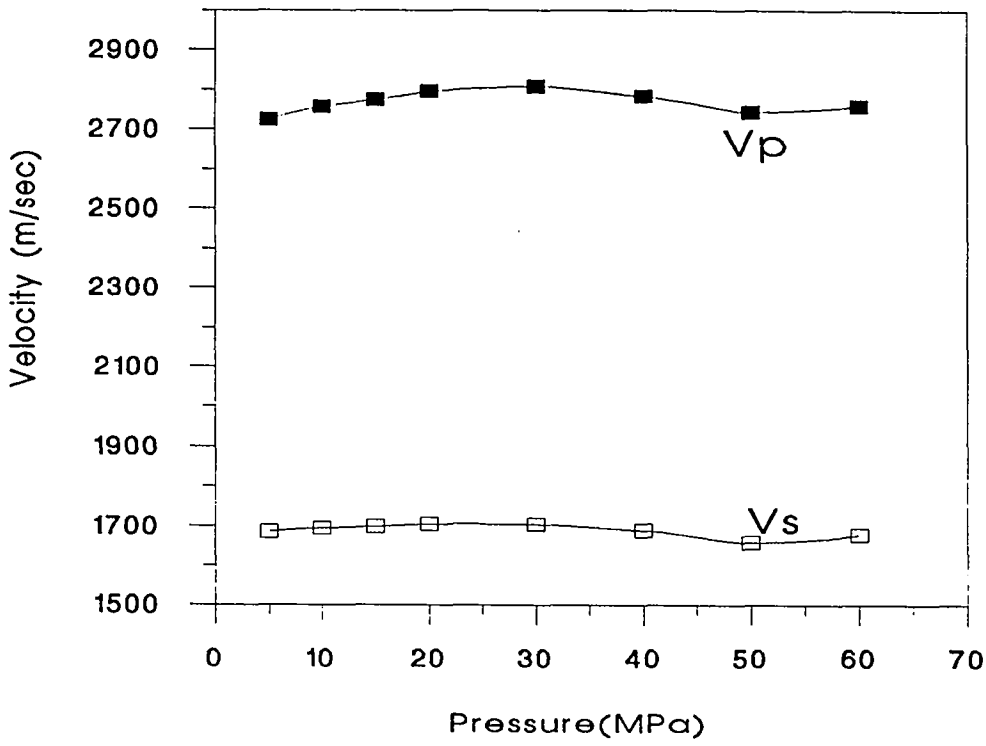

Figure 5.29a Compressional (Vp) and shear (Vs) velocities versus pressure for sample CH7/1

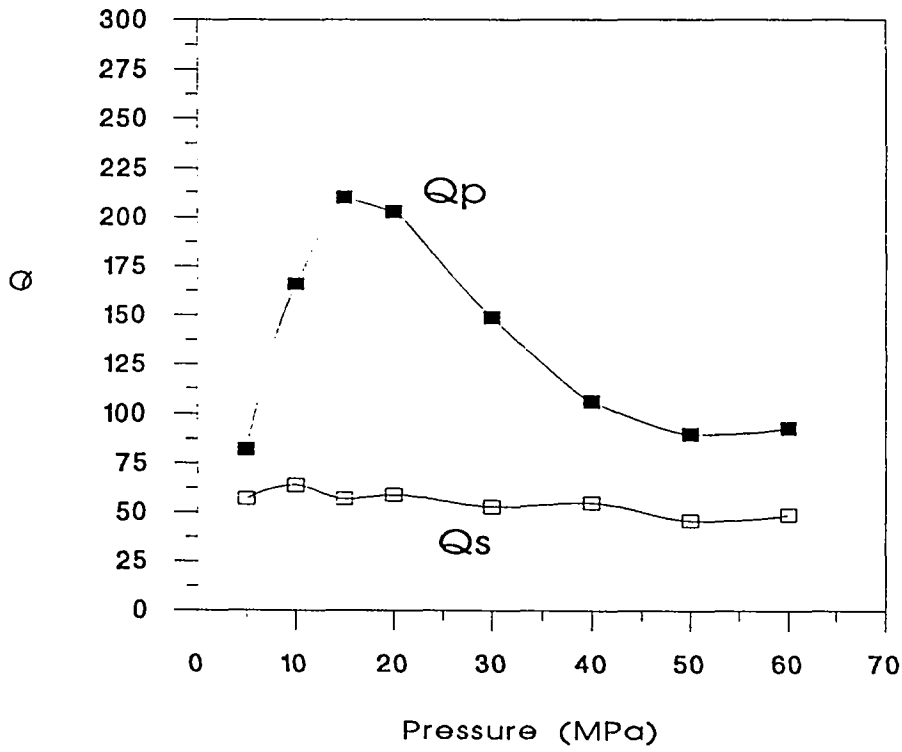

Figure 5.29b Compressional (Qp) and shear (Qs) quality factors versus pressure for sample CH7/1

The pattern of behaviour of the compressional-wave velocities and compressional-wave quality factors of Cherry Hinton samples CH5/1, CH6/1 and CH7/1 might suggest that some microfractures may exist in their original matrices. For these three samples the compressional-wave velocities show a small increase in value as the confining pressure was increased from 5 MPa to 30 MPa. At confining pressures greater than 30 MPa, the compressional velocities show the same pattern of decrease exhibited by the other chalk samples. Similarly, the compressional-wave quality factors show increases in values as the confining pressures were increased from 5 MPa to 20 MPa. However, the shear-wave velocities and quality factors show small or zero increases over the same range of confining pressures. As the consistent increases in all of the acoustic parameters, which are characteristically observed as a result of crack closure in sandstones, for example in Figures 5.1 and 5.2, are not observed in the Cherry Hinton data, it was concluded that these rocks do not contain a significant fracture density.

5.7 Conclusions

Ultrasonic measurements of the compressional-wave and shear-wave velocities and quality factors of the chalk samples demonstrate that the samples from the Shoreham Quarry, the Play Hatch Quarry and from Cherry Hinton contain an undetectable volume concentration of microfractures in the original rock matrix.

6. RESIN IMPREGNATION OF LARGE CHALK SAMPLES

6.1 Introduction

For some time it has been possible to impregnate rock with material that provides a contrast between the void space and the mineral grains (Waldo and Yuster, 1937). For the present study resin impregnation was employed to enable detailed examination of chalk matrix pore space. As discussed above, one explanation for the difference in the values of modelled and actual unsaturated zone storage (Lewis *et al*, 1993) was the slow drainage of a small proportion of the volume of unsaturated-zone matrix. It was hoped that examination of matrix pore resin casts would reveal, if present, the macropores and microfissures discussed in Section 1.3. Prior to this study, no direct evidence of these features had been forthcoming. Although macropores should be present in small chalk samples it could be argued that microfissures are unlikely to be included as the blocks from which the samples were taken would fracture preferentially along microfissures; the samples could therefore have been bounded by microfissures. The present study attempted to avoid this problem by using larger samples, of a size that must contain microfissures if they exist.

The resin impregnation method employed in the present study was developed 'in house' at Reading (Lewis (1987), Beckett and Sellwood (1991)). It has been shown to produce porecasts with faithful replication of sub-micrometre micro-fabric. The method involves evacuation of the sample to be impregnated followed by addition of resin whilst the system is maintained under vacuum. Using a pressure vessel the resin is then forced further into the sample before final curing of the resin in an oven. For the present study the heating and curing of the resin was performed under pressure using a specially developed apparatus.

The resin used in the present study, 'Transmit' resin for electron microscopy, was developed as a successor to Spurr's resin (Spurr 1969), the previous industry standard, by a pathologist in the UK. It has a viscosity at room temperature of 6.97×10^{-4} Pa s (69.7 cP) (cf. 8.4×10^{-4} Pa s for olive oil), facilitating good impregnation into chalk. It is also non-carcinogenic (unlike Spurr's resin) and exhibits electron beam stability. It does however expand by 4 per cent on curing. This expansion was unwelcome in the present study as it was feared that it might distort the resin casts of the matrix, but this disadvantage seemed to be outweighed by the other advantages. The resin is supplied by TAAB Laboratories Ltd, Aldermaston (01734 817775).

6.2 Method

6.2.1 Resin impregnation

Twenty samples for resin impregnation were taken from the larger blocks collected in the field. These samples included both natural block surfaces (fissure walls) and plain 'cut' surfaces. The samples were dried thoroughly before evacuation in a vacuum desiccator over three days. The prepared 'Transmit' resin was then slowly admitted into the sample beaker inside the desiccator (Figures 6.1 and 6.2). On completion of this step the resin-filled beaker and sample were removed from the vacuum desiccator and placed in the pressure vessel. The vessel was pressurised using nitrogen to 10.3 MPa for 48 h at ambient laboratory temperature and for a further 24 h at 70°C. The vessel was then allowed to cool and depressurised before the resin-

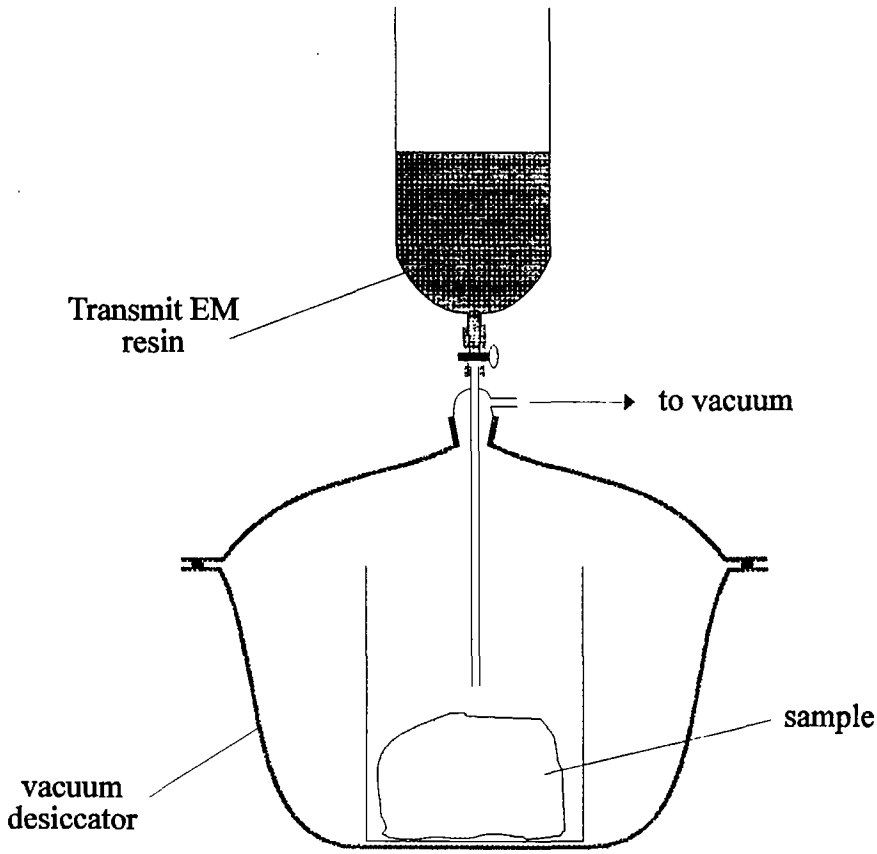

Figure 6.1 Schematic diagram of the resin introduction step

Figure 6.2 Photograph of the arrangement used for resin introduction

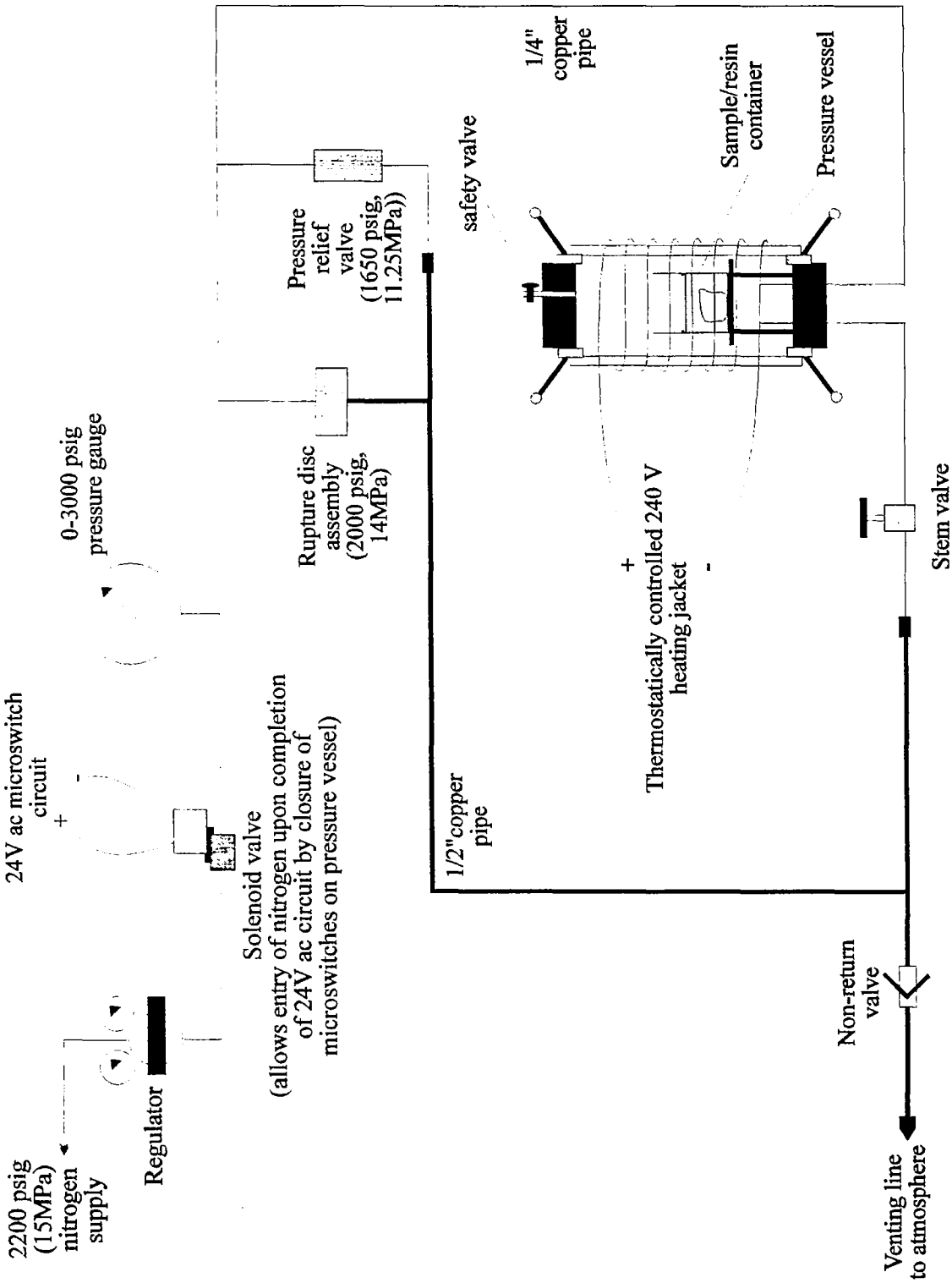

Figure 6.3 Schematic diagram of the resin-impregnation pressure vessel and its ancillary systems

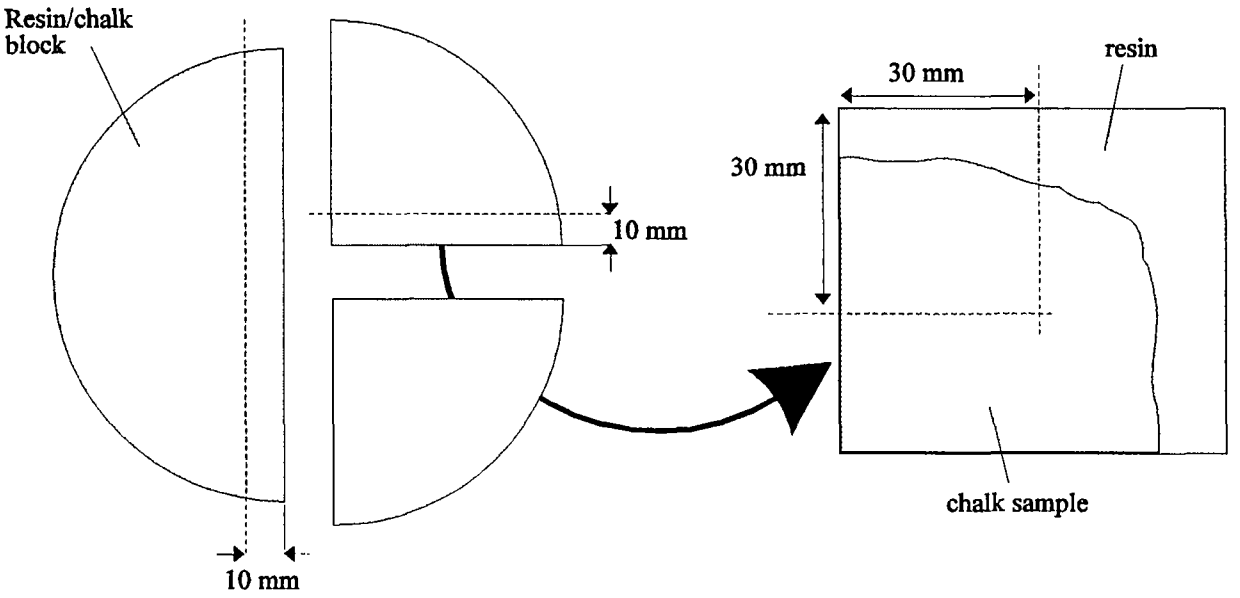

Figure 6.4 Resin/Chalk block sectioning protocol

impregnated sample was removed. Figure 6.3 is a schematic diagram showing the pressure vessel and its ancillary systems.

6.2.2 Preparation of resin pore-casts for SEM inspection

The impregnation and curing process left each impregnated sample surrounded by solidified resin in the shape of the plastic beaker. The resin/sample block was removed from the beaker and sectioned for SEM examination as shown in Figure 6.4.

For accommodation in the SEM the 100 mm sections had to be cut into small squares of maximum dimension 30 mm. The relevant face of the prepared sample was firstly ground using 240 grit abrasive paper on a rotary grinder and then polished using 0.3 μm aluminium oxide abrasive on a rotary polishing machine. The samples were then etched for 3 hours in 4 M HCl before being dried in an oven and coated with gold in preparation for SEM inspection. The polishing of the samples proved very time-consuming with the final stage often taking over three hours, depending on the hardness of the resin. When the samples were mounted in the SEM, it also frequently took a long time to attain the required vacuum. This is a common problem with chalk samples because the small pores are difficult to evacuate, but it had been expected that evacuation of resin impregnated chalk would be easier.

Figures 6.5 and 6.6 show resin impregnated chalk sections fully prepared for SEM inspection. Of technical note are the uniformly-thin, plasma-deposited gold coating of the sample, highlighted by the mirror-like finish on the highly polished resin surface, and the small dark zones of colloidal carbon suspension which provide an escape to earth for the bombarding electrons. The polished section shows the darker coloured resin surrounding the chalk sample and the larger voids in the resin-chalk interface caused by the dissolution of solid calcite shell fragments or non-impregnated areas.

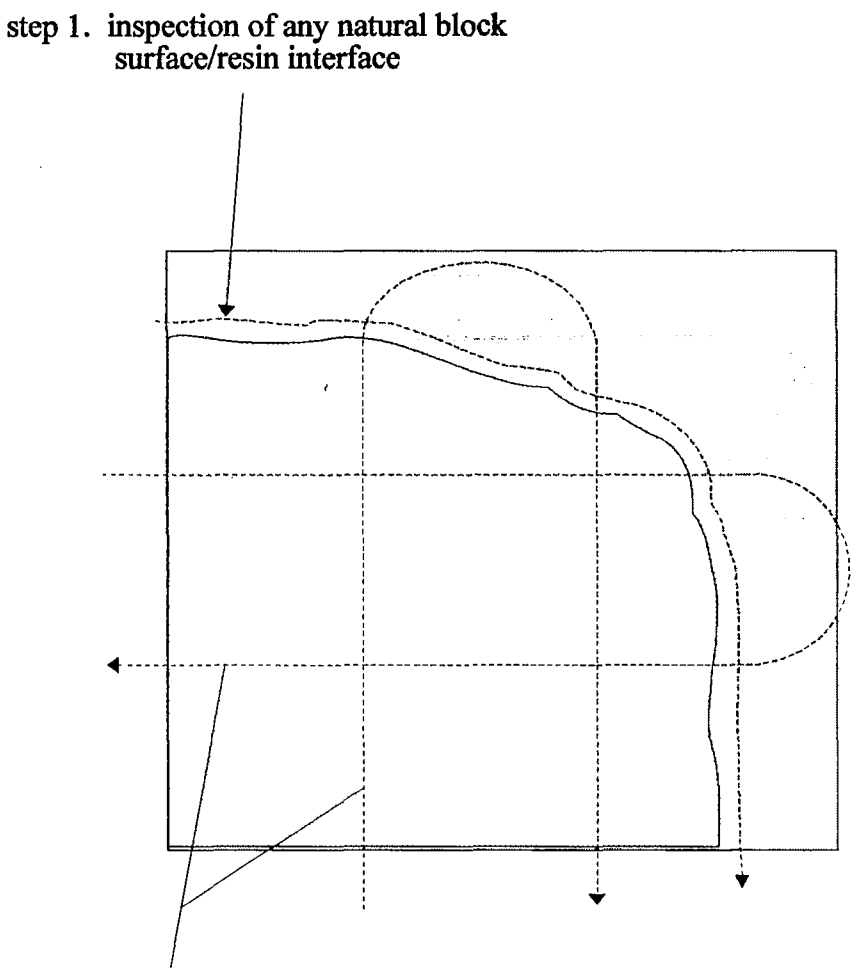

Figure 6.7 Diagram showing the protocol adopted for inspection of polished samples by SEM (except step 3)

6.3 Results

6.3.1 Quantitative estimation of the number of features in the matrix that might contribute to delayed drainage

In total, 19 polished matrix sections were examined using the SEM. No differences were apparent between samples from the three different sites. Table 6.2 presents the quantitative estimates of the frequency of relevant features (i.e. microfissures) for all the sections examined. The mean values for the three sites confirm that there is little difference between the three sites. The average for all 19 sections is 1.1×10^{-4} mm^2/mm^2. To give a tangible idea of this figure it equates to 6.7 mm^2 (e.g. a line 6.7 mm long and 1 mm thick) of two-dimensional fissure space on this A4 sheet of paper (6.2×10^4 mm^2). This means that a very small proportion of the volume of the matrix is occupied by features which might contribute to delayed gravity drainage. Indeed, as shown below, a number of the prepared sections exhibited no features of interest to the present study.

Table 6.2 Quantitative estimation of the frequency of features that might cause delayed drainage of the matrix (mm^2/mm^2)

Section	Frequency	Section	Frequency	Section	Frequency
PH2/5,1	0	SH2/6,1	3.9×10^{-4}	CH2/6,1	9.4×10^{-5}
PH4/5,1	2.8×10^{-4}	SH2/6,2	4.8×10^{-5}	CH2/6,2	2.8×10^{-4}
PH4/5,2	1.6×10^{-4}	SH5/6,1	0	CH2/6,3	5.1×10^{-5}
PH7/9,3	8.6×10^{-5}	SH5/6,2	0	CH3/6,1	2.1×10^{-4}
PH8/10,1	0	SH6/6,1	1.3×10^{-4}	CH3/6,2	0
PH8/10,2	1.3×10^{-4}	SH6/6,2	2.6×10^{-5}	CH5/5,1	0
				CH5/5,2	2.3×10^{-4}
Mean	**1.1×10^{-4}**	**Mean**	**9.9×10^{-5}**	**Mean**	**1.2×10^{-4}**

6.3.2 Some examples of features discovered in the chalk matrix during the SEM examinations

During the SEM inspection of the prepared samples a large number of monochrome photomicrographs of notable features were taken. A number of these are presented and described but, at this point, a warning is appropriate. In choosing which SEM images to preserve on film, and also in choosing the series of photomicrographs to present, one is obviously drawn to those images which are worthy of comment, i.e. those depicting various features. Hence, in comparison with the images of the samples viewed on the SEM, a disproportionate number of the following images are of features which might contribute to delayed drainage of the matrix. In forming an impression of how frequent these various features are in the matrix the reader is directed to Section 6.3.1 above.

As a number of SEM photomicrographs will be presented to demonstrate features found in the resin pore-casts a full explanation of some example plates (Figures 6.8 (from polished section number PH8/10,1) and 6.9 (PH8/10,1)) will be given. Firstly, the text at the bottom of the plates consists of (left to right) a potential difference (constant at 20 kV for the present study) through which electrons are accelerated towards the sample, a magnification (only approximate because of changes in image size during reproduction), a scale bar (accurate), and a plate identification number. The SEM model used has a range of magnification from x 50 to x 7500, but little inspection was done at magnifications exceeding x 1500 during the present study.

Figure 6.8 is a relatively high-magnification photomicrograph of a chalk matrix resin pore-cast. In all such plates that follow it should be remembered that the image is of a resin pore cast. This means that the solid resin is a three-dimensional reproduction of the pore-network while the voids represent space formerly occupied by solid carbonate particles in the matrix.

Figure 6.9 is a lower magnification photomicrograph of a natural block surface (NBS) which shows some features more relevant to the present project. To the top right of the plate is the solid resin surrounding the block and to the bottom left is the resin-impregnated matrix. A number of larger scale (5-30 μm) voids can be seen in the matrix indicating the former presence of solid calcite particles of an equivalent size. The large voids at the resin-chalk interface will be discussed in detail below.

Previous exercises in resin impregnation of carbonate rocks at Reading (Beckett and Sellwood 1991) had shown that submicrometre detail of porosity could be preserved in resin casts. Figure 6.10 (PH2/5,1) is a very high magnification photomicrograph of chalk matrix included to demonstrate the scale of detail which was reproduced by the resin impregnation technique used in the present study. The section of the matrix shown is somewhat unusual as it appears to have had regular larger spheres of carbonate (5-10 μm in diameter), possibly foraminifera, which have been removed by etching. However, the image demonstrates clearly the submicrometre detail of the pore space preserved by the resin.

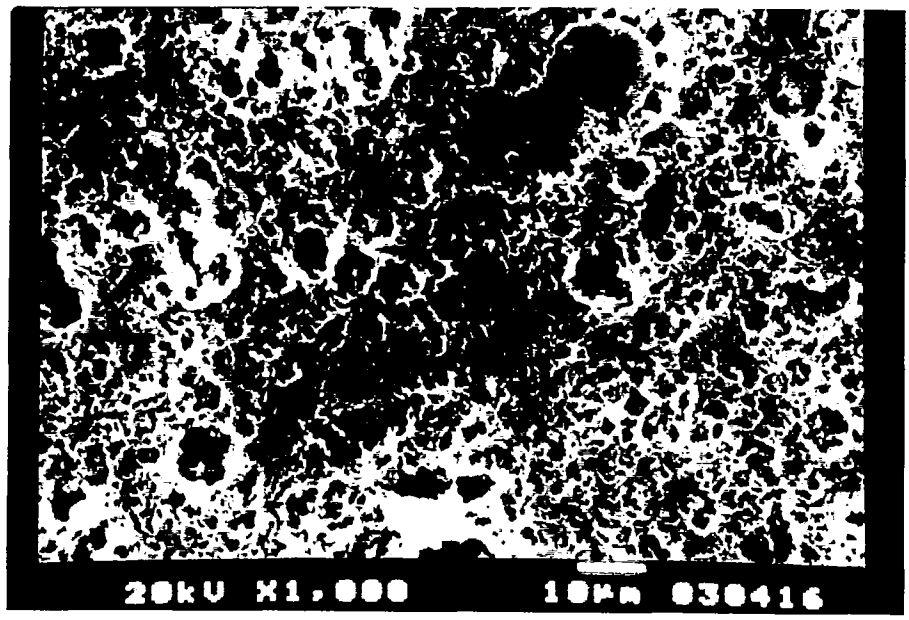

Figure 6.8 Relatively high-magnification photomicrograph of a chalk matrix resin pore cast (from polished SEM section PH8/10,1)

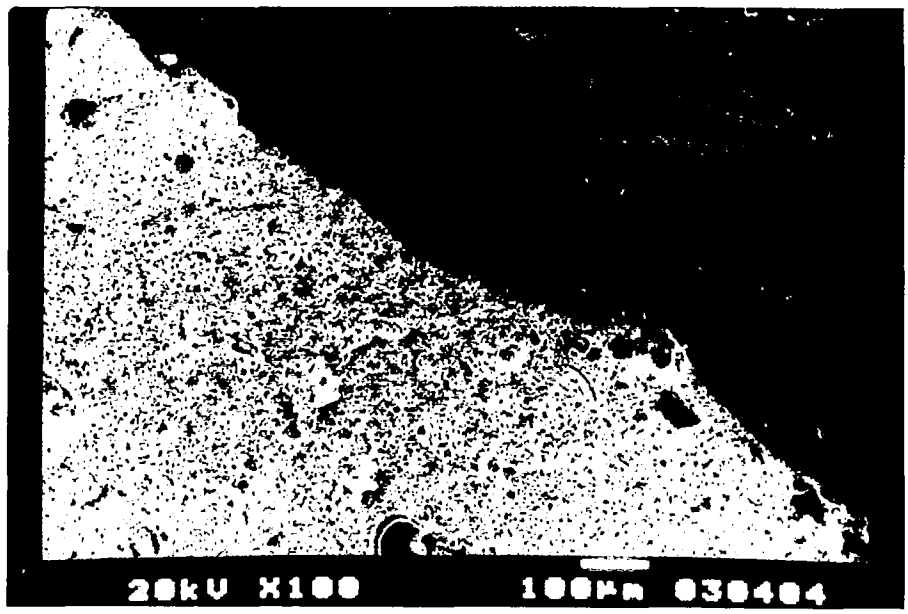

Figure 6.9 Low magnification photomicrograph of a resin cast of a natural block surface (PH8/10,1)

Section 6.3.1 above detailed the scarcity of features which could be responsible for delayed drainage within the matrix. A natural consequence of this fact was that examination of the polished sections using the SEM often consisted of viewing large areas of matrix that lacked any apparent drainable porosity. However, the matrix was rarely featureless and demonstrated a number of interesting features and variations in fabric. Figures 6.11 (SH6/6,1) and 6.12 (PH7/9,3) are highly magnified images of pore casts of the matrix from polished and non-polished sections respectively. The former was the usual highly magnified view of the matrix during routine examination of the polished sections but in many respects the latter demonstrates the important features of matrix pore casts more effectively. Considering both of these figures, the basic attributes of the chalk matrix are apparent. The pores of the resin cast are the spaces formerly occupied by the fundamental particles of chalk matrix, the coccolith laths, which range in size from 0.5-2 μm. Also apparent, especially in Figure 6.11, is the large volume of resin (pores in matrix) in relation to that of space (chalk grains) reflecting the high porosity (0.25-0.40) of the matrix. More apparent in Figure 6.12 is the small size of the connections between the pores (the pore throats), preserved as the fine 'webbing' joining the small spheres of resin (the matric pores). It is apparent that these pore throats are often less than a micrometre across, explaining the low permeability of the matrix.

Figures 6.13 (CH2/6,1) is a photomicrograph of an area of matrix with a foraminiferal concentration at the upper end of the 5 to 10 per cent range suggested by Hancock (1993). The foraminifera range in size from 20 to 100 μm and therefore could represent an important element of porosity with regard to delayed drainage of the matrix. However, two observations suggest that this is not the case. First, closer examination of Figure 6.13 reveals that most of the foraminifera are physically isolated within the fine-grained matrix. Drainage from these foraminifera will therefore be controlled by the same pore-throat sizes that control the drainage of the surrounding matrix..

Secondly, evidence suggests that the connections through the outer layer of the foraminiferal tests might be even lower than that of the fine-grained matrix. Examination of Figure 6.14 (PH8/10,1), which is a highly magnified image of parts of the outer edges of two foraminifera tests, shows that the outer layer demonstrates a tube-like porosity, represented in the resin cast by thin resin spicules leading from the inside of the foraminifera to the fine-grained matrix. The suggestion that this limited link with the matrix will also inhibit fluid movement is possibly confirmed by the observation that the resin has failed to impregnate a high proportion of foraminifera in the matrix (for example Figure 6.13).

During examination of the polished sections a number of microfissures were discovered, although again it is important to emphasise that, as confirmed in Section 6.3.1, they were very infrequent.

Figures 6.15 (SH2/6,1) and 6.16 (CH2/6,1) are typical examples of microfissures found during the SEM inspections. In both these cases the image is of part of a microfissure. A number of microfissures were of an extended length (1 to 3 mm), sometimes traversing the complete section. More often however they were of limited length (for example Figure 6.17 (PH7/9,3)) and apparently isolated within the fine-grained matrix.

Another potentially important feature discovered during the SEM inspection of the polished sections was areas of apparently enhanced porosity within the matrix. The expression of these areas varied from distinct zones of high resin concentration (almost very large pores) through

to very graded and almost indistinguishable areas of slightly increased resin concentration. The size of these features varied from less than 50 μm to greater than 2000 μm. This variation in size and form suggested a common cause was unlikely.

Figure 6.18 (CH2/6,2) shows a zone of enhanced resin concentration indicating the presence of a zone of enhanced porosity in the matrix. In this case the zone is characterised by almost solid resin which would result from the presence of a large pore but Figure 6.19 (CH2/6,2), which is a magnified view of part of the same feature, confirms that the zone is only of enhanced porosity.

A final group of interesting features was associated with the junction between some of the natural block surfaces and the adjacent solid resin. In most cases (approximately 80 % of the natural block surface inspected) this area was characterised simply by resin butting up closely to the resin cast of the chalk but in a number of cases other features were found. Figure 6.20 (PH8/10,1) is an example of the basic form of these interesting features, showing a void in the resin parallel to the natural block surface (in this case 20 to 80 μm wide). If this feature were simply an artefact of the impregnation and etching process it would indicate that there was a solid layer of calcite adjacent to the natural block surface. An alternative theory for the origin of this type of feature is that it results from the expansion of resin (up to 4 % in volume) upon curing. Hence, if the resin-impregnated matrix was able to resist this expansion whilst the outer layer of resin expanded to its full extent, a void would develop around the sample.

It seems likely then that some of the voids found adjacent to natural block surfaces (and plain cut surfaces) were caused by post-impregnation resin expansion. However, in a number of cases the void was only partial and exhibited some infilling with resin of various morphologies. Figure 6.21 (PH8/10,2) is an example of these partially infilled voids. It seems unlikely that these features are a result of differential expansion of the sample and the resin, and they are likely therefore to be a product of real features in the matrix adjacent to natural block surfaces.

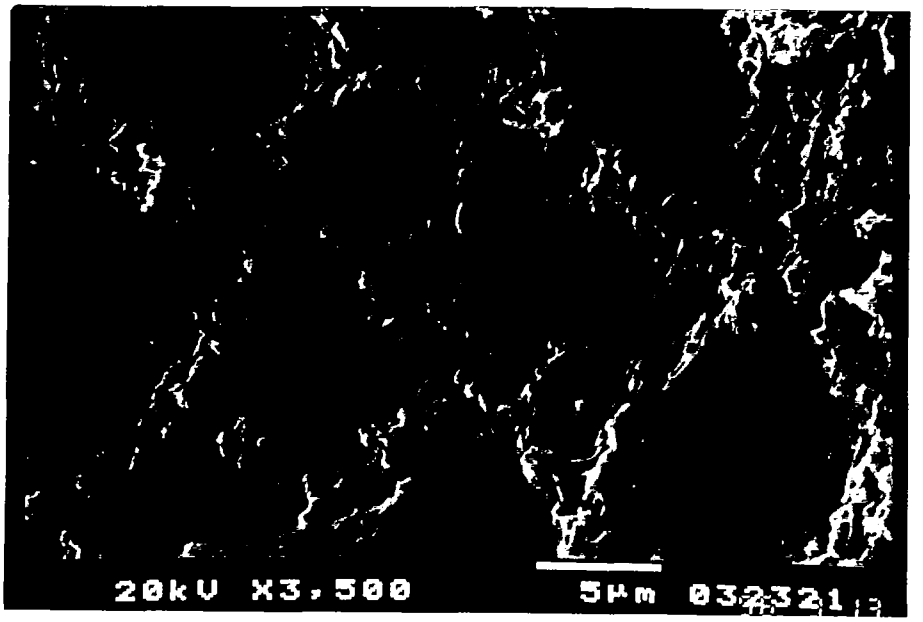

Figure 6.10 High magnification photomicrograph of chalk matrix (PH2/5,1). Note the submicrometre scale of resin 'webbing' representing the small pore throats responsible for low permeability.

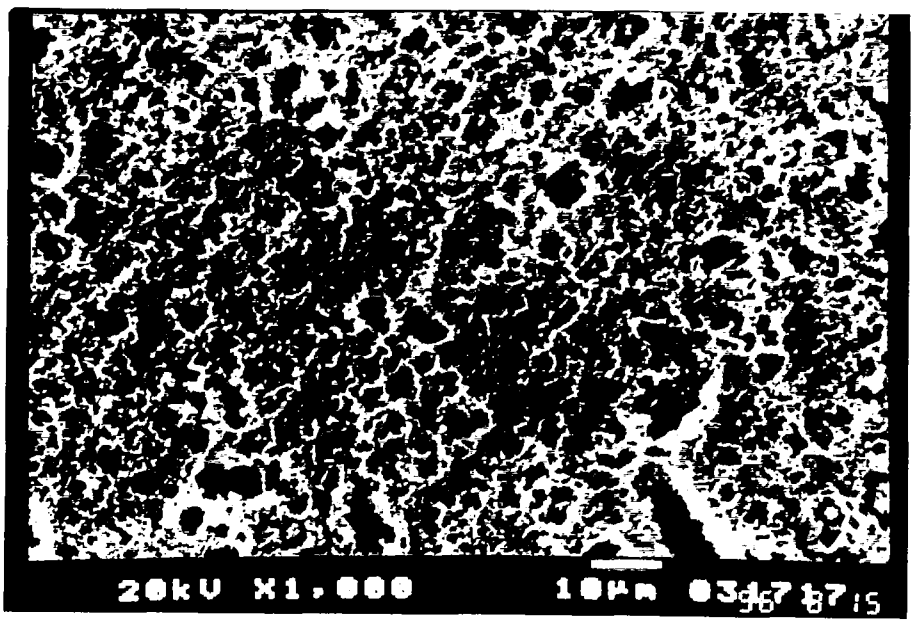

Figure 6.11 High magnification photomicrograph of chalk matrix (polished surface) (SH6/6,1).

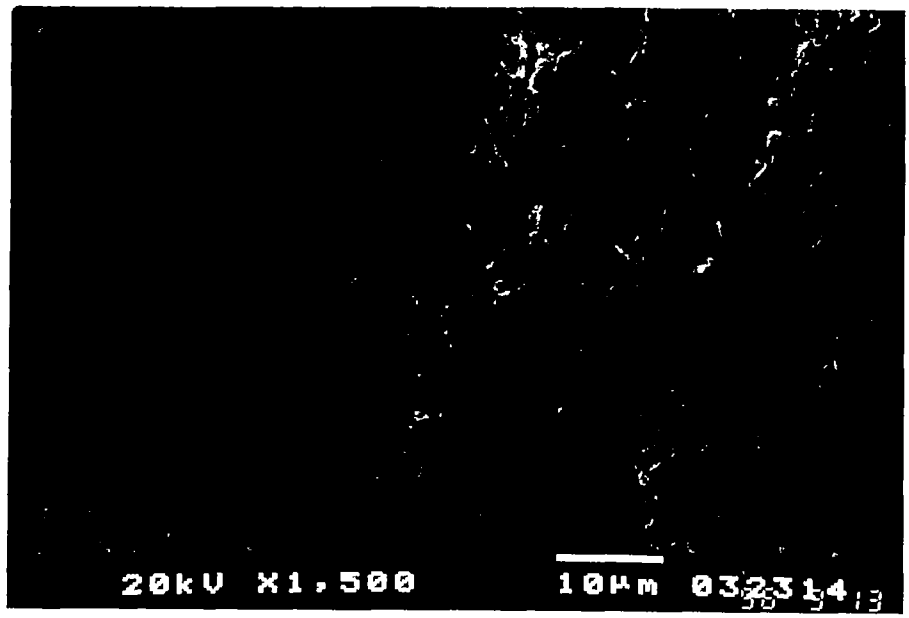

Figure 6.12 High magnification photomicrograph of chalk matrix (unpolished surface) (PH7/9,3).

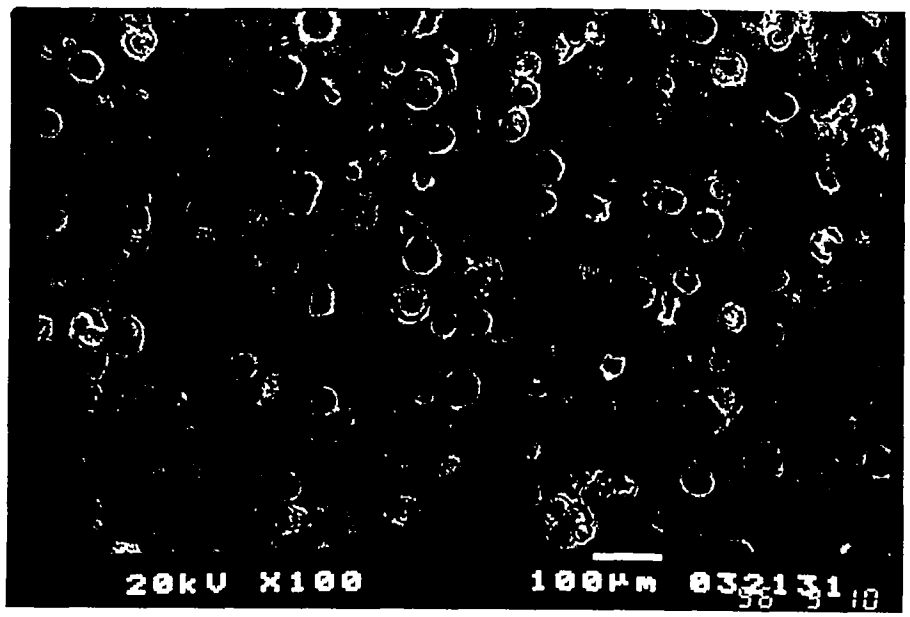

Figure 6.13 Photomicrograph of a section of foraminifera-rich matrix (CH2/6,1). Note that most of the foraminifera are surrounded by poorly-permeable matrix that will control drainage.

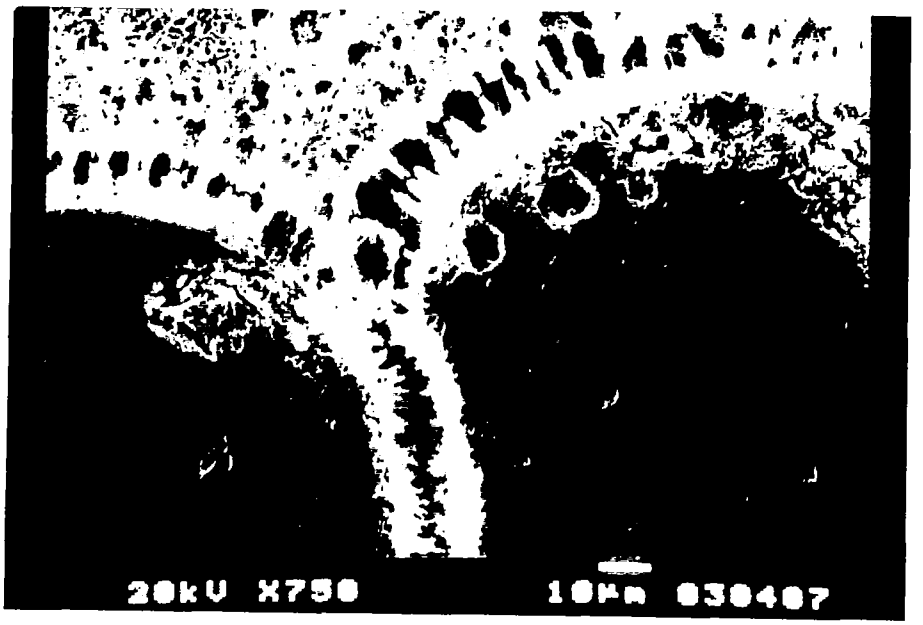

Figure 6.14 High magnification photomicrograph of the outer edges of two foraminifera tests (PH8/10,1).

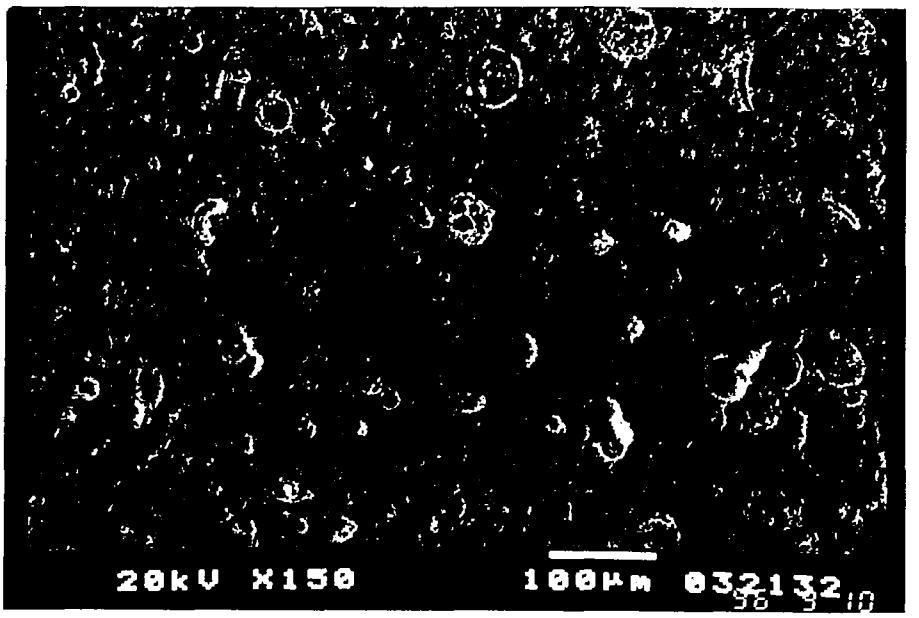

Figure 6.15 Photomicrograph of a section of a sinuous resin-filled fissure running through chalk matrix (SH2/6,1).

Figure 6.16 Photomicrograph of a section of a straight resin-filled fissure running through chalk matrix (CH2/6,1).

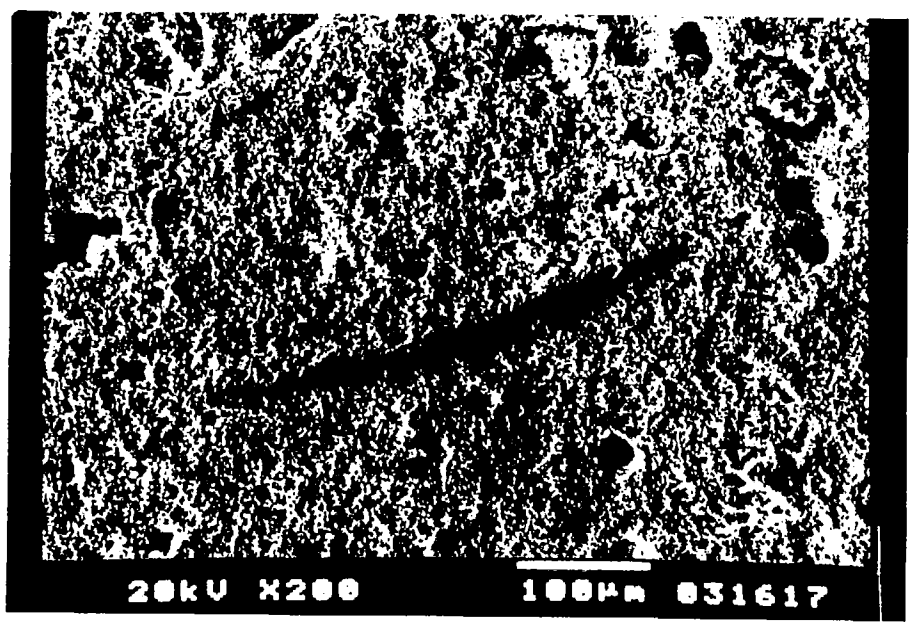

Figure 6.17 Photomicrograph of a short resin-filled fissure apparently isolated within the fine-grained matrix (PH7/9,3).

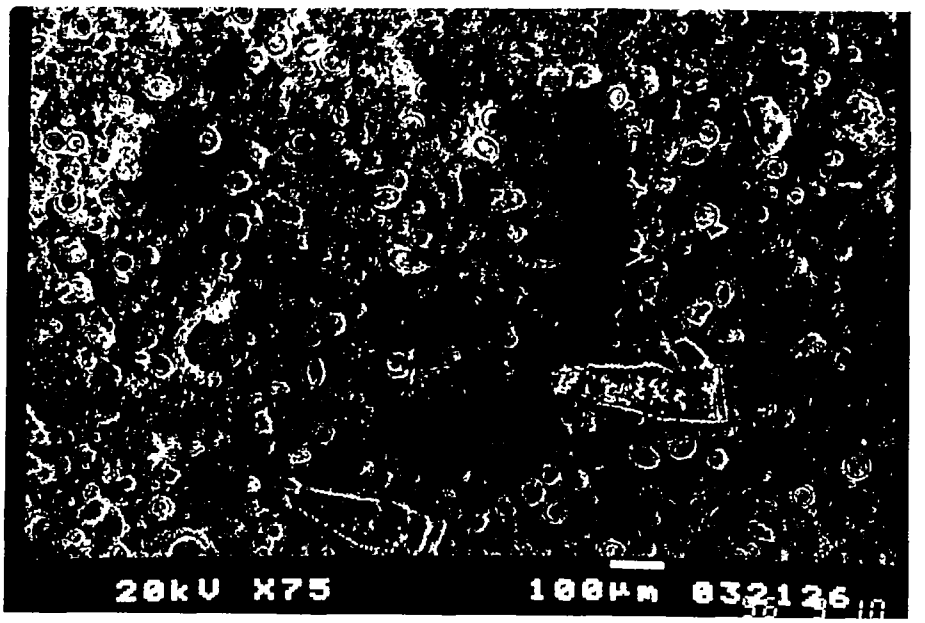

Figure 6.18 Photomicrograph of an area of apparently enhanced porosity within the chalk matrix (CH2/6,2).

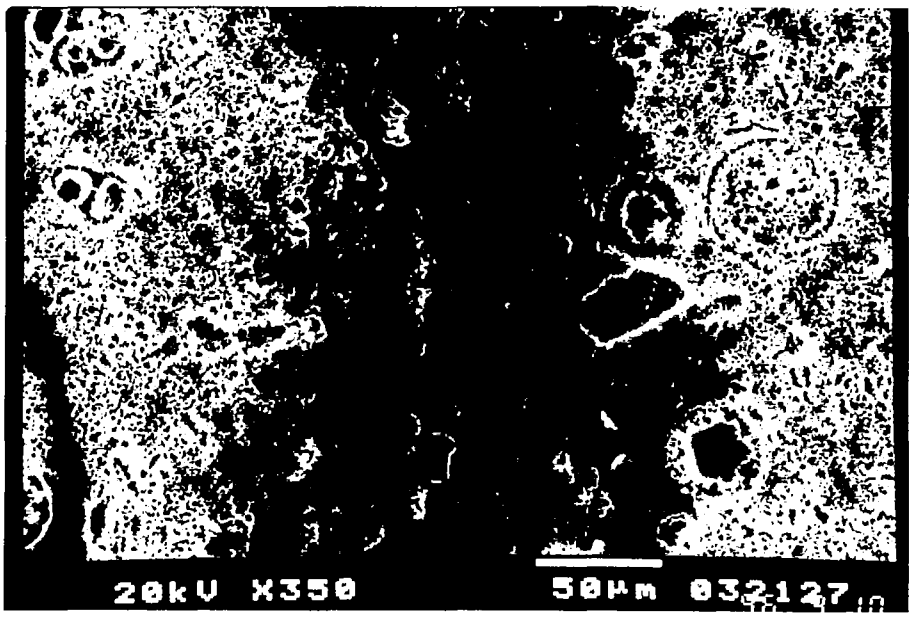

Figure 6.19 High magnification photomicrograph of part of the area of apparently enhanced porosity as shown in Figure 6.18 (CH2/6,2).

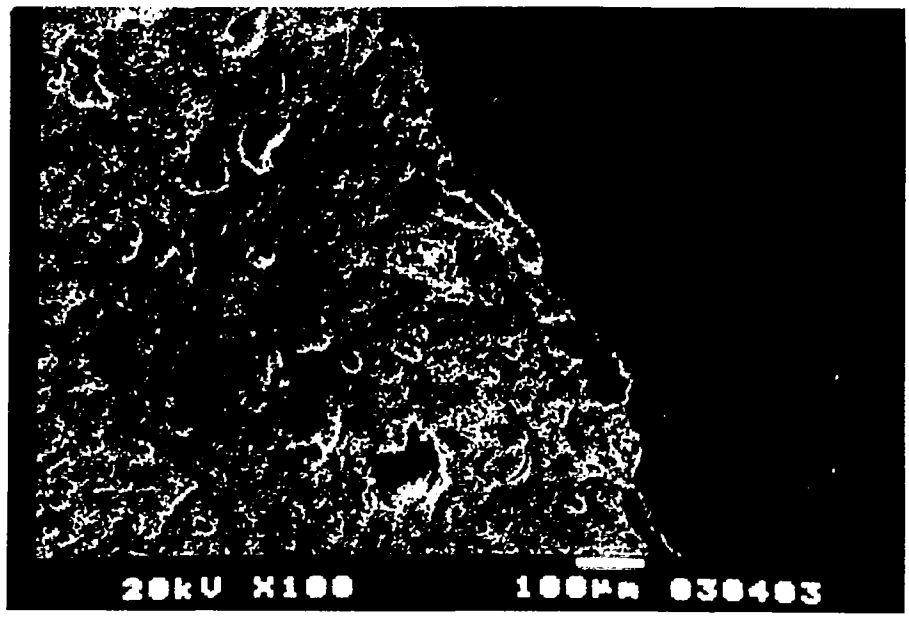

Figure 6.20 Photomicrograph showing a void in the resin cast between the resin-filled matrix and the solid resin surrounding the sample block (PH8/10,1).

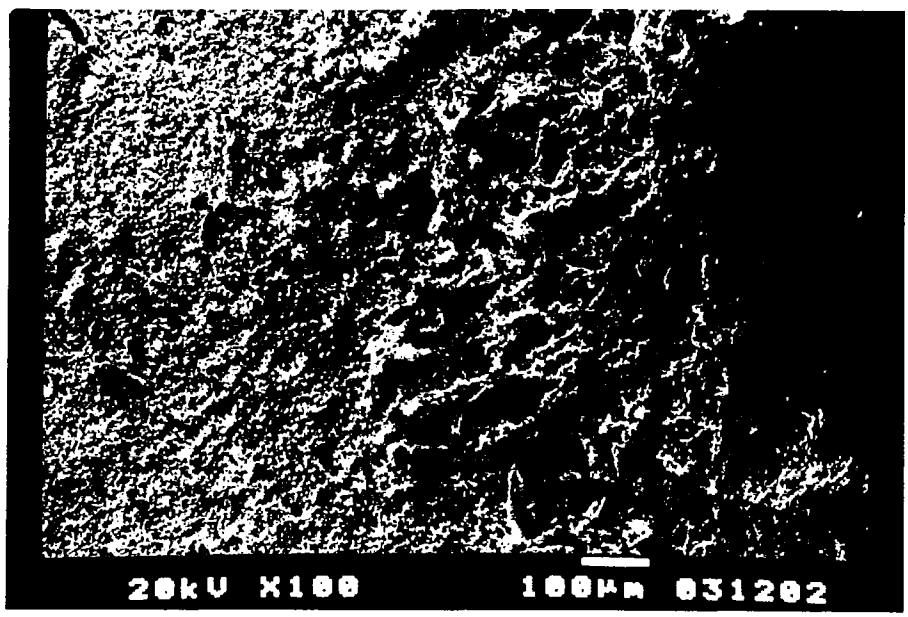

Figure 6.21 Photomicrograph showing an example of an extraordinary resin texture close to a sample block surface (PH8/10,2).

7. DISCUSSION

7.1 The findings of the present study

All discussion of the findings of the present study has to be prefaced by the comment that the study is based on relatively few samples of the Chalk from only three localities.

Neither the acoustic measurements nor the resin impregnation studies have produced evidence of the presence of any significant microfissure networks in any of the samples studied. The resin impregnation studies have shown the presence of macropores in the form of foraminiferal tests, but the communications with these macropores consist of openings which are typically no more than 1 μm in diameter. These larger pores will therefore not drain until the pore-water suctions rise to the values required to drain the narrow connections, nor will they contribute significantly to permeability. As far as drainage and permeability contributions are concerned, there is therefore no confirmation of the microfissures and macropores postulated by workers such as Reeves (1979).

The results from the AWCP studies (Section 3) imply that in the absence of irregular surfaces, such as those formed by natural fissures, drainage at suctions of 10-15 m is of the order of 0.5-1 per cent of pore space, or about 0.15-0.4 per cent of bulk volume, with the smaller value applicable to large blocks and the larger value applicable to small blocks. This variation with size of tested blocks implies clearly that there is a surface effect in the drainage behaviour. This conclusion is strengthened by the fact that drainage is significantly greater from samples that include one or more rough surfaces - either natural fissure surfaces or artificially broken surfaces. The same trend is seen in the MICP results (Section 4) which show that significantly more intrusion occurred into samples broken into fragments than into single samples of approximately the same volume.

It is not immediately clear whether all the water drainage from, or mercury intrusion into, the samples occurred into surface irregularities or whether pores within the test samples are involved. However, on the basis of the apparent absence of macropores or microfissures it might be expected that the surface irregularities are responsible for the bulk of this storage, and it is possible to demonstrate approximately that this could be so, even in the case of the samples with smooth surfaces. The samples with cut surfaces were ground on a lap with 240 grade abrasive grit. This grade number refers nominally to the number of grains per inch, which would mean that the theoretical grain size would be approximately 0.1 mm (100 μm); in fact, data from the manufacturers suggest that the median grain size will be around 60 μm. Grinding with such a medium might be expected to leave a surface relief of alternating depressions and lumps, of a size related to the size of the particles forming the grinding medium. Thus a sample finished using 240-grade grit might have depressions about 60 μm in diameter. A possible representation of such a finished surface is shown in Figure 7.1. The volume of storage represented by the hemispherical depressions on a unit area of such a surface is

$$\pi d/24$$

On a cube of side b the volume of surface depressions as a fraction of bulk volume is

$$\pi d/4b$$

which is equivalent to a specific yield of

$$(\pi d/4b) \times 100 \quad \text{per cent} \qquad (7.1)$$

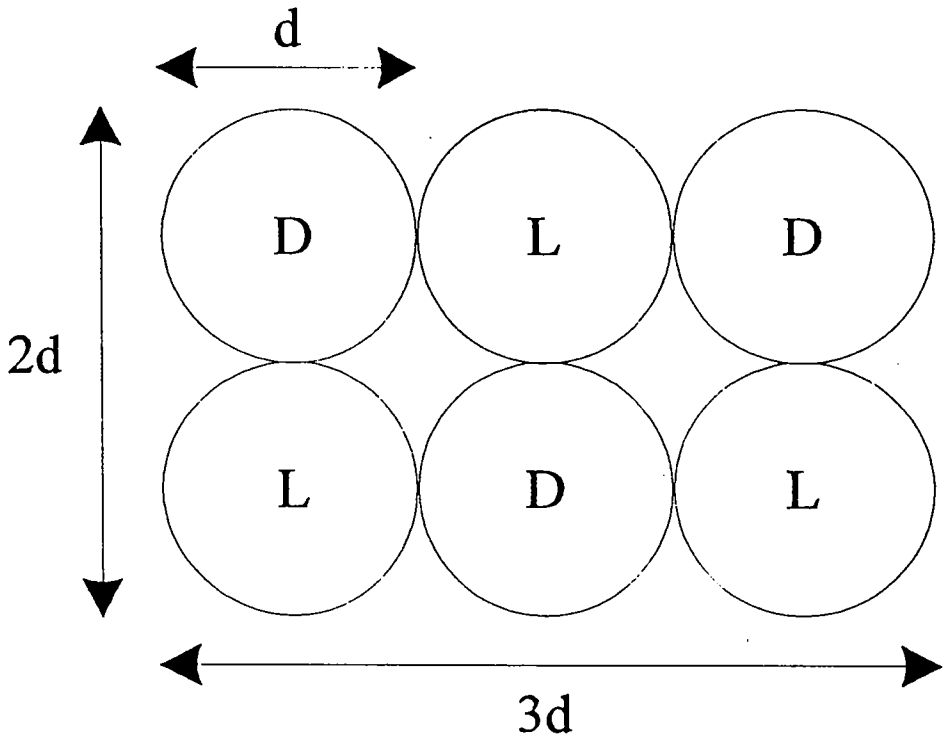

Figure 7.1 A simple model for the calculation of the drainage contribution from surface irregularities on a "smooth" block surface. D = depression, L = lump.

Table 7.1 shows the values of specific yield that would be expected as a result of drainage from depressions of various sizes (spaced according to the model of Figure 7.1) on the surfaces of cubes ranging in size from 10 to 2000 mm.

Table 7.1 Specific yields (per cent of bulk volume) that would arise from depressions of the size shown on cubes of various sizes. The calculation is based on Figure 7.1 and Equation 7.1.

cube side, b (mm)	10	50	100	200	500	1000	2000
depression diameter, d (mm)							
0.100	0.785	0.157	0.0785	0.0393	0.0157	0.00785	0.00393
0.050	0.393	0.0785	0.0393	0.0196	0.00785	0.00393	0.00196
0.020	0.157	0.0314	0.0157	0.0079	0.00134	0.00157	0.00079
0.010	0.0785	0.0157	0.0079	0.0039	0.00157	0.00079	0.00039
0.005	0.0393	0.0079	0.0039	0.0020	0.00079	0.00039	0.00020

The values of specific yield shown in Table 7.1 must not be taken to be definitive values for general use in the Chalk. They assume cubic blocks, with depressions on all six sides free to drain, and also assume the very idealised model of Figure 7.1. Nevertheless they provide an order of magnitude estimate or better of the drainage that can be expected from "smooth" block surfaces. The samples tested using the AWCP technique (Section 3) were generally between 10 mm and 100 mm across. It is interesting to note that at the suction range employed (which would drain depressions of between 0.06 mm and about 0.003 mm) the measured drainage of the samples with smooth surfaces was between about 0.2 and 0.5 per cent of bulk volume, which is in good agreement with the predictions of Table 7.1. This suggests that drainage observed from even these smooth samples could be explained as the result of drainage from surface irregularities, without the need to invoke drainage of matric pores or of hypothetical macropores or microfissures. When allowance is made of the greater surface area of samples with rough or natural fissure surfaces, it is easy to see that block surfaces can account for volumes of water of the order of those required to explain the findings of Ineson and Downing (1964) and of Lewis *et al.* (1993).

7.2 Wider implications for Chalk hydrogeology

7.2.1 Water table response

Notwithstanding the findings of Ineson and Downing (1964) and of Lewis *et al.* (1993). it is clear that there must be a component of storage within the chalk of the unsaturated zone. There is a delay before the water table rises in response to periods of substantial recharge. In the case of aquifers with deep water tables this delay may be many weeks. This evidence for storage in the unsaturated zone is additional to and quite independent of the findings of Ineson

and Downing (1964) and of Lewis *et al.* (1993). This delay can best be understood by considering the speed of propagation of a perturbation of head through a porous medium. Such a medium is a diffusive system, through which the characteristic time t for a significant response over distance x can be expressed as

$$t = x^2/D \qquad (7.2)$$

where D is the diffusivity (Barker, 1993). In the case of a saturated medium, D is defined as K/S_S, where K is the hydraulic conductivity and S_S is the specific storage.

In the case of unsaturated flow, the diffusivity becomes a function of saturation and hence of pore-water suction or potential, and is normally written $D(\psi)$, where ψ is the potential. In these cases the relationship is

$$D(\psi) = K(\psi)/C(\psi) \qquad (7.3)$$

where:

$K(\psi)$ is a the unsaturated hydraulic conductivity (a function of saturation or fluid potential, ψ)

and $C(\psi)$ is the specific moisture capacity, defined (Freeze and Cherry, 1979) as:

$$C = \frac{d\theta}{d\psi} \qquad (7.4)$$

where θ is the volumetric moisture content.

A difficulty in applying this to the Chalk has been that if the matric porosity is regarded as non-draining, the only storage available is by the filling and emptying of fissures, yet on the basis of studies of the unsaturated zone by soil hydrologists (e.g. Wellings, 1984) the fissures at many sites are rarely if ever filled. The concept of "matric" storage in the form of irregularities which can fill and drain over the ranges of suctions observed in the field removes this difficulty.

In chalk the unsaturated hydraulic conductivity at moderate suctions is close to the saturated hydraulic conductivity of the matrix (See, e.g. Wellings, 1984, Fig. 7), which for much of the Chalk is typically about 3×10^{-3} m/day. The specific moisture capacity, C, is the gradient of the pore-water characteristic or AWCP curve over the appropriate range of suctions. It can be seen from Section 3.3 and Figure 3.6 that, for suctions in the range of 1 to 15 m (10 to 150 kPa), this gradient will lie in a range which is of the order of 0.0002 to 0.001/m. Inserting these values into Equation 7.2, together with a typical depth to water of 20 m, would give response times of about 25 to 135 days.

At depths below about 10 m fracture frequency will usually decrease, so that inter-fissure block size will increase. This will lead to a decrease in specific yield as shown in Table 7.1; an increase in the length of the block by an order of magnitude decreases the specific yield (and hence C) by an order of magnitude. With C reduced by a factor of 10, propagation time over 20 m would fall to about 2.5 to 15 days, so that the response times of deep water tables would not increase unreasonably. More detailed modelling is needed to refine these results.

7.2.2 Water resources

The results of the work by Lewis *et al.* (1993) imply that storage of 0.25 per cent of bulk volume in the unsaturated zone would explain the discrepancy between calculated drainage of the aquifer and observed baseflow in the streams. The AWCP studies have shown that drainage of this order is feasible from relatively large blocks. Whether storage in the unsaturated zone occurs in or on the surface of the matric blocks, it may be significant in water resources terms. The area of the Chalk outcrop in England is about 20 000 km^2. If the typical thickness of the unsaturated zone is assumed to be 20 m, then the volume of the unsaturated zone is about 4×10^{11} m^3, and the volume of water involved in matric storage of 0.25 per cent is 10^9 m^3, or five times the gross storage volume of Kielder Reservoir. Calculations such as this could be improved by using the BGS model (Lewis *et al.*, 1993) to obtain more reliable values for the average thickness of the unsaturated zone of the Chalk.

This storage in the unsaturated zone will be replenished each winter as recharge reaches the water table, and will be available each summer, draining slowly to the water table below the zero-flux plane to augment groundwater supplies. It may help to explain why the Chalk has proved more resilient to drought than expected in some regions; even when there is only a minimal rise in the water table during a recharge season, this additional "unsaturated" storage has been replenished and is available for the following summer. With drainable storage of 0.25 per cent and an unsaturated zone 20 m in thickness, the equivalent of 50 mm of infiltration will be taken up by matric storage in the unsaturated zone. This storage can be thought of as an additional and substantial "soil-moisture deficit" that will usually be satisfied as recharge reaches the water table.

The concept of matric storage in the unsaturated zone may also help to explain anomalies such as the groundwater mounds described by Giles and Lowings (1990) which persist beneath interfluves for much longer than expected. Beneath interfluves, where the water table is usually many tens of metres below ground surface, there will be a thick unsaturated zone and hence more water in matric storage.

7.2.3 Flooding in Chalk catchments

In recent winters, most notably in 1993-94 and 1994-95, there have been cases where flooding has occurred in Chalk catchments, apparently as a result of the water table rising to the ground surface in areas distant from normal groundwater discharge areas. In some cases - Chichester was probably the most serious and most publicised example - major disruption was caused. A better understanding of the storage processes operating in the unsaturated zone may help to understand why these flood events occur.

In "normal" winters it can be expected that suctions will fall in the unsaturated zone to the point where the smaller irregularities on the fissure walls are filled with water. Larger irregularities, and the majority of the fissure volume, will remain drained; water will be passing through the profile but all the storage space will not be filled. After unusually heavy recharge the suctions will drop further, and larger depressions on the fissure surfaces will also fill. In this state, any small extra increase in the input of water is likely to trigger the filling of most of the fissures and, in effect, the rise of the water table to ground level. Again, more work, particularly modelling of the unsaturated zone, is needed to refine these ideas.

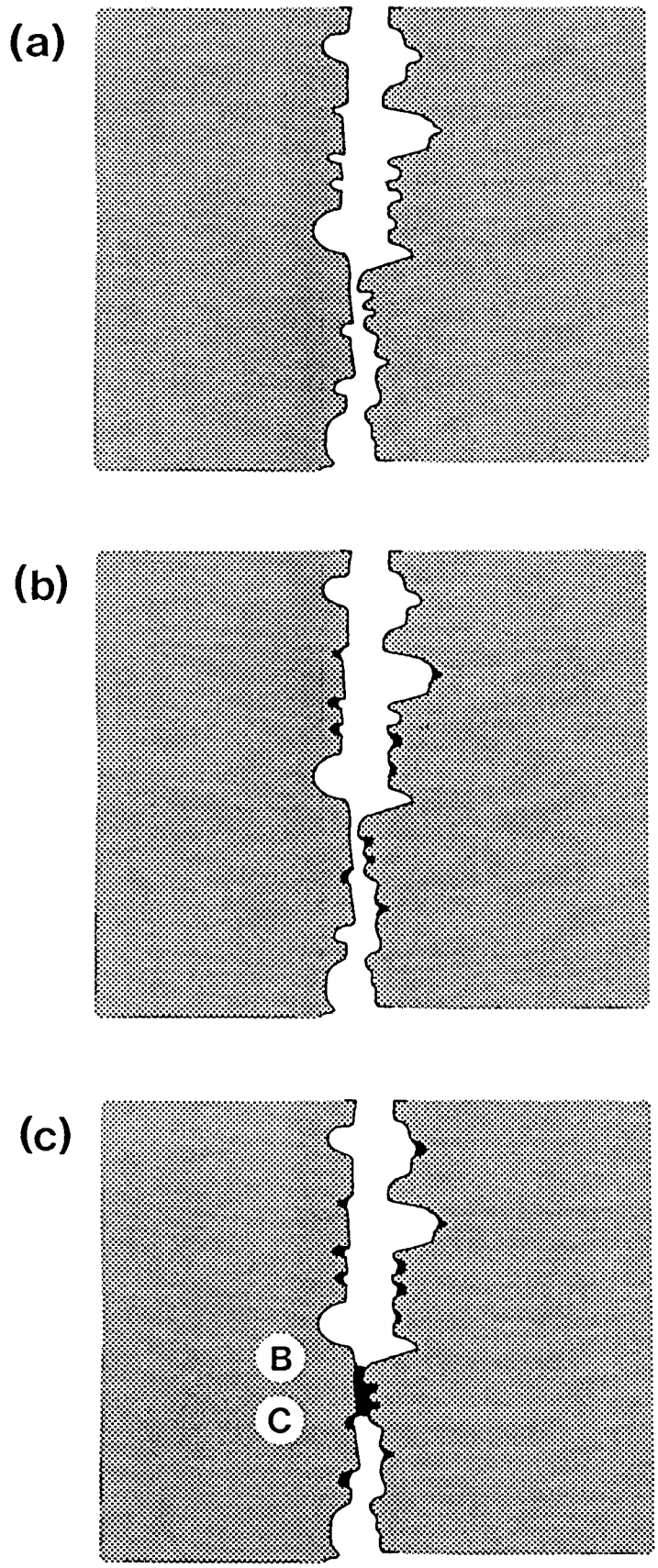
(a)
(b)
(c)
B
C

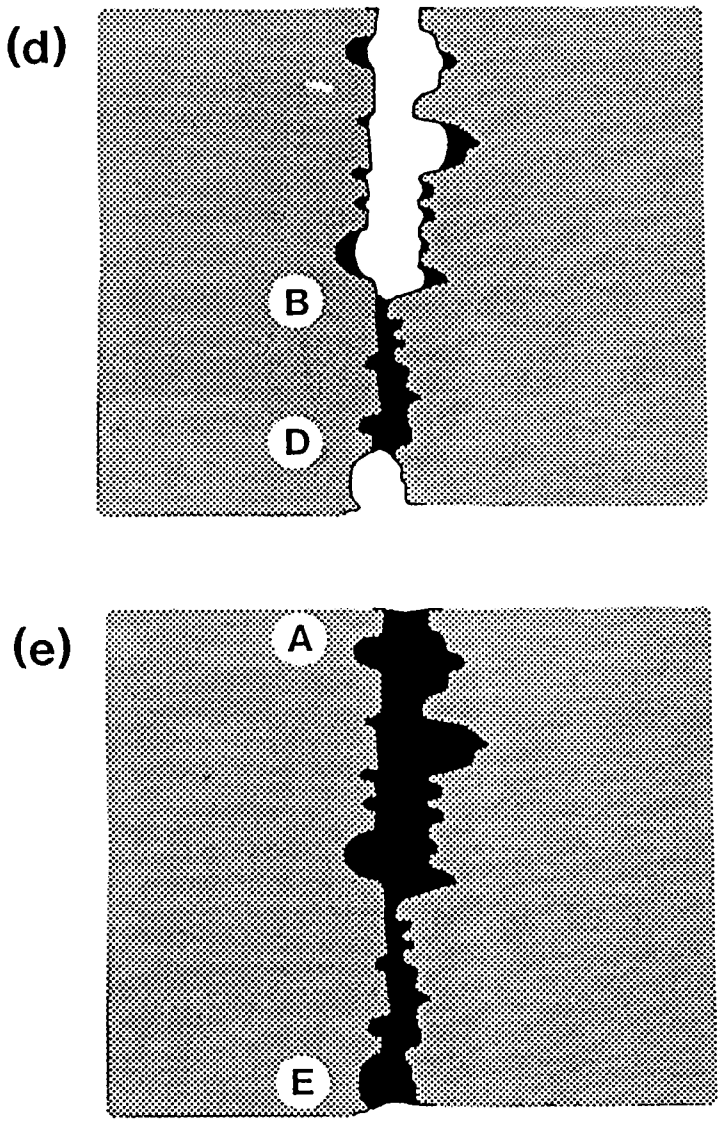

Figure 7.2 Diagrammatic representation of the initiation of flow in a fissure between two chalk blocks. Initially, only the matrix conducts water (a). As pore suctions fall, the smaller depressions on the fissure walls fill with water (b). As suctions fall further (c), larger depressions fill and the narrowest portions of the fissure (BC) begin to conduct water. At high rates of recharge, successively larger depressions fill and eventually the fissure may fill with water along its entire length (d and e).

7.2.4 Movement of recharge: generation of fissure flow

There has been much debate over whether recharge through the unsaturated zone of the Chalk occurs through fissures or matric pores. The balance of the evidence seems to be that recharge occurs through the matrix unless and until the average rate of infiltration approaches or exceeds the hydraulic conductivity of the matrix (see, for example, Price *et al.*, 1993). When this happens the matrix will not be able to carry all the recharge water unless the vertical hydraulic gradient is greater than 1, in which case the pore pressures in the unsaturated zone would rise to atmospheric pressure (the pore suctions would drop to zero) and the water table would rise to ground level. As this condition is approached the fissures will begin to fill and conduct water, greatly increasing the hydraulic conductivity in the unsaturated zone. In reality the narrower fissures will fill and become conductive first, and the wider fissures will fill only if this increase conductivity is still less than the rate of infiltration.

There seems to be a general conception that fissure flow, if generated, will begin from near the ground surface - probably from just blow the soil or the deeply weathered layer; water will then be carried downwards by fissures until at some depth the matric tensions are sufficiently high to draw the water from the fissures into the pore space. This idea appears to underlie concepts, such as that proposed by Foster (1975), that seek to reconcile rapid fissure flow of water with slow downward movements of solutes. These explanations picture water as moving downward through fissures with solutes diffusing laterally into the pore space and thus being greatly retarded relative to the water.

The evidence from the present study seems to suggest that fissure flow can be generated at any point in the profile, but will probably be initiated at levels where the matric hydraulic conductivity is relatively low. The sequence is represented in Figure 7.2. As recharge moves down through the matrix (Figure 7.2a), pore suctions will reduce to the point that depressions on the surface of the matric blocks fill, with the smaller depressions filling first followed by the larger ones (Figure 7.2b); if suctions continue to fall the finer fissures - such as the length BC in Figure 7.2c - will also fill and begin to conduct water. If recharge is at such a rate that it cannot be carried by these finer fissures, the suctions will decrease further and larger fissures (BD in figure 7.2d) will also fill. In extreme events the fissure will fill along the length AE (Figure 7.2e), but this will probably be rare. The profile of hydraulic head (and therefore the pore-water suctions) will adjust in response to the changes in hydraulic conductivity ($K(\psi)$), which will in turn vary as the pore-water suctions adjust. Again, more detailed modelling is needed to help refine these concepts.

The concept of diffusion between fissures and matrix becomes largely redundant, as water entering fissures will almost invariably have passed through higher parts of the profile as matric flow.

8. CONCLUSIONS AND RECOMMENDATIONS FOR FURTHER WORK

8.1 Conclusions

The various aspects of this project, including air-water capillary pressure (AWCP) studies, mercury intrusion (MICP) measurements, acoustic measurements at various confining stresses, and resin impregnation studies, have led us to conclude that, for the samples of chalk studied:

- there is no evidence for the presence of significant networks of microfissures;
- some large pores (macropores) are present. However, the connections from these macropores to the surrounding pores are so small that the macropores cannot make a significant contribution to specific yield or permeability;
- in studies of drainage from chalk blocks, there is a clear correlation between the drainage from the block (and hence its specific yield) and the block surface, with more water draining from blocks with rougher surfaces. This suggests that much or all of the specific yield of chalks may arise from drainage of irregularities on block surfaces;
- there is a similar relationship between drainage and block size, with smaller blocks having larger specific yields. This strengthens the conclusion that surface irregularities are a major component of specific yield, as small blocks have a larger ratio of volume to surface area than large blocks;
- simple numerical modelling of block surfaces indicates that predicted drainage from irregularities is of the same order as measured specific yield;
- measured and modelled specific yields are in good agreement with the values needed to explain the additional water released from drainage in the catchment studies described by Lewis *et al.* (1993);
- the proposed relation between drainage and block size is consistent with the decline in specific yield with depth that is reported from detailed studies for river augmentation schemes, as fissure spacing and therefore block size frequently increase with depth.

These conclusions, if valid, throw light on some other aspects of Chalk hydrology and hydrogeology that have caused debate in recent years:

- delay in the response of the water table to recharge is a function of the storage property of the unsaturated zone. It is not necessary to invoke fissure flow to explain this storage, as storage can be contributed by irregularities on the surfaces of fissures as well as by the emptying and filling of fissures;
- the unexpected resilience of the Chalk aquifer in periods of drought can be partially explained by the additional water in storage in the unsaturated zone which drains slowly to the water table to augment groundwater reserves in the absence of hydrologically effective precipitation;

- in turn, this means that, as predicted by Lewis *et al.* (1993), water levels in the aquifer may not be an accurate indication of water resources; for the same water-table level there will be significantly more storage in the unsaturated zone at the end of a recharge season than at the beginning of the following one;

- the rapid rise of the water table to ground level, which has led to widespread flooding in some Chalk catchments after unusual recharge, may be related to the state of storage in the unsaturated zone;

- the debate over whether recharge occurs through matric flow or fissure flow, and the difficulty of reconciling conflicting observations, is moderated by the understanding that flow can be generated in fissures over limited depth intervals in the unsaturated zone. Fissure flow is generated not by water moving down a fissure from the soil, but by the suction in the surrounding blocks falling to a level where first the irregularities on the surfaces of the blocks are filled with water and then the narrower fissures also become filled;

- the concept of solutes moving between matric pores and fissures by diffusion is largely redundant, as fissure flow will be generated in effect from within the matrix rather than by direct flow down fissures.

8.2 Recommendations for further work

The findings of the present study are based on results from a limited number of samples from only three sites, all in southern England. It was not possible to complete all of the measurements even on the limited number of samples involved - for example, some blocks were impregnated with resin but have not been examined under the SEM. These shortcomings were inevitable given the time-consuming nature of the measurements and techniques used and the short duration of the study, coupled with the fact that some of the techniques and equipment were developed specifically for this project. However, they do raise concerns as to the general applicability of the results. For example, because of the desire to obtain large blocks to give the best chance of finding microfissures, it is possible that the chalks collected may have been taken only from the harder beds.

To address these concerns, and to make the findings of the study as useful as possible, the following additional studies are suggested:

1. Completion of the sectioning, polishing and SEM examination of the samples that have been impregnated.

2. A systematic study, similar to the one just carried out, to determine the presence or absence of microfissures and the degree of any matric drainage, on a series of samples taken at fixed intervals from borehole core. This would avoid any problem of sampling bias, which is difficult to avoid when taking samples from a surface exposure. Ideally existing core should be used, but if none is available a cored borehole should be drilled at a site with a relatively thick unsaturated zone. The methods used should include AWCP and acoustic measurements; MICP studies would probably not be necessary. The impregnation technique should be used sparingly, mainly to check any samples which on the basis of the acoustic studies seem to contain microfissures.

3. The AWCP equipment should be refined to provide improved control and measurement of low pressures, to permit better definition of the drainage curve at suctions between 0 and 1 m of water.

4. Modelling should be undertaken of the unsaturated zone profile, its drainage towards equilibrium and its response to recharge events. The modelling should make use of the properties obtained in the present study and those from the proposed measurements on the borehole core. It should concentrate on elucidating the relationships between matric and fissure flow, the change of total head gradients and matric suctions in response to recharge, and the response of the water table (including occasions when it may rise rapidly).

REFERENCES

Barker, J A (1993). Modelling groundwater flow and transport in the Chalk. In *The hydrogeology of the Chalk of North-West Europe* (ed. R A Downing, M Price and G P Jones) 59-66. Clarendon Press, Oxford.

Beckett, D and Sellwood, B W (1991). A simple method for producing high-quality porecasts of carbonate rocks. *Sedimentary Geology*, **71**, 1-4.

Benson, G C and Kiyohara, O (1974). Tabulation of some integral functions describing diffraction effects on the ultrasonic field of a circular piston source. *J. Acoust. Soc. Am.*, **55**, 184-185.

Bloomfield, J P, Brewerton, L J and Allen, D J (1995). Regional trends in matrix porosity and dry density in the Chalk of England. *Quarterly Journal of Engineering Geology*, **28**, S131-S142.

Foster, S S D (1975). The Chalk groundwater tritium anomaly - a possible explanation. *Journal of Hydrology*, **25**, 159-165.

Freeze, R A and Cherry, J A (1979). *Groundwater*. Prentice-Hall, Englewood Cliffs, New Jersey.

Giles, D M and Lowings, V A (1990). Variation in the character of the chalk aquifer in east Hampshire. In *Chalk* (ed. J B Burland) 619-626. Thomas Telford, London.

Ineson, J and Downing, R A (1964). The ground-water component of river discharge and its relationship to hydrogeology. *Journal of the Institution of Water Engineers*, 18 (7): 519-541.

Klimentos, T and McCann, C (1990). Relationships between compressional wave attenuation, porosity, clay content and permeability of sandstones. *Geophysics*, **55**, 998-1014.

Lewis, M A, Jones, H K, Macdonald, D M J, Price, M, Barker, J A, Shearer, T R, Wesselink, A J and Evans, D J (1993). *Groundwater storage in British aquifers: Chalk.* R&D Note 169, National Rivers Authority, Bristol.

McCann, C and Sothcott, J (1992). Laboratory measurements of the seismic properties of sedimentary rocks. In *Geological applications of wire-line logs 2* (ed. A Hurst, P F Worthington and C Griffiths) *Special Publication of the Geological Society*, **65**, 285-297.

Peacock, S, McCann, C, Sothcott, J and Astin, T R (1994a). Seismic velocities in fractured rocks: an experimental verification of Hudson's theory. *Geophysical Prospecting*, **42**, 27-80.

Peacock, S, McCann, C, Sothcott, J and Astin, T R (1994b). Experimental measurements of seismic attenuation in micro fractured sedimentary rock. *Geophysics*, **59**, 1342-1351.

Price, M, Bird M J and Foster, S S D (1976). Chalk pore-size measurements and their significance. *Water Services*, **80**, (968): 596-600.

Price, M, Downing, R A and Edmunds, W M (1993). The Chalk as an aquifer. In *The hydrogeology of the Chalk of North-West Europe* (ed. R A Downing, M Price and G P Jones) 35-58. Clarendon Press, Oxford.

Reeves, M J (1979). Recharge and pollution of the English Chalk: some possible mechanisms. *Engineering Geology*, **14**, 231-240.

Ritter, H L and Drake, L C, (1945). Pore-size distribution in porous materials. *Industrial and Engineering Chemistry: Analytical Edition*, **17**: 782-786.

Spurr, A R (1969). A low viscosity resin embedding medium for electron microscopy. *J. Ultrastruct. Res.* **23**, 31-43.

Vavra, C L, Kaldi, J G and Sneider, R M (1992). Geological applications of capillary pressure: a review. *American Association of Petroleum Geologists Bulletin,* **76**, 840-850

Waldo, A W and Yuster, S T (1937). Method of impregnating porous materials to facilitate pore studies. *American Association of Petroleum Geologists Bulletin,* **21**, 259-267.

Wellings, S R (1984). Recharge of the Upper Chalk aquifer at a site in Hampshire, England. 1. Water balance and unsaturated flow. *Journal of Hydrology*, **69**, 259-273.

Winkler, K and Plona, T J (1982). Techniques for measuring ultrasonic velocity and attenuation spectra in rocks under pressure. *Jour. Geophys. Res.*, **87**, 10776-10780.